



Titre: Polyethylene Terephthalate (PET) Films Surface Modification
Title: Through Blending

Auteur: Ahmad Rezaei Kolahchi
Author:

Date: 2014

Type: Mémoire ou thèse / Dissertation or Thesis

Référence: Rezaei Kolahchi, A. (2014). Polyethylene Terephthalate (PET) Films Surface Modification Through Blending [Thèse de doctorat, École Polytechnique de Montréal]. PolyPublie. <https://publications.polymtl.ca/1368/>
Citation:

 **Document en libre accès dans PolyPublie**
Open Access document in PolyPublie

URL de PolyPublie: <https://publications.polymtl.ca/1368/>
PolyPublie URL:

Directeurs de recherche: Abdellah Ajji, & Pierre Carreau
Advisors:

Programme: Génie chimique
Program:

UNIVERSITÉ DE MONTRÉAL

POLYETHYLENE TEREPHTHALATE (PET) FILMS SURFACE MODIFICATION
THROUGH BLENDING

AHMAD REZAEI KOLAHCHI

DÉPARTEMENT DE GÉNIE CHIMIQUE
ÉCOLE POLYTECHNIQUE DE MONTRÉAL

THÈSE PRÉSENTÉE EN VUE DE L'OBTENTION
DU DIPLÔME DE PHILOSOPHIAE DOCTOR
(GÉNIE CHIMIQUE)

MARS 2014

UNIVERSITÉ DE MONTRÉAL

ÉCOLE POLYTECHNIQUE DE MONTRÉAL

Cette thèse intitulée:

POLYETHYLENE TEREPHTHALATE (PET) FILMS SURFACE MODIFICATION
THROUGH BLENDING

présentée par : REZAEI KOLAHCHI Ahmad

en vue de l'obtention du diplôme de: Philosophiae Doctor

a été dûment acceptée par le jury d'examen constitué de :

M. FAVIS Basil, Ph.D., président

M. AJJI Abdellah, Ph.D., membre et directeur de recherche

M. CARREAU Pierre, Ph.D., membre et codirecteur de recherche

M. DUBOIS Charles, Ph.D., membre

Mme. DEMARQUETTE Nicole Raymonde, Ph.D., membre

DEDICATION

“To my best friend Ali”

ACKNOWLEDGEMENTS

I would like to express my endless gratitude to my lovely wife, Mansoureh, *who did more than her* share around the house as I sat at the computer, to our little daughter Asra who her charm made it possible throughout the tough times and my beloved family specially Akram and Davoud, Words are unable to reflect what I feel in my heart towards them.

My sincere appreciations go to Prof. Abdellah Ajji for supervising my PhD research program, for believing in me, supporting me and challenging me; for his patience, and all the productive discussions.

Prof. Carreau is someone I will remember until the end of my life as the coolest, knowledgeable, wise and kind professor I have ever met. It was a pleasure to work with him, and he taught me lots of lessons that will help me in all aspects of my life.

My special gratitude to the staff and technicians of Ecole Polytechnique de Montreal, chemical engineering department and Lavergne Group Inc. who have been of great help during my experiments: Florin, Doru, Guillaume, Martine, Gino, Robert, and Jean.

I am especially grateful to Marie for translating the abstract of this thesis to French. And special thanks also go to Mélina Hamdine, Weawkamol Leelapornpisit, and Claire Circlé who helped me during my study.

Finally my most sincere thanks to my friends: Ali Yaghoobi, Mohammad Savoji, , Navid, Khalil, Ahmad, A Zolali, Vahid, Salman and Ali Jafary.

RÉSUMÉ

Contrôler l'adhérence de la surface des polymères est un problème clé de la technologie des surfaces, les polymères étant des matériaux communément utilisés depuis de nombreuses années. Deux aspects différents de la modification de surface sont abordés dans cette étude. Le premier est l'amélioration du caractère hydrophile, le second est la création d'une rugosité de surface du film de PET.

Dans cette thèse, nous développons une approche nouvelle et simple pour modifier la surface d'un film de polyéthylène téréphtalate (PET) par un mélange de polymères en extrusion double-vis. Un exemple décrit dans la thèse utilise le polyéthylène glycol (PEG) dans le polyéthylène téréphtalate (PET) pour modifier la surface du film de PET. Le PEG est un polymère hydrophile avec un groupe fonctionnel carbonique et un pourcentage élevé d'oxygène par carbone dans sa structure chimique. Pour augmenter le taux de migration du PEG vers la surface du film, une faible quantité de polystyrène (PS) a été ajoutée dans le système comme troisième composant. Cette nouvelle méthode a été utilisée car les chaînes polymères du PEG, qui sont courtes, migrent facilement à la surface et reviennent dans la masse du polymère pendant la phase de refroidissement. Le PS à haut poids moléculaire étant fortement incompatible avec le PET stabilise les molécules de PEG dans la couche à la surface du film. L'enrichissement de la surface en PEG a été observé à l'interface polymère/air du film polymère composé du système PET-PEG-PS tandis que pour le système binaire PET-PEG, une plus grande quantité de PEG a été distribuée au cœur de l'échantillon. Un autre exemple décrit la morphologie de la surface du film de mélange ternaire de polymères. Dans cette partie de l'étude, l'apparence de la surface du polymère tient compte de la migration des molécules du constituant minoritaire vers la couche supérieure en surface des films. Différents polymères, comme le PS, le PBAT, le PCL, le PMMA et le PLA, ont été utilisés en tant que seconde phase minoritaire dans un système contenant du PET et du PEG. Un taux de migration plus élevé du PEG vers l'interface polymère/air a été observé dans les systèmes avec des morphologies hydrophobes et le plus haut taux de migration pour le mélange PET/PS/PEG. L'énergie de surface la plus élevée est 54 mN/m pour le film composé de PET avec 5% en masse de PS et 7% en masse de PEG, la concentration optimale de PS par rapport à la concentration de PEG à la surface est alors 7% en masse.

De plus, une nouvelle méthode a été proposée afin de créer une surface rugueuse des films de PET. Nous avons considéré l'épaississement de la phase de PS dans les films extrudés de PET. Afin de rendre la surface des films de PET rugueuse, une faible quantité de résine phénoxy PKHH a été utilisée pour changer la tension interfaciale du système PS/PET. Les effets compatibilisants du PKHH ont provoqué la formation de gouttelettes de PS plus petites, qui ont alors été capables de migrer plus facilement à travers la matrice de PET. Par la suite, aboutissant à une concentration élevée de PS localisée proche de la surface du film, cela a pris la forme de gouttelettes encapsulées juste sous la surface. La transformation de Fourier rapide en 2D des images AFM a indiqué que l'intensité de fluctuation des longueurs d'ondes à la surface du film pendant le recuit suivait une relation en loi puissance en fonction du temps et cette instabilité entraînerait l'apparition de la rugosité.

ABSTRACT

Controlling the adhesion of the polymer surface is a key issue in surface science, since polymers have been a commonly used material for many years. The surface modification in this study includes two different aspects. One is to enhance the hydrophilicity and the other is to create the roughness on the PET film surface.

In this thesis, we developed a novel and simple approach to modify polyethylene terephthalate (PET) film surface through polymer blending in twin-screw extruder. One example described in the thesis uses polyethylene glycol (PEG) in polyethylene terephthalate (PET) host to modify a PET film surface. PEG is a hydrophilic polymer with carbonic functional group and high percentage of oxygen per carbon in its chemical structure. Low content of polystyrene (PS) as a third component was used in the system to increase the rate of migration of PEG to the surface of the film. This novel method was effective because short PEG polymer chains migrate easily to the surface and move back toward the bulk of polymer during the cooling process. High molecular weight PS as a very incompatible polymer with PET stabilizes PEG molecules at the surface layer of the film.

Surface enrichment of PEG was observed at the polymer/air interface of the polymer film containing PET-PEG-PS whereas for the PET-PEG binary blend more PEG was distributed within the bulk of the sample. Another example described the surface morphology of the ternary polymer blend film. In this part of the study the polymer surface make up considered by the migration of minor component molecules to the top surface layer of the films. Different polymers as a second minor phase such as PS, PBAT, PCL, PMMA and PLA were used in a system containing PET and PEG. Higher migration rate of PEG to the polymer/air interface was observed in the systems with non-wetting morphology and the highest in the PET/PS/PEG blend. The highest surface energy is 54 mN/m, for the PET-5wt%PS-7wt%PEG film so the optimum concentration of PS with respect to PEG concentration at the surface is 7wt%.

Furthermore, a novel method to create roughness at the PET film surface was proposed. We considered the phase coarsening of PS in extruded thin films of PET. In order to roughen the surface of PET film, a small amount of PKHH phenoxy resin to change PS/PET interfacial

tension was used. The compatibility effect of PKHH causes the formation of smaller PS droplets, which were able to migrate more easily through PET matrix. Consequently, resulting in a locally elevated concentration of PS near the surface of the film, took the form of encapsulated droplets just below the surface and coarsening the minor phase. The local concentration of PS eventually reached a level where a co-continuous morphology occurred, resulting in the instabilities on the surface of the film. 2D fast Fourier transforms of the AFM images indicated that the intensity of wavelength fluctuations at the film surface during annealing followed a power-law relationship as a function of time and the roughness appeared due to this instability.

TABLE OF CONTENTS

DEDICATION	III
ACKNOWLEDGEMENTS	IV
RÉSUMÉ.....	V
ABSTRACT	VII
TABLE OF CONTENTS	IX
LIST OF TABLES	XIV
LIST OF FIGURES.....	XV
CHAPTER 1 INTRODUCTION AND OBJECTIVES	1
1.1 Introduction	1
1.2 Objectives.....	3
CHAPTER 2 LITERATUREREVIEW	5
2.1 PET.....	5
2.2 Surface properties of polymers	6
2.2.1 Adhesion.....	7
2.2.2 Wettability	11
2.2.3 Surface tension and surface energy	12
2.3 Printing.....	15
2.3.1 Printing methods	15
2.3.2 Printing Inks	16
2.3.3 An example of printing ink formulation for polymer surface	21
2.3.4 Ink drying and curing	22
2.3.5 Problems frequently encountered during the ink printing on surfaces.....	22
2.3.6 Mechanism for bonding between polymer surface and inks.....	23

2.4	Molecular bonding mechanism for adhesion	24
2.5	Surface treatment and modification	26
2.5.1	Physico – chemical treatment.....	27
2.5.2	Chemical modification	31
2.5.3	Bulk modification.....	32
2.6	Migration of macromolecules under flow	36
2.6.1	Thermodynamic theory of migration	37
2.6.2	Kinetic theory of migration	38
2.7	Polymer blending	39
2.7.1	Thermodynamic of polymer blends	40
2.7.2	Phase separation	42
2.7.3	Morphology of polymer blends.....	44
2.8	Effect of material parameters on morphology.....	44
2.8.1	Interfacial tension.....	44
2.8.2	Viscosity ratio	45
2.8.3	Composition	45
2.8.4	Shear stress	46
2.8.5	Elasticity ratio	46
2.9	Summary of literature review and problem identification	46
2.10	Originality of the work.....	49
CHAPTER 3 ORGANIZATION OF THE ARTICLES		50
CHAPTER 4 ARTICLE 1: ENHANCING HYDROPHILICITY OF PET SURFACE THROUGH MELT BLENDING		52
4.1	Abstract	52
4.2	Introduction	53

4.2.1	Surface migration of the minor components	56
4.3	Experimental section	58
4.3.1	Materials and sample preparation	58
4.3.2	Characterization	59
4.4	Results and discussion.....	61
4.4.1	Effect of PEG molecular weight on migration.....	61
4.4.2	Binary blend	62
4.4.3	Ternary blend	65
4.5	Conclusion.....	78
4.6	Acknowledgment	79
4.7	References	79
CHAPTER 5 ARTICLE 2: SURFACE MORPHOLOGY AND PROPERTIES OF TERNARY POLYMER BLENDS: EFFECT OF THE MIGRATION OF MINOR COMPONENTS.....		82
5.1	Abstract	82
5.2	Introduction	83
5.3	Experimental section	87
5.3.1	Materials.....	87
5.3.2	Samples preparation	87
5.3.3	Characterization	88
5.4	Results and discussion.....	90
5.4.1	Surface free energy.....	90
5.4.2	Film surface morphology	93
5.4.3	Surface oxygen content	98
5.5	Conclusion.....	99

5.6	Acknowledgment	100
5.7	References	100
CHAPTER 6 ARTICLE 3: SURFACE ROUGHENING OF PET FILMS THROUGH BLEND PHASE COARSENING		104
6.1	Abstract	104
6.2	Introduction	105
6.3	Experimental section	108
6.3.1	Materials and sample preparation	108
6.3.2	Characterization	109
6.4	RESULTS AND DISCUSSION	113
6.4.1	XPS analysis.....	113
6.4.2	SEM results	117
6.4.3	Depth profiling and AFM results	119
6.4.4	Phase coarsening kinetics.....	123
6.4.5	Surface roughness	125
6.4.6	Adhesion test.....	126
6.5	Conclusion.....	127
6.6	Acknowledgments.....	128
6.7	References	129
CHAPTER 7 GENERAL DISCUSSION		136
CHAPTER 8 CONCLUDING REMARKS AND RECOMMENDATIONS.....		140
8.1	Conclusions	140
8.2	Recommendations	142
CHAPTER 9 INDEX		144
9.1	Index A.....	144

9.2	Index B	145
9.3	Index C	146
9.4	Index D	147
9.5	Index E	147
REFERENCES		148

LIST OF TABLES

Table 2.1: Recycled plastic collected in Canada [26]	6
Table 2.2: Common printing ink pigments (Kroschwitz 1999).	18
Table 2.3: Combinations of binders and solvents for different printing methods (ÖZMAN 2008).	21
Table 2.4: Flexographic ink for polyethylene film (Saad 2007)	22
Table 2.5: Surface modification methods (Awaja, Gilbert 2009)	26
Table 4.1: Relative content (in %) of the carbon bonds and oxygen atoms at the surface of the neat PET, PET-PS, PET-PEG and PET-PS-PEG films. C1: C-C bonds, C2: Ether carbon atoms, C3: Ester carbon atoms, O1: Ester oxygen atoms, O2: Ether oxygen atoms.	68
Table 5.1: List of the materials and their characteristics.....	87
Table 5.2 : Interfacial tension of pairs of polymers in PET blends and spreading coefficient	96
Table 6.1: High-resolution XPS spectra of PET and PET-5wt% PS-5wt% PKHH film surfaces.	115

LIST OF FIGURES

Figure 2-1: Rigid plastics recycled by resin category (Moore 2012).....	6
Figure 2-2: Bond energies and bond length of adhesive forces.	8
Figure 2-3: Schematic illustration of dispersive adhesion between two surfaces.....	9
Figure 2-4: Schematical illustration of diffusive adhesion between two surfaces.....	10
Figure 2-5: Schematic image of mechanical interlocking between adhesive and substrate due to solid rough surface.	10
Figure 2-6: Sessile drop on a surface indicating.	11
Figure 2-7: Schematic image of wettability and contact angle.	12
Figure 2-8: Liquid solid interfaces.	13
Figure 2-9: Typical graph of Zisman plot to obtain critical surface tension with a series of liquids.	14
Figure 2-10: Printing ink components.....	17
Figure 2-11: The difference between pigments and dyes.	19
Figure 2-12: Schematic illustration of Molecular bonding between two surfaces.....	25
Figure 2-13: Mechanism of adhesion promoter bonding (Awaja, Gilbert et al. 2009).....	25
Figure 2-14: Variation of surface energy of polyethylene by flame treatment (Brewis 2002)	27
Figure 2-15: Schematical diagram of corona discharge generator.....	28
Figure 2-16: Parallel plate system for cold plasma treatment in a vacuum chamber. There are two electrodes: the anode, which is polarized with the radiofrequency, and the grounded cathode. The plasma is formed between the two electrodes and results in the formation of excited species, which then act on the surface of the sample.	30
Figure 2-17: NaOH attack on PET chains (Situma, Wang et al. 2005).	32
Figure 2-18: Creation of grafted surface by: a) direct polymer-coupling reaction; b) graft polymerization.....	32

Figure 2-19: Schematic diagram of the self-assembly of a surface-active end-functional block copolymer at the surface of a polymeric substrate at an air–polymer interface and subsequent reorganization when it is exposed to water vapor.	35
Figure 2-20: A typical image illustrating migration of minor component to the surface during extrusion.	39
Figure 2-21 : Schematic diagram of free energy of mixing versus composition in binary polymer mixture.	41
Figure 2-22: Phase diagram showing LCST and UCST behavior for polymer blends.	42
Figure 2-23 : Schematic illustration of the phase separation a) nucleation and grow, b) spinodal decomposition.	43
Figure 4-1: Water contact angle for the PET-PEG blends containing 5wt% of different M_w PEGs (35, 20, 8 kDa).....	62
Figure 4-2: Water contact angle of the original PET and PET- 5wt%PEG films.	63
Figure 4-3: XPS survey spectra of the PET-5wt%PEG blend sample.	64
Figure 4-4: O/C atom ratio for the original PET and PET-5wt%PEG.....	65
Figure 4-5: Water contact angles for PET, PET-5wt%PEG, PET-5wt%PS and PET-5wt%PS-5wt%PEG films.....	66
Figure 4-6: O/C atom ratio for PET, PET-5wt%PEG, PET-5wt%PS, PET-5wt%PS-5wt%PEG.	68
Figure 4-7: XPS high-resolution spectra of carbonyl groups on the surfaces of the neat PET, PET-5wt%PS, PET-5wt%PEG and PET-5wt%PS-5wt%PEG films.	69
Figure 4-8: Surface energies of the neat PET, PET-5wt%PEG, PET-5wt%PS and PET-5wt%PEG-5wt%PS films.....	71
Figure 4-9: Results of TOF-SIMS imaging of the PET PET-5wt%PEG and PET-5wt%PS-5wt%PEG film surfaces.	73
Figure 4-10: SEM cross-sectional images from (a) PET-5wt%PS and (b) PET-5wt%PEG (etched) (c) PET-5wt%PEG (non-etched) (d) PET-5wt%PS-5wt%PEG (etched) (e) PET-5wt%PS-5wt%PEG (non-etched).....	75

Figure 4-11 : DSC thermograms of the cooling cycle for the neat PET, PET-5wt%PEG, PET-5wt%PS and PET-5wt%PS-5wt% PEG films.....	77
Figure 4-12: Crystallinity percentages calculated from DSC on the neat PET, PET-5wt%PEG, PET-5wt%PS and PET-5wt%PS-5wt%PEG DSC films	77
Figure 5-1: Possible morphologies in a ternary polymer blend composed of two minor phases A and C and one major phase B, as predicted by the spreading coefficient. a) Polymer A encapsulated by polymer C. b) A and C are two polymers dispersed in matrix B. c) Polymer C encapsulated by polymer A. d) Partial wetting morphology of polymer A and C.	85
Figure 5-2: Surface free energy of samples of the neat PET and PET containing 5wt%PEG and 5wt% of a different second minor phase (PCL, PBAT or PLA, PMMA and PS).	92
Figure 5-3: Water contact angle and surface energy of the neat PET film and prepared films with different concentrations of PET, PS or PEG.	92
Figure 5-4: SEM cross-sectional images of the ternary polymer blend films composed of 90wt%PET, 5wt%PEG and 5wt% of the second minor phase. a,b) PET-PBAT-PEG. c,d) PET-PS-PEG. e,f) PET-PMMA-PEG. g,h) PET-PLA-PEG.	95
Figure 5-5: AFM images from the surface morphology of the samples containing PET, 5wt%PEG and 5w% of the second minor phase. a) PET-PBAT-PEG. b) PET-PCL-PEG. c) PET-PS-PEG. d) PET-PMMA-PEG. e) PET-PLA-PEG.	97
Figure 5-6: AFM images from the PET-PS-PEG film surfaces for different concentrations of PS and PEG. a,b) PET-5wt%PS-5wt%PEG. c) PET-5wt%PS-3wt%PEG. d) PET-5wt%PS-7wt%PEG.	98
Figure 5-7: O/C atom ratio of the neat PET, PET-PS-PEG (92-5-3wt%), PET-PS-PEG (90-5-5wt%) and PET-PS-PEG (88-5-7wt%) film surfaces. The top inset shows XPS survey spectra of PET (left side) and PET-5wt%PS-5wt%PEG (right side).	99
Figure 6-1: Schematic illustration of roughness and liquid anchoring on a solid surface	106
Figure 6-2: Schematic image of pull-off adhesion test	112

- Figure 6-3: Sinusoidal distortions on the PS thread with diameter 55 μm , embedded in the PET matrix. The measurement was performed at 240 $^{\circ}\text{C}$; the times at which subsequent photographs were taken are: $t=20, 40, 60, 80$ s.....113
- Figure 6-4: a) Chemical structure of PET. b) High-resolution XPS spectra of: 1 C1s PET, 2 C1s PET-5wt%PS-5wt%PKHH, 3 C1s PET-5wt%PS, 4 O1s PET, 5 O1s PET-5wt%PS-5wt%PKHH, 6 O1s PET-5wt%PS.116
- Figure 6-5: SEM images from a) PET film surface. b-1) Cross section of PET-5wt%PS. b-2) PET-5wt%PS film surface. c-1) Cross section of PET-5wt%PS-5wt%PKHH films. c-2) PET-5wt%PS-5wt%PKHH film surface.118
- Figure 6-6: Volume fractions of dPS from FRES depth profiles of PET-5wt%dPS-5wt%PKHH film surface for a) Non-annealed sample. and annealed samples at 250 $^{\circ}\text{C}$ for b) 120 s c) 600 s. d) 1200 s. and AFM phase images of PET-5wt%dPS-5wt%PKHH film surfaces for e) Non-annealed sample and annealed samples at 250 $^{\circ}\text{C}$ for f) 120 s. g) 600 s. h) 1200 s. Scan sizes are 2.5 $\mu\text{m} \times 2.5 \mu\text{m}$. (Dark region is PET and bright region is PS).122
- Figure 6-7: Characteristic wavenumber versus annealing time for the PET-PS-PKHH blend at three different temperatures (240, 245 and 250 $^{\circ}\text{C}$). The left inset shows RMS surface roughness as a function of annealing time at different temperatures (240, 245 and 250 $^{\circ}\text{C}$) and the right inset shows 2d FFT image of PET-5wt%PS-5wt%PKHH film.....125
- Figure 6-8: RMS surface roughness for the neat PET, PET-5wt%PS, PET-5wt%PKHH and PET-5wt%PS-5wt%PKHH films surfaces in a) 472 μm length scale and b) 5 μm length scale. 126
- Figure 6-9: Adhesion test results on the surface of PET, PET-5wt%PS, PET-5wt%PKHH and PET-5wt%PS-5wt%PKHH film.127

CHAPTER 1

INTRODUCTION AND OBJECTIVES

1.1 Introduction

Plastic articles and products based on polyethylene terephthalate (PET) are numerous, from packaging films, bottles and containers to automotive parts. In most of these applications, surface structure and behavior of PET are of utmost importance, since wetting, adhesion, friction, abrasion, adsorption, and penetration phenomena are involved (Noeske, Degenhardt et al. 2004; López-Santos, Yubero et al. 2010; Liu, Sheng et al. 2013).

The surface of PET is prone to printability, dyeability, wettability and adhesion to the other surfaces due to its relatively low surface energy (Pandiyaraj, Selvarajan et al. 2010; Shin, Lee et al. 2012). Therefore it should be treated for good performance in these applications (Dong, Lyoo et al. 2010; Dastjerdi, Mojtahedi et al. 2012; Parvinzadeh Gashti and Moradian 2012). For example, surface treatment prior to printing has been the most efficient route to add desired surface properties and overcome specific problems. These operations represent an additional cost in the manufacturing process, while if dyes or inks adhere directly to the surface, significant cost savings and extension of use to other types of products and applications would be allowed.

In general, specific surface characteristics with regard to chemical composition, hydrophilicity, roughness, crystallinity, conductivity, lubricity and cross-linking density are required by successful applications. Hence, surface modification techniques, which can transform this inexpensive material into a highly valuable finished product, are of great scientific and technological interest (Favaro, Rubira et al. 2007; Slepicka, Vasina et al. 2010; Vandencastele, Broze et al. 2010).

Being able to change a material's surface properties during its manufacturing process will provide commercial benefits and eliminating an extra post-processing step will benefit the industry. The homogenous surface properties for complex shapes also can be obtained by this kind of modification. Our aim is to control useful surface properties like hydrophilicity while at the same time keeping the valuable mechanical properties of the bulk material (Morisada, Fujii et al. 2006; Wang, Shi et al. 2009).

Among all surface modification methods, blending is an attractive method to change surface properties because of its simplicity, reproducibility and commercial availability of desired additives, polymers and copolymers (Lee, Losito et al. 2001; Kim, Lee et al. 2009; Sanaeepur, Ebadi Amooghin et al. 2012). Modification for low-energy surfaces, which provides an opportunity to control properties, adhesion, wetting, and mobility, can be achieved by adding only a small amount of another component (Hardman, Muhamad-Sarih et al. 2011; Hardman, Hutchings et al. 2012). Such polymers or additives should show high efficiency at low concentrations in order to minimize or prevent possible negative effects on polymer processing, mechanical properties and the cost of the final products. They should also migrate and locate quickly on the surface of the host polymer (PET). The selection of a suitable material with appropriate cost/performance characteristics is a first objective of this project. Preliminary results obtained in our laboratory are encouraging as shown in the subsequent sections of this dissertation.

In order to make an adhesion between PET film surface and ink, surface hydrophilicity is not the only requirement, but equally important is the mechanical interlocking of ink on PET surface (Awaja, Gilbert et al. 2009; Tsao and DeVoe 2009). This phenomenon allows the ink to anchor

physically into the substrate, which would be achieved by roughness of the film surface. Therefore, another part of this study is to provide suitable roughness on PET film surface.

This thesis is based on three articles that have been published or submitted to scientific journals and comprised the following sections:

- **Chapter 2** provides a critical literature review regarding the related issues and followed by the summary of literature review, problem identification and originality of this dissertation.
- The summary and organization of the articles are described in **Chapter 3**.
- The main achievements of the thesis are given in the format of three scientific papers in **Chapters 4, 5 and 6**.
- **Chapter 7** presents a general discussion of the main results.
- Finally **Chapter 8** presents the final conclusions of this study and the recommendations for future works.

1.2 Objectives

The principal target of the present research is to develop a novel method to improve the printability of PET film surface, with good uniformity of modification for complex shapes. Among the different types of surface modification techniques, surface modification via polymer blending was identified as a significant potential to be done by extrusion process. Therefore, our main objective in this PhD project is:

To modify the surface properties of PET film in terms of hydrophilicity, roughness and adhesion through blending with other polymers and/or copolymers and/or additives

The general objective can be divided into the following specific objectives:

- To investigate the effect of low concentration of a hydrophilic polymer with PET on the surface of PET film
- To induce the migration of hydrophilic minor component molecules to the air/polymer interface
- To study the surface morphology of ternary polymer blend and its effect on the migration of the minor components
- To create rough PET film surface by phase separation/coarsening of a minor phases at the surface layer of the film

CHAPTER 2

LITERATUREREVIEW

This chapter includes a comprehensive literature review covering many aspects of ink composition, the requirement for good interaction between ink and polymer surface, polymer surface properties, the techniques to modify the surface of polymers and important parameters in polymer blending, which form the backbone of this research.

2.1 PET

Polyethylene terephthalate (PET) is a semi-crystalline polyester with excellent thermal, mechanical, gas barrier properties and chemical resistance. Its crystallinity variety can make it highly transparent, opaque and off-white in color. PET offers many different advantages and can be found in many different forms, from semi-rigid to rigid. It is a widely used plastic that can be made into a number of products including the packaging for many food products, clothes, sleeping bags, shoes, luggage, automotive parts and many more (Ballara and Verdu 1989; Foulc, Bergeret et al. 2005).

PET is synthesized by the esterification of either terephthalic acid or dimethyl terephthalate with ethylene glycol (Al Ghatta, Cobror et al. 1997; Biscardi, Monarca et al. 2003). Using copolymer of PET is becoming increasingly common for manufacturers due to certain of their advantages over homopolymer PET with regard to mechanical properties and resistance to degradation. PET is commonly recycled, which can be reused in a number of things (Guerrica and Eguiazabal 2009).

As for other recyclable materials, using PET is a good option in terms of preventing

environmental pollution. Moore Recycling Associates (Moore 2012) publish an annual survey about postconsumer plastic recovered in Canada. According to its 2011 report, around 268.5 million tons of recyclable plastics were collected in Canada, this was a 24% increase compared to 2010. Table 2.1 shows three years statistics of collected recycle plastic in Canada.

Table 2.1: Recycled plastic collected in Canada (Moore 2012)

Year	Recycle plastics (kg)
2011	268,533,314
2010	217,181,619
2009	188,104,289

Figure 2-1 also presents the breakdown of the recycled polymers in 2011 by resin.

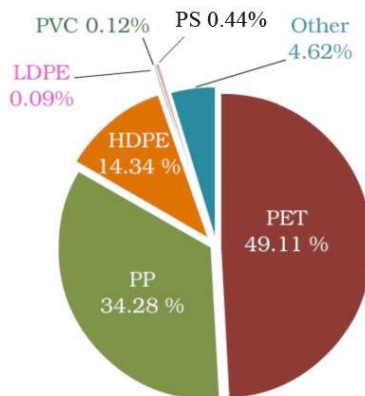


Figure 2-1: Rigid plastics recycled by resin category (Moore 2012).

The data show that there is good opportunity in the market of recycled PET to particularly make a more valuable compound to be used for many applications (Moore 2012).

2.2 Surface properties of polymers

In many industrial sectors, the surface properties of polymers are of particular importance. This applies for instance to the coating and painting of the surface of polymeric objects. In coating and painting processes, problems sometimes occur due to the relatively poor wetting and adhesion of

the plastic surfaces. This is directly related to the low surface free energy of the polymers and the absence or lack of polar surface functional groups resulting in weak mechanical interaction between two contacting surfaces (Pandiyaraj, Selvarajan et al. 2010; Shin, Lee et al. 2012). A desired polymer surface cannot often be obtained from the material itself but through some kinds of modification such as; plasma, corona or surface etching treatments. In this way, the active functional groups are introduced on the surface to increase the surface free energy and have a greater tendency to bond with other active materials. Some techniques also are used to increase the physical interaction between two contacted surfaces (Favaro, Rubira et al. 2007; Slepicka, Vasina et al. 2010; Vandencastele, Broze et al. 2010).

Several factors such as the chain length and the difference between the surface tension of polymer chain ends and middle segments can influence the surface of polymers. The surface composition is a critical parameter, which is affected by all the mentioned factors that control thermodynamic properties such as wettability and surface energy (Lee, Losito et al. 2001; Bodas, Patil et al. 2004; Lee, Ha et al. 2004; Esteves, Lyakhova et al. 2013). Therefore the treatment must be applied on the surface of polymers before coating and it has to introduce polar groups into the surface, consequently bringing into play strong forces that strengthen the bond with applied agents, e.g., inks. It also has to strengthen the cohesively weak boundary layer (Wampler 1989; Migdal and Schreiber 1995).

2.2.1 Adhesion

Adhesion is bonding between two dissimilar surfaces that can be divided into three types including specific adhesion, mechanical adhesion and effective adhesion. Specific adhesion is molecular level interaction between two-contacted surfaces whereas the mechanical adhesion is

resulted from a mechanical interlocking between the surfaces. In addition, effective adhesion is combination of specific and mechanical adhesion where there are both molecular bonding and mechanical interlocking between the surfaces. It can be concluded that the strength of adhesion between two surfaces depends on their interactions; therefore, many parameters can affect the surface adhesion that will be explained in the following sections (Wake 1978; Kinloch 1980; Packham 1992; Fourche 1995; Allen 2000).

2.2.1.1 Chemical adhesion

There is a chemical adhesion when two-contacted surfaces produce a strong interaction by ionic or covalent bonds or by weaker hydrogen bonds. The hydrogen bond is formed when a hydrogen atom of one material is attracted to another atom, an electron donor, such as oxygen. Therefore, chemical adhesion is a kind of adhesion when two surfaces (adhesive and adherent) form ionic, covalent or hydrogen bonds. It is also demonstrated that the bond length of the adhesive forces must be large enough in addition to having high strength and make a stable bond between two surfaces. Figure 2-2 shows the bond energies and bond lengths of adhesive forces (Fourche 1995; Marshall, Bayne et al. 2010).

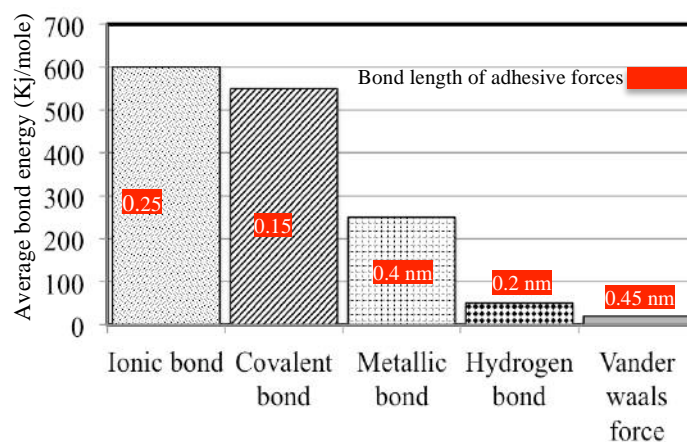


Figure 2-2: Bond energies and bond length of adhesive forces.

2.2.1.2 Dispersive adhesion

Dispersive adhesion is an adhesion between polar and non-polar surfaces. In this kind of adhesion, van der Waals force holds the surfaces together. The molecules are polar with a region of negative or positive charge and the polarity is a transient effect because of random electron motion within the molecules and then the electron will be concentrated in one-region known as London forces. However, the length of van der Waals bond is longer than the other forces (see Figure 2-2), it is not long enough for all distances and it acts over small distances at the range of a nanometer. It is shown schematically in Figure 2-3 how the dispersive adhesion is produced between two materials (Fraunhofer 2012; Shan, Du et al. 2012).

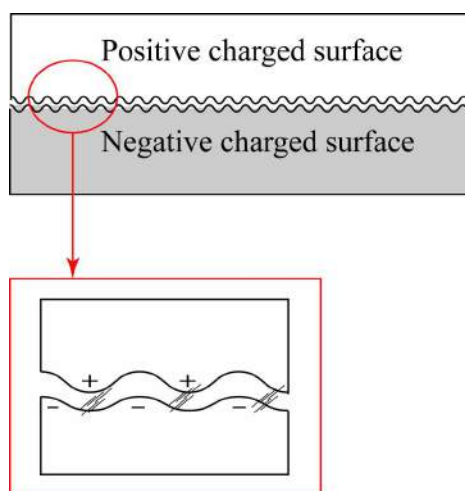


Figure 2-3: Schematic illustration of dispersive adhesion between two surfaces.

2.2.1.3 Diffusive adhesion

Diffusive adhesion may be formed when both contacted materials are soluble and mobile in each other at the molecular level. However, the polymer chain mobility strongly influences the molecular diffusion at the material interfaces. Cross-linked polymers are not able to diffuse as much as non-cross-linked polymers due to their restricted mobility. A stronger adhesion between two surfaces is achieved when there is enough time and the surfaces are allowed to interact by the

diffusion process. Figure 2-4 schematically shows the diffusive interaction between two surfaces (Hong, Chang et al. 2011).

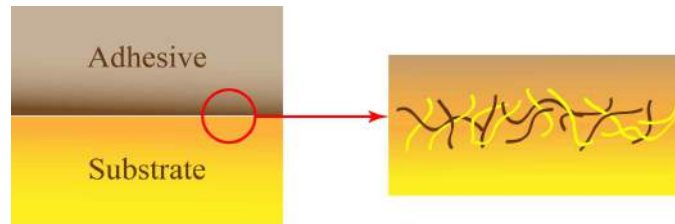


Figure 2-4: Schematic illustration of diffusive adhesion between two surfaces.

2.2.1.4 Mechanical adhesion

Mechanical adhesion occurs when one material flows on a solid material with rough and porous surface and penetrates into the cavities. In this mechanism, the adhesion is due to the interlocking of the coated material with the target surface. The materials may attach on the surface even without chemical compatibility with the surface. It is believed that roughness can increase the surface area, which produces more molecular bonding interaction. Some researchers noted that the roughness factor should be combined with some other forces to make strong bond and adhesion between two materials. Mechanical interlocking is referred to as micromechanical adhesion as shown in Figure 2-5 (Packham and Johnston 1994; Biresaw and Carriere 2001).



Figure 2-5: Schematic image of mechanical interlocking between adhesive and substrate due to solid rough surface.

2.2.2 Wettability

Wetting is a process of spreading a liquid across the surface of a solid to produce a uniform and continuous surface. Wettability is determined by a balance between the adhesive and cohesive forces. The liquid spreads upon the surface of the solid when the adhesive force between the solid and liquid overcomes the cohesive forces within the liquid (Lee, Khang et al. 2003).

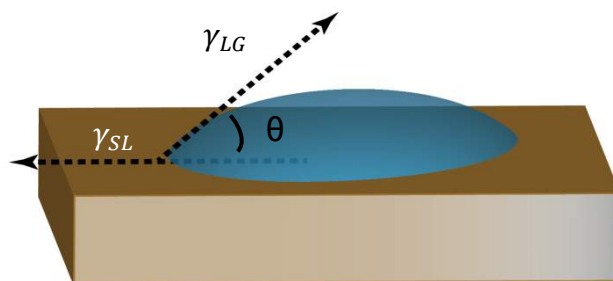


Figure 2-6: Sessile drop on a surface indicating.

Gluing, painting, inking and washing are good examples for practical situations where a good contact is sought between a liquid and solid. The good interaction between ink and solid surface is achieved when it wets and makes a strong adhesion to the surface. Measurement of the contact angle between a solid and a liquid is a technique to measure the ability of the liquid to wet a surface. A contact angle of 0 degree indicates a complete wetting and the liquid will cover a surface, while a contact angle of 180 degrees indicates the liquid form a bead on a surface. Generally, the wetting phenomenon is defined differently for two kinds of surfaces; smooth surfaces and rough surfaces. Figure 2-6 shows schematically a contact angle of a liquid drop on solid surface.

The contact angles are generally measured to evaluate a surface tension of the solid since it is not possible to be measured directly. Therefore, the calculation of surface energy through the contact

angle has been of interest to researchers for many years. Various degrees of wetting are depicted in Figure 2-7 (Good 1993; Kato, Uchida et al. 2003; Marmur 2003; David and Neumann 2013).

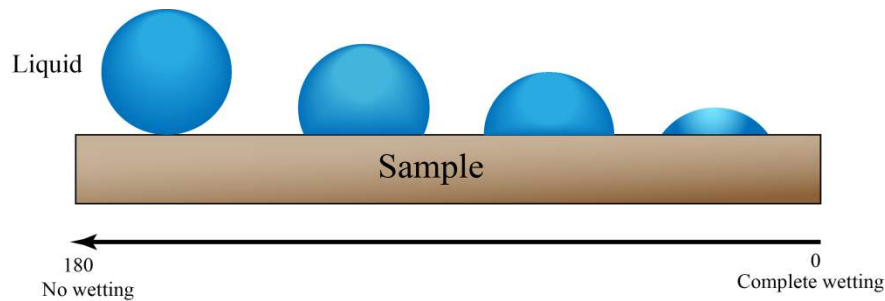


Figure 2-7: Schematic image of wettability and contact angle.

2.2.3 Surface tension and surface energy

Surface tension is a thermodynamic parameter that plays an important role in numerous industrial processes. Three interphases are involved in the interactions at the interface between a liquid and solid: the liquid-vapor, the solid-liquid and the solid-vapor interfaces. The spherical shape of the liquid drop is changed to spread across the surface of a solid and wet the surface. Work is needed in order to change the drop shape and also reshape it. This work per unit area is called surface tension. Surface tension is usually expressed as dynes/cm or it is given in SI units of N/m or J/m² (Hansen, 2004). In fact, each interface has an associated surface tension (γ), which represents the energy required to create a unit area of that particular interface. Since it is not possible to measure the surface tension of a solid film directly, contact angle is used as an indirect approach for this purpose. The contact angle (θ) between a drop of liquid and the surface of a solid corresponds to the surface tensions of the three interfaces as the Young's equation:

$$\gamma_{lg} \cos \theta = \gamma_{sg} - \gamma_{sl} \quad (2.1)$$

where γ_{sg} , γ_{sl} and γ_{lg} are the surface tensions of solid-gas, solid-liquid and liquid-gas interfaces respectively. Figure 2-8 shows the liquid solid interfaces in different conditions of liquid wetting.

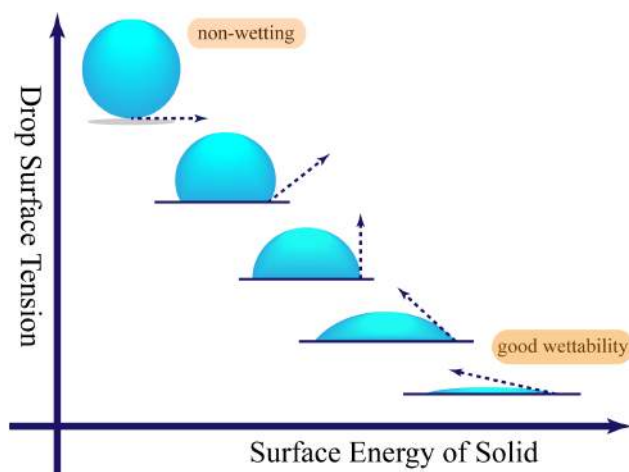


Figure 2-8: Liquid solid interfaces.

Surface tension of untreated polymer surfaces is around 30 mN/m at 25 °C. With polymer with a surface tension less than 37 mN/m, it is not possible to achieve good adhesion and consequently there is a problem with spreading of liquids upon the surface (Wu 1974; Gao, McCarthy et al. 2009).

Fox and Zisman created the concept of critical surface energy theory in 1950. They introduced a linear relationship between the surface tension of a series of liquids and cosine of the advancing contact angle. In the Zisman theory, the surface energy is determined using critical surface tension (γ_c), which differs from the quantity of γ_s . The concept of the Zisman theory is based upon wetting the surface with a liquid with a surface tension less than or equal to its surface tension.

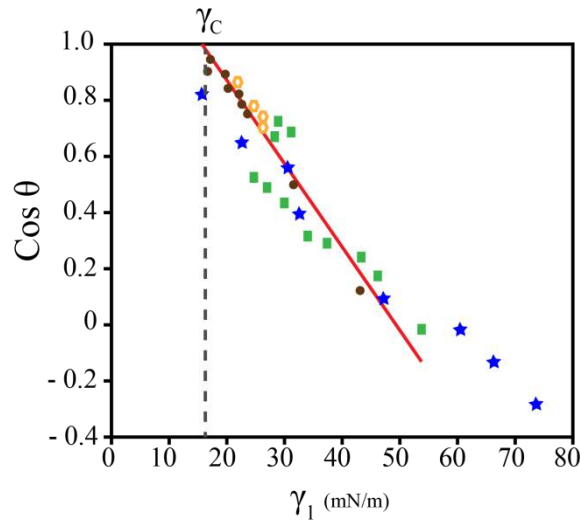


Figure 2-9: Typical graph of Zisman plot to obtain critical surface tension with a series of liquids.

In other words, the liquid/solid interfacial tension must be equal to zero ($\gamma_{SL} \approx 0$). In order to find the γ_c value, a series of contact angles are measured using different liquids with progressively smaller surface tensions. Then the plot of surface tension of the liquids versus cosine value of the corresponding contact angle is prepared. The solid line of the best fit for the measured points is extrapolated to intersect with the value of $\cos \theta = 1$. As shown in Figure 2-9 (typical Zisman plot), the perpendicular line to the x-axis at the point of the intersection (dashed line in Figure 2-9) drawn to the x-axis, obtains a value of γ_c . At present, however, it is not commonly applied, mainly because of insufficient theoretical justification and time-consuming investigation procedures (Kinloch 1987; Zenkiewicz 2007).

Fowkes and his group developed a theory in 1962, which defines the surface tension as a sum of the independent terms. They represent particular intermolecular forces such as polar (p) and dispersion (d). The combination of the equations results in determination of the surface energy by the properties of two liquids (polar and dispersion surface tension) and the contact angle of the two liquids with the solid surface as follows:

$$\frac{(\gamma_{IA}^d)^{1/2}}{\gamma_{IA}} (\gamma_S^d)^{1/2} + \frac{(\gamma_{IA}^p)^{1/2}}{\gamma_{IA}} (\gamma_S^p)^{1/2} = \frac{\gamma_{Sl}(1 + \cos\theta)}{2} \quad (2.2)$$

$$\frac{(\gamma_{IB}^d)^{1/2}}{\gamma_{IB}} (\gamma_S^d)^{1/2} + \frac{(\gamma_{IB}^p)^{1/2}}{\gamma_{IB}} (\gamma_S^p)^{1/2} = \frac{\gamma_{Sl}(1 + \cos\theta)}{2} \quad (2.3)$$

$$\gamma_S = \gamma_S^p + \gamma_S^d \quad (2.4)$$

where γ_{IA} and γ_{IB} are the surface tensions of liquid A and B, respectively, γ_{IA}^d and γ_{IB}^d are the dispersion component of the surface tension of the liquid A and B, γ_{IA}^p and γ_{IB}^p are the polar components of the surface tension of the liquid A and B, γ_S is the surface energy of the solid, γ_S^d and γ_S^p are the dispersion and polar components of the surface energy of the solid and γ_{Sl} is the interfacial tension between the solid and liquid.

This equation set is solved for $(\gamma_S^d)^{1/2}$ and $(\gamma_S^p)^{1/2}$ and γ_S will be obtained from Eq.(2.4).

Usually, one polar (e.g., water) and one nonpolar (e.g., methylene iodide) liquid are used. This method is commonly called ‘two-liquid method’. Fowkes method is being used in many laboratories for the determination of the surface free energy of polymers (Fowkes 1968; Kinloch 1987; Zenkiewicz 2007).

2.3 Printing

2.3.1 Printing methods

Nowadays, printing is widely used technique to decorate and display information on objects in the presentation of many products. This approach is being used with impressive success at various scales on many different surfaces ranging from aluminum cans and plastic bottles as well as paper. Water and solvent base inks are used in different applications such as packaging systems, which the printing process is an important step in the development of the final products.

Seven major methods are employed for printing on the solid materials including Letterpress, lithography, gravure, flexography, electrostatic printing, silkscreen printing and ink-jet. These techniques can be utilized for different kinds of surfaces depend on their applications and are as follows:

- a) On plastic films: flexographic and rotogravure printing
- b) On paper, paperboard and multilayer paperboard: flexographic, rotogravure and also sheet feed lithography

Ink-jet is used mainly for information, which may change as the expiry dates, manufacturing details and etc. (Leach and Pierce 1993; Kahn and Kahn 2008).

2.3.2 Printing Inks

The ink formulation comprises a variety of materials. Choosing the substances for given ink are dependent on many factors such as:

- a) The printing process
- b) The type of printing press used
- c) Printing speed being applied
- d) The type of the substrates

Figure 2-10 shows all printing ink components. As shown in this figure, the inks are divided into two main different components: Colorant and vehicle that will be explained in the following sections (Leach and Pierce 1993; Micheli 2000).

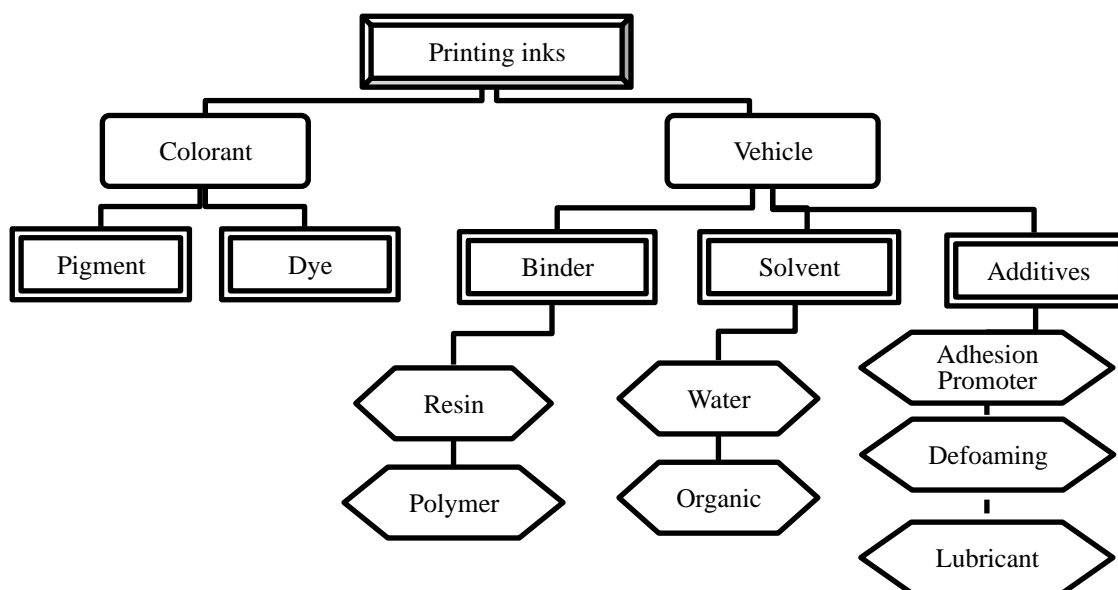


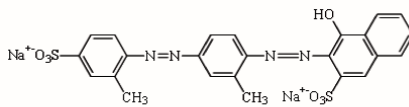
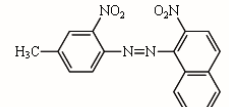
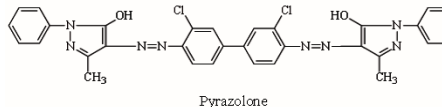
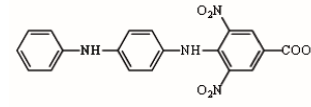
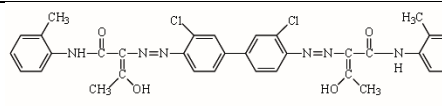
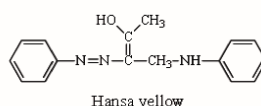
Figure 2-10: Printing ink components.

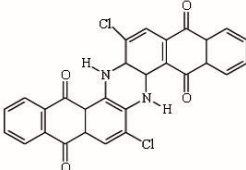
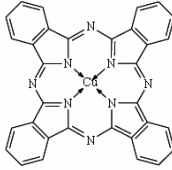
Colorants are classified into pigments and dyes. They are substances that impart colour to materials. The term “colorant” is often used for both dyes and pigments. They are obtained from both natural and synthetic sources and can be further subdivided into the chemical types: organic and inorganic. The most used colorants in inks are organic and synthetic origin. Dyes and pigments have main difference in terms of their interaction with liquids, which is called solubility (the tendency to dissolve in a liquid). Dyes are usually soluble—or can be made to be soluble—in water or other solvents. Depending on the type of printer, inks could be categorized into two common types including dye-base and pigment-base. The type of the used ink will allow us to have photo prints, black and white text, or colour graphics. In order to develop the colour strength on the target surface, the dyes must be dissolved into the vehicle, whereas in using the pigment, it should be dispersed within the vehicle (see Figure 2-11). Pigments are used in the majority of printing inks rather than dyes. For some of the printing inks, called semi-pigmented inks, a few which contain pigments, are mixed with dye. To dissolve the pigments in water, oil, or other solvents, they should be first ground into a fine powder and thoroughly mixed with the

vehicle. The mixture is then spread on the material to be coloured. Therefore the pigment is held in place on the material after drying and dispersing on the surface (Svanholm , Mendel, Bugner et al. 1999; Pekarovicova, Bhide et al. 2003; Desie, Deroover et al. 2004). Table 2.2 is a list of common pigments that are used in the printing inks (Warson 1991; Allen, Segurola et al. 1999; Micheli 2000). All major difference between pigments and dyes used in ink printing can be categorized as follows:

- Pigments are dispersed in the medium while dyes are dissolved.
- Pigments can control some particulate properties of the ink such as light and heat resistance, while dyes do not.
- The ink containing pigments are more resistant to fading than dyes (Zollinger 1987).

Table 2.2: Common printing ink pigments (Kroschwitz 1999).

Class	Example	
Inorganic white (opacifiers)	Titanium dioxide (TiO ₂) - in either rutile or anatase form	Zinc oxide (ZnO)
Extenders	Calcium carbonate (CaCO ₃)	Talc - mixed oxides of magnesium, Calcium, Silica and aluminum
Inorganic black	Carbon black	
Organic red	 Lithol (C.I. 26670 ³)	 Toluidine derivative (C.I. 12120)
Organic orange	 Pyrazolone (C.I. 21110)	 Dinitroaniline (C.I. 10390)
Organic yellow	 A di azo pigment (C.I. 21095)	 Hansa yellow (C.I. 11660 derivative)

Organic green	Phthalocyanine green	PMTA
Organic blue	 Indanthrene (C.I. 69825)	 Phthalocyanine blue (C.I. 74160)

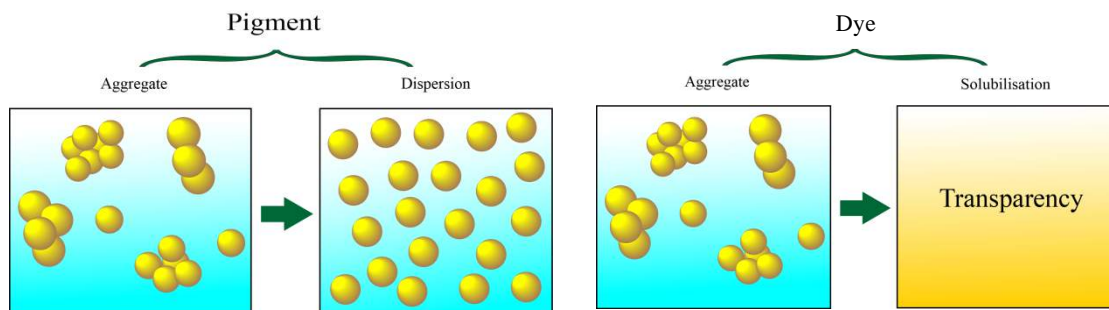


Figure 2-11: The difference between pigments and dyes.

The liquid portion of the ink to carry the pigment to the substrate is called vehicle. The main job of the vehicle is to hold the pigment on the surface and provide many desirable properties. Therefore, the vehicle composition can change the characteristics of the ink (Cantu 2009).

A material is needed to bind ink components one to another and therefore to the substrate. Binder, is a resin that holds the paint together once it has dried. Different types of resins are utilized to modify the physical and chemical properties of the printing ink and categorized into two basic classifications: natural and synthetic. The major usage of the natural resin is found in lithographic and letterpress inks. In the other hand, synthetic resins are the type of resins, which can impart special characteristics to ink. The most common used synthetic resins are listed as follows:

- a) Acrylic resins, which has excellent adhesion to packaging films through flexographic, gravure or screen inks process
- b) Vinyl resins, which is usually used in screen inks
- c) Maleics for using in lithographic and flexo inks
- d) Polyamides, which are used in flexographic and gravure inks
- e) Epoxy resins for using in offset metal decorating inks

Two or more of these resins can be mixed to capture the desired and specific characteristics (Lin 1990).

The ink must be liquid to be transferred easily to and be printed upon the surface. The role of solvents is keeping the ink liquid during the printing process. At the target surface, the solvent must be separated from the ink components to allow the colorant to bind to the surface. The solvents dissolve the solid components of the inks before being used in printing inks. The solvents or diluents are selected based on many factors including the type of ink being manufactured (pasty or liquid), the substrate, drying mechanism, the volatility and the evaporation speed (drying time of ink film). Important examples of solvents include:

- a) Toluene, Xylene, Acetone
- b) Mineral spirits
- c) Methyl Isobutyl Ketone (MIBK), Methyl Ethyl Ketone (MEK)
- d) Propyl acetate, Isobutyl acetate

- e) Methoxy propanol, Ethoxy propanol, Methanol, Ethanol, Iso-propanol, n-propanol
- f) Water

We can conclude that a solvent and a binder are required for printing inks as a complex. The most common combinations of binders and solvents using in different printing techniques are listed in Table 2.3 (Ozman 2008).

Table 2.3: Combinations of binders and solvents for different printing methods (Ozman 2008).

Process	Binder	Solvent
Newsprint	Hydrocarbon resins, e.g. asphalt	Mineral oil
Offset	Drying oils, alkyd resins, modified rosin, hydrocarbon resins	Mineral oil
Metal decorating	Alkyd resins, melamine resins	Mineral oil
Publication, gravure	Modified resin, hydrocarbon resins	Toluene
Flexography, packaging gravure	Polyvinyl acetate, polyamide resins	Alcohols, Esters, Ketones, mineral spirits
Water based flexo, packaging gravure	Maleic resins, acrylic resins, shellac	Water, Alcohols

Additives are materials, which can greatly affect the performance of the ink with the desired properties. It is usually part of the confidential information of ink manufacturer companies. The most known additives include optical brighteners, driers, anti-skinning agents, thixotropy promoters, adhesion promoters, surfactants, plasticizers, defoaming agents, biocides, deodorants and micro-encapsulated perfumes (Saad 2007).

2.3.3 An example of printing ink formulation for polymer surface

Since this study is concentrated on improving the PET surface properties in terms of printability, it is appropriate to have a practical example of printing ink on a kind of polymer surface. As the

ink formulation used for printing on polyethylene film is available, we have tabulated it in table 2.4 that might be useful for other applications as well.

Table 2.4: Flexographic ink for polyethylene film (Saad 2007)

Ingredient	Function	Amount (%wt)
Titanium dioxide	White pigment and opacifier	35
Alcohol soluble nitrocellulose	Resin	5
Alcohol soluble polyamide	Resin	15
Dibutyl phthalate	Plasticizer	1
Polyethylene wax	Prevents damage to the ink Film from rubbing	1
Amide wax	Prevents damage to the ink Film from rubbing	1
Ethanol	Low boiling point solvent	30
n-propyl acetate	Low boiling point solvent	8
n-propanol	low boiling point solvent	4

2.3.4 Ink drying and curing

After applying the ink on the surface of the medium, it must adhere to the surface properly. This can happen simply as a result of the ink drying, or can take place by cross-linking process and polymerization reactions that form a film and bind the ink to the printed surface. It is important to understand the difference between "drying" and "curing". However, after printing, the ink may become dry to the touch, but must achieve full internal curing to obtain durability (Cantu 2009).

2.3.5 Problems frequently encountered during the ink printing on surfaces

Regarding ink printing process on surfaces, sometimes there is a poor bonding over the film surfaces due to the following reasons:

- a. Unsuitable binder for selected substrates
- b. Surface active slip additives in the inks

- c. Low substrate surface energy (Inadequate surface treatment of film)
- d. Incorrect ink for selected substrate
- e. Incomplete curing
- f. Ink or primer not completely dry

In order to find the durable printed ink on the surfaces, only one important parameter is associated to the substrate. The substrate must have appropriate properties in term of surface energy and functionality (Blythe, Briggs et al. 1978).

2.3.6 Mechanism for bonding between polymer surface and inks

The ink composition contains the solvent, colorant, vehicle and additives. As explained in the previous sections, nowadays, pigment base inks are usually utilized to have durable ink printing on surfaces (especially polymer surfaces). Pigment-based inks provide printouts with particles of pigment spread throughout the polymer surface. The colors become more durable to external forces like evaporation or oxidation.

In order to obtain good printing on the surface of polymers, two steps including spreading and bonding must be met. In the first step, the ink must be spread out completely on the surface. Among the ink components, vehicle plays main role in this phenomenon. Alcohols, ester and ketones are the commonly used solvents for the ink printing on polymer surfaces, whose surface energy is less than 40 dyne/cm. In order to get good and stable printing, the magnitude of surface tension of a polymer must be at least 10 units greater than the surface tension of the vehicle while the surface tensions of the most common used vehicles are less than 40 dyne/cm. The next step is bonding between the ink and substrate. This adhesion is due to chemical bonding between these

materials and target surface. Adhesion promoters are often used in ink formulation to improve adhesion of the ink to the substrate.

2.4 Molecular bonding mechanism for adhesion

The molecular bonding between two materials is due to intermolecular forces such as van der Waals¹, dipole-dipole interaction² and chemical interaction between the substrates. We review some articles showing a relationship between the hydrophilic³ properties of the surface and the polarity, which can be the factors to obtain a good adhesion. Figure 2-12 shows schematically the intimate contact between two substrates, which is essential for their surface adhesion. The adhesion, which occurs at the interfaces by chemical bonding, is stronger than the one with other methods. In this mechanism some bridges are made between the substrates through the interaction of the chains. In fact, a suitable functionality is necessary for this kind of interaction (Awaja, Gilbert et al. 2009). In order to achieve high adhesion strength, it was found that roughness is one important factor due to the mechanical interlocking of the polymer surface. In some applications such as polymer-paint interface, using an adhesion promoter can also increase the adhesion.

1 Van der Waals forces include attractions between atoms, molecules, and surfaces

2 Dipole-Dipole interactions are caused by permanent dipoles in molecules.

3 A hydrophilic molecule or portion of a molecule is one that is typically charge-polarized and capable of hydrogen bonding, enabling it to dissolve more readily in water than in oil or other hydrophobic solvents.

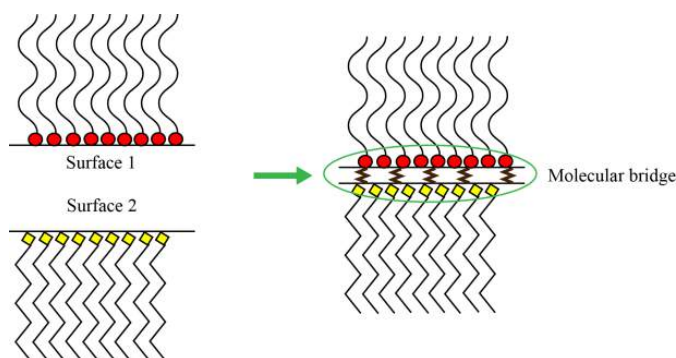


Figure 2-12: Schematic illustration of Molecular bonding between two surfaces

Tyzor titanates and zirconates have been designed to be utilized as an adhesion promoter in the existing ink formulation. The binder and substrate must contain functional groups (e.g. -OH, -COOH) to achieve a reaction with the titanate or zirconate. The diagram below (Figure 2-13) illustrates how the titanate cross-links the polymer chains and increases adhesion to the substrate (Zollinger 1987; Fourche 1995).

Although some adhesion promoters improve the adhesion to many substrates, plastic substrates require prior surface modification in order to create reactive functional groups at the contacting surface.

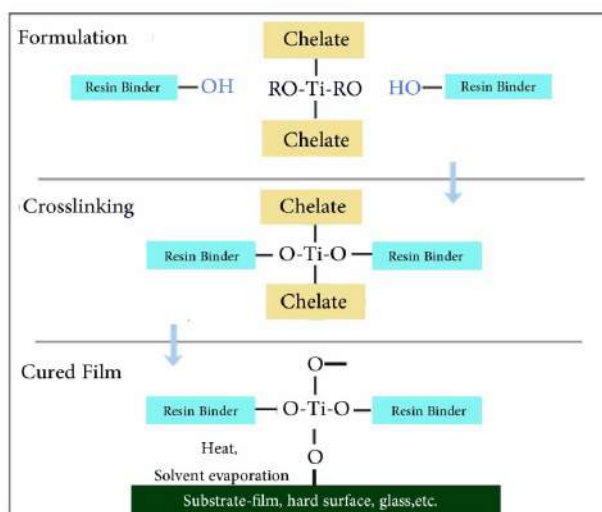


Figure 2-13: Mechanism of adhesion promoter bonding (Awaja, Gilbert et al. 2009).

2.5 Surface treatment and modification

The treatments are applied at the surface of the polymeric objects to generate well-defined and active surfaces with an affinity for the coating. The surface energy (γ) of modified surface must also be sufficient and prepared for coating liquids to be wet and spread out. This condition is fulfilled when the surface energy of the solid is larger than the surface energy of the liquid ($\gamma_s > \gamma_l$). It is known that the surface energy of most polymers are in the range of 15 to 40 mJ.m⁻². smaller than the surface energies of the most commonly used organic solvents. In order to increase the surface energy of polymers, several methods are used as surface modification techniques. These kind of treatments are classified in two main categories as listed in Table 2.5. (Awaja, Gilbert 2009)

Table 2.5: Surface modification methods (Awaja, Gilbert 2009)

Kind of treatment	Example
Physical modification	Flame treatment
	Corona treatment
	Cold plasma treatment
	Hot plasma treatment
	UV treatment
	Laser treatment
	X-ray and γ -ray treatment
	Electron beam treatment
	Ion beam treatment
	Metallization
	Sputtering
Chemical modification	Wet treatment
	Surface grafting

2.5.1 Physico – chemical treatment

The physical modification of polymer surfaces can be introduced in two categories including chemically altering the surface layer and depositing the other external layer on top of the main polymer surface. This kind of treatment has been used in industry to date. This technique is applied for polymer materials to increase the dyeability and printability or generally for improving the adhesion property of the surfaces.

Flame treatment is usually used to introduce oxygen-containing function at polymer surfaces. In this method, the substrates are exposed to the flame of a burner with a fixed air/gas mixture in order to obtain a stable and oxidizing flame. The most commonly used gases in this method are methane, propane or butane. The technique is quite simple: it consists of a flame, which is held at a fixed distance from the sample. It also can scan the surface at controlled speed. Polyolefins are the most frequently used materials in flame treatment method. For example Figure 2-14 shows the variation of surface energy of polyethylene as a function of flame treatment time (Brewis 2002; Desai and Singh 2004; Goddard and Hotchkiss 2007).

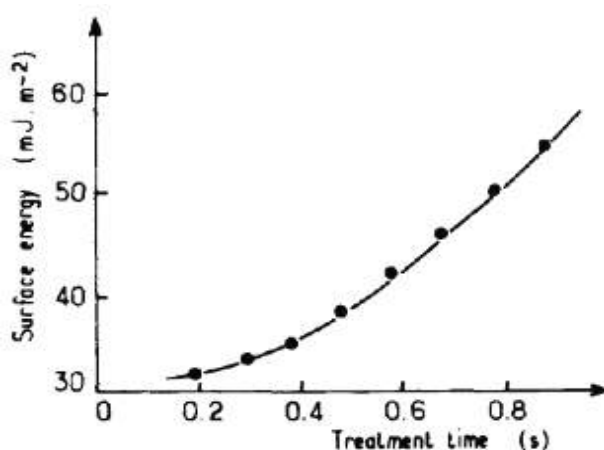


Figure 2-14: Variation of surface energy of polyethylene by flame treatment (Brewis 2002)

The corona discharge technique utilizes the formation of high-energy electromagnetic fields near to specific points with consequent ionization of their adjacent area. It can be done even in atmospheric pressure and low temperature. The apparatus consists of an electromagnetic field generator thin wire and the important variables are electromagnetic properties such as voltage, frequency and electrode geometry. The corona discharges have been used industrially for many years to treat polymeric films, fibers, and flat objects. This process is especially used for polyolefin (polyethylene and polypropylene) and some polyesters (polyethylene terephthalate). The electrical discharge between two electrodes is obtained under atmospheric pressure from a high voltage alternative current as shown in Figure 2-15 (Ozdemir, Yurteri et al. 1999; Abbasi, Mirzadeh et al. 2001; Brewis 2002). The electrons generated in the discharge impact the surface of polymer placed in the discharge path. They have enough energy to break the molecular bonds and create very reactive free radicals on the surface. These free radicals in the presence of oxygen can form various chemical functional groups, which are the most effective at increasing surface energy and enhancing chemical bonding to the other material like inks and paints. These include carbonyl ($-C=O-$), carboxyl ($HOOC-$), hydroperoxide ($HOO-$) and hydroxyl ($HO-$) groups.

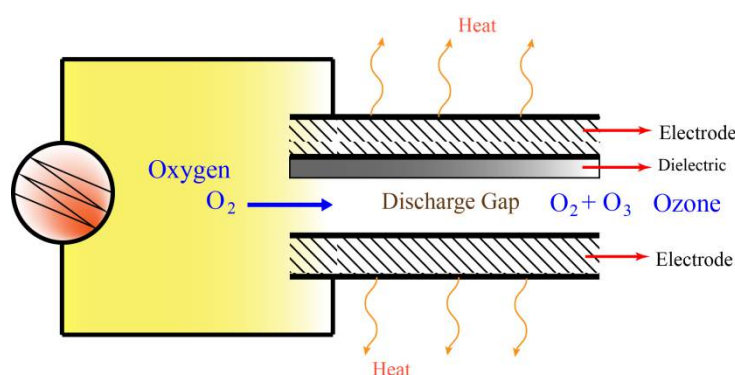


Figure 2-15: Schematical diagram of corona discharge generator

Plasma is an ionized gas generated in a high-voltage electric field in a vacuum. Depending on the nature of the plasma gas, the surface energy will be either increased or decreased. Therefore,

using oxygen, nitrogen, ammonia, argon or helium gases causes increasing of surface energy. The main difference between plasma and corona treatment is using a vacuum in the plasma technique thus the vacuum chamber in the apparatus set up (Figure 2-16) is essential. This chamber is needed to maintain a suitable pressure and composition of the required gas. The most applications of plasma treatment are in the field of biomaterial to allow coating of some specific materials. It is often utilized in microelectronic fabrication technology usually to etch inorganic⁴ (silicon, silicon dioxide) surfaces and much less frequently for organic materials. Many papers have been dedicated to the effect of non-polymerizing plasma on surface chemistry, which is related to printability and adhesion on the surface of polymers. In addition, plasma has more degree of freedom such as selecting the required gas and some processing parameters (pressure, gas flow rate and etc.) in comparison with corona treatment (Ozdemir, Yurteri et al. 1999; Aouinti, Bertrand et al. 2003).

Low wavelength photons are energetic species, which are usually used to activate many chemical reactions. Polymer surfaces are treated through UV using a UV lamp. Cross-linking by activated photons and also fragmentations of polymer coating are two kinds of most-common application of this treatment. The wavelength of the UV lamp is approximately 250-400 nm in this application.

Lasers are source of photons, which are characterized by high intensity energy. The application of these photon sources is like other techniques for promoting cross-linking or scission effects. The apparatus is also similar to the UV treatment apparatus (Nahar, Naqvi et al. 2004; Situma, Wang et al. 2005; Xing, Deng et al. 2005).

⁴ Silicon, silicon dioxide

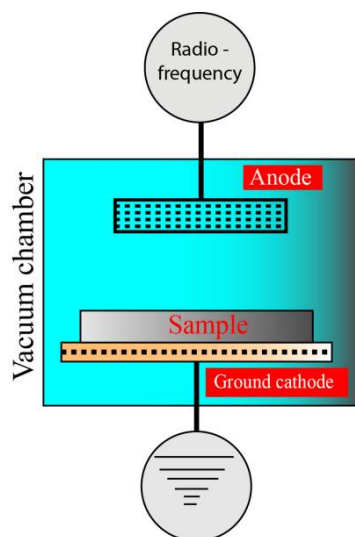


Figure 2-16: Parallel plate system for cold plasma treatment in a vacuum chamber. There are two electrodes: the anode, which is polarized with the radiofrequency, and the grounded cathode. The plasma is formed between the two electrodes and results in the formation of excited species, which then act on the surface of the sample.

The main application of the X and γ -ray treatments is similar to UV for cross-linking of polymeric coating. High-energy photon causes the formation of radical sites at surfaces in the presence of oxygen. They can react with atmospheric oxygen forming oxygenated functions. Most literature publications involve the study of chemical effects of radiation exposure or radiation-induced curing of coating (Ozdemir, Yurteri et al. 1999).

High energy electrons are used to cross-link the macromolecular chains for many applications such as tubing, curing of coating and cables due to possessing high mean free paths, which are more than 100 micrometers up to a few millimeters

The metallization and sputtering technique involves coating of polymer surfaces by a layer of metal. The coating process takes place by evaporation of metal and depositing on the surface. For example, in industry, some polymers are coated by aluminum for electrical or packaging applications like decorative. Sputtering is another coating method to change the surface

properties by depositing on polymer surface but without evaporating because sometimes evaporation is not possible. It is used to create ions and accelerating them on a target, forming atoms and deposit them on the target surface (Ozdemir, Yurteri et al. 1999; Situma, Wang et al. 2005).

2.5.2 Chemical modification

Chemical modification is a surface modification by altering the surface chemical composition of the polymer by direct chemical reactions. These reactions can be performed in the given solution environment or also by covalent bonding of appropriate molecular chains to the polymer surface (grafting). The chemical modification is divided into categories: wet treatment and surface grafting.

Wet treatment was a first modification technique used to improve the polymer surface properties. Since this method is applied to change the surface chemical composition of the polymer, having an appropriate knowledge of the general chemistry is an essential need to design the suitable processing conditions. Furthermore, the functional groups reactivity depends on the solvent-polymer interaction. Therefore, enough information about the solvents and their functional groups activities are required. In fact the main goal of this modification is to create well-defined functional surfaces. Sodium etching, oxidizing, hydrolysis of esters (see Figure 2-17) are the most common wet treatments of polymeric surfaces (Ozdemir, Yurteri et al. 1999; Situma, Wang et al. 2005).

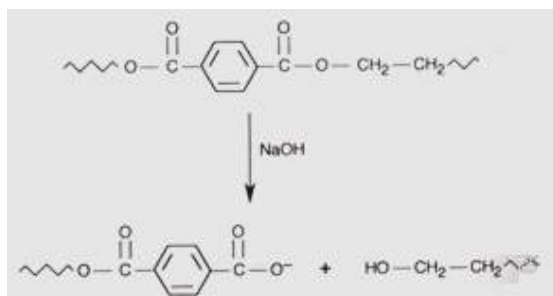


Figure 2-17: NaOH attack on PET chains (Situma, Wang et al. 2005).

The new surface properties of the polymers can be achieved by covalent bonding of some other macromolecule on the surface of the main polymer. This fundamental step can be carried out chemically or by irradiation. The grafting process involves chemical linking to the substrate and polymerization of the chains. Figure 2-18 shows the schematic of the grafted surfaces made by direct polymer coupling and graft polymerization (Uyama, Kato et al. 1998; Coad, Lu et al. 2012).

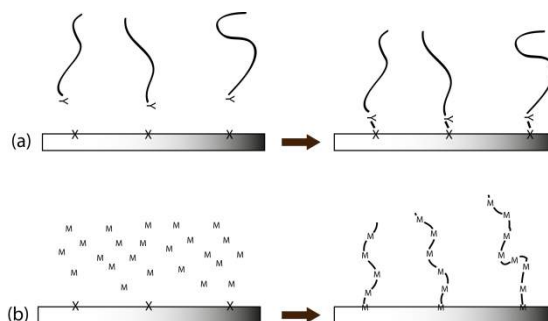


Figure 2-18: Creation of grafted surface by: a) direct polymer-coupling reaction; b) graft polymerization.

2.5.3 Bulk modification

In this surface modification method the surface structure is arranged through the bulk multi-component polymeric system. The relationship between the bulk and the surface structure of macromolecular system is considered in bulk modification study. It was mentioned previously that the surface composition is changed and modified by the external treatment (plasma, grafting,

etc.), whereas in the bulk modification method the surface composition is designed by the presence of the specific components resulting of their migration from the bulk of the polymer blend to the surface.

Blending of polymers is interesting way to improve the bulk properties. The polymer blending has been described in a lot of articles and books but the knowledge on the polymer surface through blending is much less considered. Recently some publications have discussed the several variables affecting the nature of the blend and polymer surface. Many articles also have described the effect of block copolymers on polymer surfaces with respect to their bulk properties (Li, Andruzzi et al. 2002).

It has long been known that low molecular weight additives blended in a polymer host might migrate to the surface of the host polymer under the shear field in melt processing equipment (Li, Andruzzi et al. 2002; Andruzzi, Hexemer et al. 2004). Such migration is a powerful mechanism to transport many desired materials with suitable functional groups to polymer surfaces during normal melt processing. The migration method is highly attractive because it utilizes physical processes to design and modify the chemical make-up of polymer surfaces and therefore does not require extra processing steps or new equipment. Furthermore, some specific surface properties could be imparted by flow-induced migration such as adhesion, printability, biocompatibility and lubricity. However, traditional surface modification methods have the drawbacks of requiring extra processing steps and providing little control over the resulting non-equilibrium surface structure and also no uniformity of modification. The problem is more pronounced when the shapes of the object is complex. It has been well known that in multi-component polymeric systems, the component with lower surface free energy preferentially migrates to the air/polymer interface in order to minimize the interfacial free energy.

Two objectives can be considered with respect to surface modification of polymers: increasing the surface energy and surface potential (e.g. adhesion promotion) or decreasing the surface energy and surface interaction with a given material. In general, we can say that all surface modification methods share a common goal to control the number of chemical functional groups⁵ at the polymer surfaces.

If decreasing of surface energy is the goal of the modification, some specific functional groups (low energy) are desired at the surface such as $-\text{CH}_2-$, $-\text{CH}_3$, $-\text{CF}_2-$ and $-\text{CF}_3$ and the interaction is only London dispersive⁶. Such low energy functional groups would like migrating to the surface due to the fundamental thermodynamic theory. In order to get a high-energy surface, the specific high-energy functional groups or some nature reactive materials have to be delivered to the surface. For this goal of modification the incorporation of dipole-dipole interaction or hydrogen bonding can increase the thermodynamic work of adhesion.

Additionally, the control of the stability of the additives at the surface of polymer is one of the important steps within the modification process. Because surfaces are intended thermodynamically to lower their surface energy, therefore the high-energy surfaces created by the treatment methods are often unstable and susceptible to reorganization processes resulting in rapidly loss of surface functionality (Li, Andruzzi et al. 2002; Andruzzi, Hexemer et al. 2004).

5 Functional groups are specific groups of atoms within molecules that are responsible for the characteristic chemical reactions of those molecules.

6 The London dispersion force is the weakest intermolecular force. The London dispersion force is a temporary attractive force that results when the electrons in two adjacent atoms occupy positions that make the atoms form temporary dipoles.

It is desired to use of functional polymers as additives due to cost and kinetic factors that can affect on polymer surface by blending with nonfunctional polymer host. Surface-active block copolymers are perhaps the best-known examples of this class of additives.

In order to create a high-energy polymer surface, adding a small amount of polymer containing high-energy functional group cannot segregate to the surface. In fact, high-energy functional groups of additive molecules would not be located in the subsurface layer but would be dispersed throughout the polymer matrix. The solution for this problem is the use of a surface delivery vehicle, which can deliver high-energy functional groups to the surface. The simplest molecular design for a surface delivery vehicle is an end-functional block copolymer. The one side of this block copolymer comprises the same polymer as the substrate or a polymer that is miscible with the polymer substrate and the other block of the copolymer is a surface-active that causes the entire molecule to segregate preferentially to the surface. (Koberstein, Duch et al. 1998; Anastasiadis, Retsos et al. 2003; Andruzzi, Hexemer et al. 2004). Figure 2-19 shows illustration of the mechanism by end functional copolymer schematically.

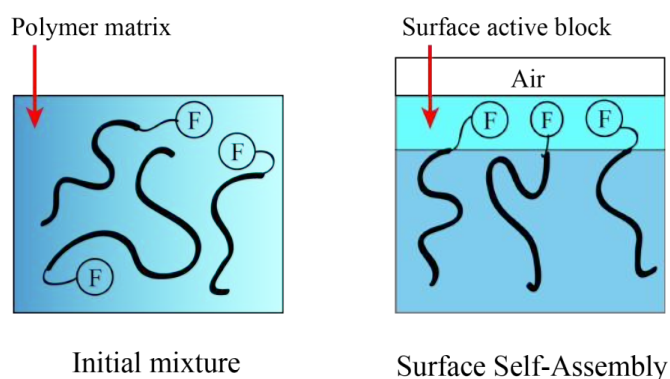


Figure 2-19: Schematic diagram of the self-assembly of a surface-active end-functional block copolymer at the surface of a polymeric substrate at an air–polymer interface and subsequent reorganization when it is exposed to water vapor.

2.6 Migration of macromolecules under flow

The minor phase is dispersed in the bulk of the main polymer during the extrusion process (Figure 2-20). Several factors, such as molecular weight (in the case of two polymer mixtures), compatibility and solubility can result in one-phase or two-phase system. Some enrichment of the additive or polymer in the surface region of the polymer film can occur during the actual film formation in the die. Upon cooling, right after exiting from the die, when the crystalline structure develops, more migration can occur and the minor phase might move to the amorphous region after being pushed out of the crystalline region. However, no studies related to this aspect could be found in literatures.

Experiments indicate that during shear flow, flexible polymer molecules in a matrix migrate away from solid boundaries, leading to the formation of depletion layers and apparent slip at the boundaries.

Schreiber and Storey extruded polyethylene and found more low molecular weight components near the surface of the film compared to the bulk (Schreiber and Storey 1965). Fodor and Hill used a new technique involving dielectric measurements to measure the flow-induced fractionation of polystyrene melt (Fodor and Hill 1992). They observed an increased concentration of fast relaxing species near the wall indicating a buildup of low molecular weight chains. Pangelinan et al. used internal reflection (IR) measurements and found that high molecular weight component were moving away from walls in blends of two different molecular weight polymer melts (Pangelina, McCullough, Kelley 1994). The accumulation of low molecular weight component in the high shear wall region during capillary flow has been observed in all the studies above.

The driving force for the migration of the component is mostly thermodynamic where the component with lower surface tension tends to go to the air/polymer interface to lower the interfacial energy. The mobility of the component, which depends on the size of its domains, compatibility of the component with the host polymer, molecular weight and the environmental factors can influence the kinetics of migration toward the interface.

2.6.1 Thermodynamic theory of migration

Many researchers interpreted the phenomenon of polymer migration as due to the changes in entropy arising out of the deformation of the molecules. Garner and Nissan first proposed that the concentration of the polymer solutions is decreased in a high shear layer next to the pipe-wall (Garner and Nissan 1946). They explained that in a deforming fluid, the macromolecules become stretched and aligned, thus creating spatial free energy differences. Concentration gradients are induced in order to compensate for the spatial variation in the free energy levels. Therefore the polymer molecules migrate towards regions of low stress levels. (Garner and Nissan 1946; Schreiber and Storey 1965)

In addition, the miscibility and mobility of the component influence the kinetic driving force toward the interface. It has been suggested that solubility/compatibility of the minor components with the host polymer, which involve solubility parameters or the free energy of mixing, influence their migration to the air/polymer interface.

The essence is that the thermodynamic theory suggests that the shear gradient drives the polymer toward low shear regions to attain the maximum possible configurational entropy; therefore, the polymer will migrate to the centerline where the local shear rate is minimized. But, in addition to thermodynamic factors, kinetic factors are also important.

2.6.2 Kinetic theory of migration

Dill and Zimm observed radial migration of minor component in a blend during cone and plate flow measurements. They explained that the molecular migration is essentially a result of the curvilinearity of the streamlines by “hoop stress” argument. They also developed an approximate expression for the radial migration velocity (Garner and Nissan 1946).

$$v_m \approx \frac{\eta_s \dot{\gamma}^2}{rk_B T} R_0^5$$

where v_m is the radial migration velocity, r is the radial position, R_0 is the average un-disturbed end-to-end distance of the polymer chains, η_s is the solvent viscosity, K_B is Boltzmann's constant and $\dot{\gamma}$ is the shear rate.

Curtiss and Bird initiated the investigation of polymer migration due to nonuniform velocity gradient fields, in terms of kinetic theory arguments (Curtiss and Bird 1996). They modeled the polymer as linear elastic dumbbell (with end-to-end vector R) suspended in a fluid subjected to non-uniform deformation field (v). They calculated the average velocity of the migration as following expression:

$$\langle v^m \rangle = \frac{1}{8} \langle RR \rangle : \nabla \nabla v.$$

According to Brunn and Chi interpretation, the flux created by polymer migration is balanced by the diffusional flux under the concentration gradient at equilibrium (Brunn and Chi 1984), so established:

$$\frac{\partial}{\partial r} \cdot (nD) = n \langle v^m \rangle$$

where $n(r)$ is the polymer density and D is the translational diffusivity tensor.

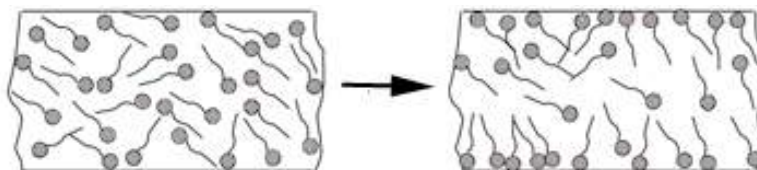


Figure 2-20: A typical image illustrating migration of minor component to the surface during extrusion.

2.7 Polymer blending

Blending of polymers is a promising method for obtaining desirable properties using already known polymers. The performance of polymer blends is controlled by morphology. Certainly, compounding is the critical step in the polymer blends technology (Takayama and Todo 2006; Zhang, Wu et al. 2009). It has to combine the fundamental knowledge of polymer behaviors such as thermodynamic and rheology, inside the mixing machine. The reason for blends include providing materials with extended useful properties by improving the properties of the pure polymers, or by adjusting the processing characteristics and reducing the cost. Most pairs of polymers are immiscible with each other. When immiscible polymers are mixed together they form a two-phase system rather than a single-phase. Several methods can be used to blend the various blend components such as melt blending, solution blending, latex blending, fine powder mixing, mill mixing technique, freeze-drying (Yu, Dean et al. 2006).

2.7.1 Thermodynamic of polymer blends

The phase behavior of the components is the most characteristic of a mixture of polymers. Polymer mixtures can be miscible, immiscible or various levels of mixing in between the extremes (partial miscibility), depending on the properties that are desired. Miscibility is a phenomenon in which changes in thermodynamic parameters are important. The most important parameter, which determines the miscibility of dissimilar components in the polymer mixture, is the free energy of mixing ΔG_m , which is given by the following equation:

$$\Delta G_m = \Delta H_m - T\Delta S_m \quad (2.5)$$

where ΔH_m is the enthalpy of mixing (heat of mixing), ΔS_m is the entropy of mixing and T is the absolute temperature (K). For complete miscibility to occur, two requirements must be met; 1- the free energy of mixing must be negative ($\Delta G_m < 0$). 2- Second derivative of the free energy with respect to concentration must be positive (Eq. (2.6)):

$$\left(\frac{\partial^2 \Delta G_m}{\partial \phi_1^2} \right)_{T,P} > 0 \quad (2.6)$$

Negative values of Eq. (2.6) can yield an area of the phase diagram where the mixture will separate into a phase rich in component 1 and a phase rich in component 2. ΔS_m is very small for most polymers due to the high molecular weight of them and ΔH_m is positive for most non-polar polymers.

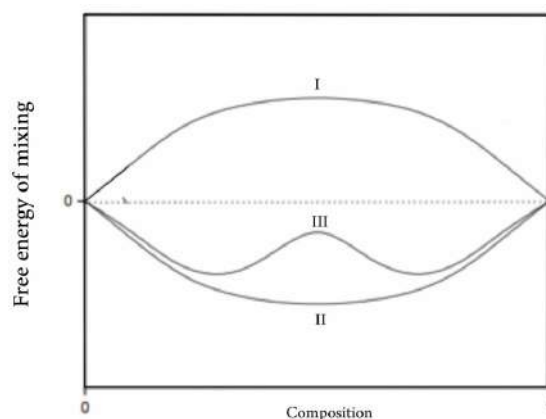


Figure 2-21 : Schematic diagram of free energy of mixing versus composition in binary polymer mixture.

Figure 2-21 exhibited three possible ways in which the free energy of mixing might vary with composition. In case I, two components are immiscible over the whole composition range due to the positive energy of mixing whereas in the case of II, it is inverse and two components are completely miscible. In the case III, in some range of the compositions, ΔG_m exhibits a negative curvature and the curve splits into two phases resulting in miscibility gap or partial miscibility. In the blend of low molecular weight materials, increasing the temperature promotes the miscibility as the entropic term ($T\Delta S_m$) increases and leads ΔG_m to more negative values (McMaster 1973).

Polymer-polymer mixtures generally exhibit lower critical solution temperature (LCST) while polymer-solvent mixtures usually exhibit upper critical solution temperature (UCST). These phase behaviors of polymer blends are illustrated in Figure 2-22.

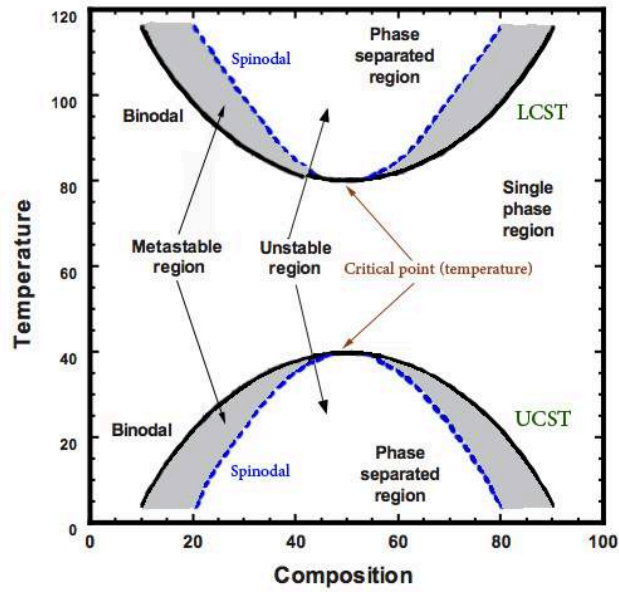


Figure 2-22: Phase diagram showing LCST and UCST behavior for polymer blends.

The figure shows two curves (binodal and spinodal) for the both LCST and UCST behaviors. The spinodal curve is related to the position where the second derivative of free energy of mixing with respect to the composition is zero (Eq. (2.7)). The binodal curve is also described by the equality of chemical potential of components (Eq. (2.8)).

$$\left(\frac{\partial^2 \Delta G_m}{\partial \phi_i^2} \right)_{T,P} = 0 \quad (2.7)$$

$$\Delta \mu_1^a = \Delta \mu_1^b, \Delta \mu_2^a = \Delta \mu_2^b \quad (2.8)$$

where μ represents the chemical potential, a,b represent the phases and 1,2 represent the two components (Flory, Orwoll et al. 1964).

2.7.2 Phase separation

In polymer blends, phase separation might occur either upon heating or cooling. It can occur either by spinodal decomposition or nucleation and growth. In the nucleation and growth

mechanism, small droplets of a minor component develop over time in a mixture and they are brought into the metastable region of the phase diagram (Figure 2-22). Spinodal decomposition occurs when a polymer blend is quenched from the miscible region in the phase diagram into the unstable (immiscible) state. Cahn and Hillard were the first one who described this process theoretically (Cahn and Hillard 1958). In general, phase separation is controlled by concentration fluctuation and the decrease of bulk energy in the early stage and it is controlled by diffusion and convection, and the decrease of surface energy at the later stage.

As illustrated in Figure 2-23, a disordered co-continuous two-phase structure may result from spinodal decomposition. Immediately after forming the co-continuous pattern, the size of droplets increases due to reduction of surface area. This process is driven by interfacial tension between the polymers. In both mechanisms (nucleation and growth and spinodal decomposition), the driving force behind coarsening is the minimization of the interfacial tension through a reduction in interfacial area (Bruder and Brenn 1992; Katzen and Reich 1993; Karim, Slawek et al. 1998).

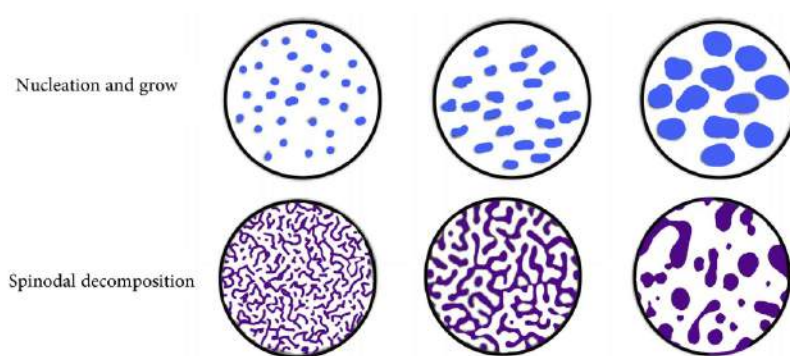


Figure 2-23 : Schematic illustration of the phase separation a) nucleation and grow, b) spinodal decomposition.

2.7.3 Morphology of polymer blends

Morphology of a mixture of polymer indicates the shape, size and spatial distribution of each phases (components) with respect to the others. When two or more polymers are blended, the shape, size and distribution of the components in the matrix depend on two major parameters; 1- material parameters including viscosity ratio, composition, interfacial tension and elasticity ratio, 2- processing conditions such as time, temperature, intensity and type of mixing. Therefore, controlling the melt flow during processing and interfacial interactions to manipulating the polymer structure might be a greatest challenge in the field of polymer blends (Bordereau, Carrega et al. 1992; Inoue 2003).

2.8 Effect of material parameters on morphology

2.8.1 Interfacial tension

Poor interfacial adhesion between a polymer blend components is due to the high interfacial energy and low interfacial thickness between the phases. The other phenomenon in a polymer blend system is coalescence of the dispersed phase, which results in larger and un-uniform morphology. Therefore, reducing the interfacial tension between the phases and decreasing the incidence of coalescence under quiescence condition are the keys to overcome the problem corresponded to the weak adhesion between the phases and coarse morphology in a polymer mixture(Chen and White 1993; Mekhilef, Favis et al. 1997; Willemse, Posthuma de Boer et al. 1999; Hong, Ahn et al. 2005; Virgilio, Desjardins et al. 2010; Yang, White et al. 2010; Fortelný, Juza et al. 2011).

2.8.2 Viscosity ratio

Several researchers have studied the effect of viscosity ratio on the morphology of immiscible polymer blend. The viscosity ratio is the ratio (k) of the viscosity of the dispersed phase to the viscosity of the matrix phase:

$$k = \frac{\mu_d}{\mu_m} \quad (2.9)$$

where μ_d and μ_m are the viscosities of the dispersed phase and the matrix, respectively. When all the factors are kept constant except the viscosity of the minor component, less viscous component results in smaller droplets in more viscous matrix. Wu's suggested a minimum particle size for a system with viscosity ratio equal to 1. When the viscosity moves away from unity (lower or higher) the dispersed particles become larger (Mekhilef, Favis et al. 1997; Willemse, Posthuma de Boer et al. 1999; Virgilio, Desjardins et al. 2010).

2.8.3 Composition

Many researchers have studied the influence of the concentration of minor phase in a blend. It is found that when the concentration of the minor component increases, the dispersed droplet size will increase due to coalescence of the droplets, it continues until the blend phase inverts and the dispersed component becomes the matrix and vice versa. A co-continuous phase structure will be generated around the phase inversion point. Many advantages have been reported for polymer blends with co-continuous morphology including synergistic mechanical properties, controlled electrical conductivity and selective permeability (Favis and Chalifoux 1988; Lee and Han 2000).

2.8.4 Shear stress

Some researchers suggested that shear stress has an inverse effect on the size of the minor components. They noted that high shear stress results in much finer dispersed phase in a matrix of polymer. It is also found that there is a critical minimum drop size as the shear rate changes and this can be due to the polymer elasticity. It is suggested that if the shear rate is increased, the viscosity of the matrix decreases and the elasticity of drop increases, therefore, the drop resists to a greater extent. As a conclusion, the finest dispersion is obtained at the optimum shear rate of the system (Huneault, Shi et al. 1995; Cercle, Sarazin et al. 2013; Taghizadeh, Sarazin et al. 2013).

2.8.5 Elasticity ratio

Van Oene found very interesting results regarding the effect of elasticity ratio on the morphology of polymer blends. He suggested that in a blend containing components with different elasticity, the phase with higher elasticity encapsulates the one with lower elasticity. Some researchers also have found the effect of elasticity on the region of co-continuity. They demonstrated that the phase inversion point and co-continuity is influenced by elasticity and viscosity ratio (Lee and Han 1999; Bhadane, Tsou et al. 2011).

2.9 Summary of literature review and problem identification

In many applications of polymer materials the surface properties are of vital importance. Adhesion of polymer coating on various surfaces has great importance recently on account of applications. The surface wettability of polymer materials is closely related to printing, spraying and dyeing. The lack of polar groups on polymer surface causes it to have lower surface energy

and poor wettability. It is often difficult to find a polymer material with the right combination of bulk and surface properties. Several methods to alter the surface properties by changing the chemical composition of thin surface layer without significant influence of bulk characteristics have been developed. Therefore many different methods as surface modification techniques are used in industry in order to get desired surface properties and they have been classified as; physical treatment (Flame treatment, Corona treatment, Cold plasma treatment, Hot plasma treatment, UV treatment, Laser treatment, X-ray and γ -ray treatment, Electron beam treatment, Ion beam treatment, Metallization, Sputtering) and chemical treatment (Wet treatment, Surface grafting). Surface treatments are used to change the chemical composition, increase surface energy and modify the surface properties. Most surface modification methods involve an additional treatment of the polymer material that consumes a large amount of fuel and cannot modify complex shape surfaces uniformly.

Other applicable treatment is bulk modification. By this technique PET can be mixed with some other polymers, which have higher surface energy, bear high-energy functional groups or blended with suitable copolymers of PET, which the other block is a polymer with high-energy functional groups. Bulk modification of PET can transform this inexpensive material into a highly valuable finished product by easy process resulting in improving of surface wettability. The increase in surface free energy is mainly due to the increase in the polar components incorporated onto the PET surfaces. As the durability of the surface modification is of interest, copolymer surface modification should be appropriate because of migration of minor phase from the surface to the bulk in the case of blending of two polymers. We hope that a large number of oxygen polar functional groups are introduced on the treated PET surface, which strengthens the interaction

between the dipole-dipole in the vertical direction of the interface. This is a main reason for improving the wettability of PET film.

2.10 Originality of the work

One idea that was explored is to use of a third immiscible polymer in binary polymer blend to push desired polymer to the air-polymer interface. Since the surface active minor phase has short chains compare to the another one, they can move to the surface quickly by applying shear force on the blend and the second minor phase should keep them on the surface top layer and prevent their migration back to the bulk.

In ternary systems, the morphology is one of the important parameters that should be taken into account besides other parameters such as shear stress and crystallinity. Using of ternary polymer blend approach to improve surface properties of host polymer has not been used before.

In order to make an adhesion between the PET surface and inks, surface hydrophilicity is not only the requirement for printability, but also mechanical interlocking of ink on PET surface. In this case, the adherent surface should have enough roughness. Hence another part of the study was to provide suitable roughness on PET surface. We also proposed a novel idea to make roughness on the surface of PET film based on the migration of one minor phase in a ternary polymer blend to the surface. A phenoxy resin and polystyrene were used as minor phases to roughen the PET film surface. We decided to put the narrow depletion of the blend in the unstable region of the phase diagram by controlling the composition of the film in that region. Therefore, the phase coarsening will occur in the surface layer. Consequently, the co-continuous phase morphology caused the instability at the surface of PET film. There is also no published work on surface roughening of polymeric films through blending of three polymers.

CHAPTER 3

ORGANIZATION OF THE ARTICLES

The major achievements of this PhD project are presented in the form of three scientific papers in the following three chapters:

Chapter 4 represents the results of the first paper, which is dedicated to study the wettability of PET films. This article is entitled: “Enhancing Hydrophilicity of PET Surface through Melt Blending” that is published in Polymer Engineering and Science. In this work we focused on the increase of the hydrophilicity and wettability of the PET film through blending via a twin-screw extruder, which is more convenient compared to the physical or chemical surface modification. We used a PEG (8 kDa) polymer to blend with PET due to its good hydrophilicity, low toxicity, biocompatibility and the mobility of its short chains. In this regard, we expected good surface migration of PEG molecules within PET matrix. The surface characterization techniques showed that there is not high enough PEG at the surface layer to make suitable surface hydrophilicity for many applications. We used a novel and second approach by adding a small amount of third component, polystyrene (PS), to the blend. It resulted in a remarkable surface enrichment of PEG at the polymer/air interface for the ternary polymer blend (PET-PEG-PS).

Chapter 5 presents the second article “Surface Morphology of Ternary Polymer Blends: Effect of the Migration of Minor Components” that has been submitted to The Journal of Physical Chemistry. In this work, the relation between the surface morphology of ternary polymer blends and the migration of minor component molecules to the top surface layer of the films were investigated. Different polymers such as polystyrene (PS), poly (butylene adipate-co-terephthalate) (PBAT), polycaprolactone (PCL), polymethyl methacrylate (PMMA) and polylactide (PLA) with different surface tensions were used to mix with the PET-PEG system. It was found that the separated droplets morphology leads more PEG migration to the surface of the film. Among all polymer mixtures with this morphology, PET-PS-PEG ternary blend exhibited the highest migration rate of PEG to the polymer/air interface. A dendritic crystalline structure was observed for PET-PS-PEG blend whereas for the other blends only some PEG droplets were found on the surface layer of the film. Furthermore, the optimum concentrations of the minor components as well as the mechanical properties of the PET-PS-PEG film were obtained.

Chapter 6 presents the third paper “Surface Roughening of PET Film Through Blend Phase Coarsening” that has been submitted to ACS Applied Material & Interface. In this study, we focused on an increase of the surface roughness of PET film through the blending process. The roughness was created by phase coarsening of the PS polymer droplets at the surface layer of the film. We used low concentrations of PS and poly (hydroxyl ether) of bisphenol A (Phenoxy resin, PKHH) in the blend. PKHH increased the viscosity of the system and could affect the PET-PS interface. It could make smaller droplets of PS in the blend. They could migrate faster to the surface by a suitable driving force then the local concentration of PS eventually reaches a level where a continuous morphology occurs, resulting in the distortion on the surface of the film.

CHAPTER 4

ARTICLE1: ENHANCING HYDROPHILICITY OF PET SURFACE THROUGH MELT BLENDING⁷

Ahmad Rezaei Kolahchi, Abdellah Ajji*, Pierre.J. Carreau

4.1 Abstract

In many industrial sectors, the surface properties of polymers are of particular importance. This applies, for instance, to painting, printing and any coating on surface of polymeric objects. Hydrophilicity and wettability characteristics are known to be determined by the chemical makeup of the polymer surface. Blending with an additive or a polymer containing high-energy functional groups is widely recognized as a potential technique to overcome disadvantages of low surface energy of polymers due to its convenient processing. Surface migration of polyethylene glycol (PEG) in PET host was investigated using a low molecular weight PEG (8 kDa) because of its good hydrophilicity, low toxicity, biocompatibility and chain mobility. A twin-screw extruder was used to blend the materials and prepare the polymer blend films. The results of surface characterizations showed that PEG renders the PET surface more hydrophilic, but not high enough for many applications. In a second approach the addition of a third component, polystyrene (PS) to the blend in a small amount of resulted in a remarkable surface enrichment of PEG at the polymer/air interface for the ternary polymer blend (PET-PEG-PS). Surface analysis revealed that the surface concentration of PEG in the ternary polymer blend film was significantly larger than that of the binary one.

⁷ Published in Polymer Engineering & Science, February 2014

4.2 Introduction

Surface wettability is an important property of polymer surfaces and is strongly dependent upon the composition. A proper control of the surface wettability has been the subject of considerable interest because of its advantages for various applications such as printability, dyeability, adhesion, absorbency and comfort of the products [1]. The low polarity and hydrophilicity of most polymers limits their applications in many areas such as membranes and biomaterials and printing, dying and adhesive properties of hydrophobic polymers are poor. Polyethylene terephthalate with its low cost, desirable mechanical, physical and thermal properties as well as ever growing commercial applications is widely used in different fields, from packaging films, bottles, containers and automotive parts to many biomedical applications [2]. Like most polymers, PET has relatively low surface energy due to its molecular structure, lack of hydrophilicity and active functional groups. Therefore, printing inks and paints do not adhere strongly to PET surface [3]. Consequently, a modification aimed at the creation of a more polar and hydrophilic surface is an important issue for applications where wettability and adhesion are required [4].

There are several popular methods one can use to modify the surface of polymer films in order to get desired properties. These include topical finishes, corona, plasma and flame treatments. Each of these techniques has disadvantages and limitations regarding the processing and the stability with time of the treated sample, and these have made them less attractive for commercial applications [5-7]. Since inks or other finishes are incorporated onto the polymer surfaces mostly by physical adhesion, they usually exhibit poor durability and can easily be removed by contact with a fluid and other surfaces [8]. All of these methods lead to an immediate hydrophilicity that deteriorates rapidly with time. Another disadvantage of these techniques is the limitation to treat complex shaped surfaces (such as automotive parts) where a uniform treatment cannot be achieved. Chemical grafting and surface derivatization

(transformation of a chemical compound of the surface to the desired one) methods can also be conducted on any solid material, of any shape. Concerns associated with the use of these techniques are related to their high cost, difficulty to implement, possibility of polymer degradation and scale-up problems for industrial productions [9].

A most promising technique appears to be the blending of polymers with low content of surface-active additives carrying suitable functional groups and then transferring them to the surface [10]. It is the objective of this work to develop and verify such a technique capability.

The extrusion process is currently used as the preferred method for blending the materials containing suitable functional groups with the polymer matrix in order to obtain polymer films with new surface properties. As a result of the applied shear field in the extrusion process, the added molecules segregate to the surface of the film [11]. The phenomenon of an additive or a minor phase polymer moving from the bulk to the surface is sometimes referred to as blooming or surface migration [12, 13]. Surface migration of additives is a pivotal part of the process to change the surface composition and achieve new properties for low concentration minor phases without altering the bulk properties. It is true that in such a surface modification, the concentration of the additives at the film surface depends upon the interplay of several driving forces such as shear, diffusion, etc. [14-16]. It has been suggested that the migration mechanism is based on surface tension gradient, molecular weight differences and polymer–additive miscibility [12, 17]. The effects of some of these parameters can be eliminated or at least minimized depending on the polymer film preparation technique. Basic principles for the additive selection and the optimization of processing conditions to enhance the surface migration of additives or minor polymer components in a polymer host can be found in the work of Lee and co-workers [12, 17, 18].

The main objective of this study is to develop an effective method for imparting hydrophilicity to PET film surface using melt blending via an extrusion process. This is based on a fundamental understanding of the formation of a hydrophilic surface for PET films. This study involves an investigation of the possible interactions between PET and other polymeric materials leading to a hydrophilic surface through their migration. Hence, the enhancement of wettability is investigated by blending some hydrophilic polymers at different concentrations with PET. The hydrophilicity of the PET film surface is explored using contact angle, X-ray photoelectron spectroscopy (XPS), time-of-flight secondary ion mass spectrometry (TOF-SIMS) and atomic force microscopy (AFM).

Since PEG is a strongly hydrophilic polymer [19, 20] and exhibits a high oxygen/carbon atom ratio, its presence on the PET film surface should enhance the hydrophilicity. In our preliminary tests, we found that PEG was the most effective polymer for enhancing the hydrophilicity of PET surface compared to polyethylene terephthalate glycol (PETG), polyethylene oxide (PEO) and many more polymers. It was observed that for a blend of PEG with PET, prepared via a twin-screw extruder, the surface energy and the polar contributions of the PET film were enhanced. This was due to the migration of some PEG chains to the surface, resulting in an increased surface wettability. Since it was found that PEG was still distributed uniformly in the entire matrix, the next step was to find a method to favor the migration of a maximum of PEG chains to the surface by lowering the interaction between PET and PEG and thereby facilitating PEG migration to the surface layer. The novel idea was to add an immiscible polymer component with the PET to the PET-PEG blend to favor migration of PEG molecules to the polymer/air interface. Since PEG chains are very short (very low molecular weight) compared to those of the third component, they can be moved along the surface (polymer/extruder barrel interface) easily under an applied shear force. Polystyrene (PS) was selected as a second minor phase to be added to the PET-PEG binary blend. Immiscibility of PS with PET, low price and its high molecular weight (350

kDa), which reduces its mobility compared to the PEG molecules, were the main reasons for choosing PS. Consequently, we investigated the effect of the second minor component on the migration of PEG to the film surface and also the effect of the minor components on the crystallinity of PET films.

4.2.1 Surface migration of the minor components

It has been demonstrated that the migration in absence of any shear forces is driven by surface free energy differences between the host polymer and additives or minor components [21, 22]. Lee et al. [12, 18, 23] investigated the quiescent (non-flow) surface migration of polystyrene-b-polydimethylsiloxane (PS-b-PDMS) and polystyrene-b-polymethyl methacrylate (PS-b-PMMA) copolymer additives in narrow molecular weight distribution PS hosts. They found that differences in surface energy and/or molecular weight between the copolymer additives and the host polymer play important roles in the migration of the additives. However, when the polymer mixture was subjected to a shear field such as in extrusion, the molecular size (or molecular weight) was the main factor that influenced the migration [18]. It has been found that a low molecular weight polymer distributed within a host polymer could easily move to the surface under shear forces [24, 25]. This is a very simple and physically based processing method that can be widely used to impart desired properties to the surface of polymers without further modifications.

Flow-induced migration of polymeric species has been widely studied mostly for dilute polymer solutions [26]. For example, Dill and Zimm [27] explored the following empirical expression for the radial migration velocity of a polymer in a dilute solution towards the center of cone-and-plate flow device:

$$v_m \approx \frac{\eta_s \dot{\gamma}^2}{r k_B T} R_0^5 \quad (4.1)$$

where v_m is the radial migration velocity, r is the radial position, R_0 is the average un-disturbed end-to-end distance of the polymer chains, η_s is the solvent viscosity, K_B is Boltzmann's constant and $\dot{\gamma}$ is the shear rate. The strong effect of molecular weight (through R_0) and the stress contribution through the viscosity and shear rate can be clearly observed in Eq. (4.1).

Generally, there are two main schools of thought regarding the migration of the components in polymer mixtures. One believes that the driving force of the surface migration is controlled by the difference in surface free energy of the host polymer and the components. To keep the minimum surface energy of the whole system, the concentration of the minor component at the surface must be different from the bulk of the polymer mixture [28-32]. The other school of thought believes that the polymer migration could be affected by molecular configuration near solid walls [33-35]. This theory contends that, in a system containing different molecular weight (M_w) polymers, the highest M_w component experiences a much larger reduction of its configuration entropy than smaller molecules near the surface. This allows the lower M_w components to enrich the surface and maintain a minimum surface energy. Hence, a non-homogeneous flow field will deplete high M_w polymer molecules from high stress regions (specifically near the surface) and thereby enhance the concentration of smaller polymer chains in those regions. It will take place when sufficient time is allowed for diffusion of the components to the surface during flow [12, 26, 33-38].

It has been also reported that annealing can increase the rate of migration [39, 40]. Besides, it was observed that the migration to a polymer/air interface is different from that to a metal/polymer or glass/polymer interface. This has been explained by the difference in their surface energies [40].

The minor phase mobility can be characterized by a diffusion coefficient that describes the permeation of small molecules through a polymer by:

$$P = D * S \quad (4.2)$$

where S is the solubility and D is the diffusion coefficient. The diffusion process minimizes the Gibbs free energy and can be described by Fick's law. Therefore, solubility and diffusivity are important factors for the migration of the minor components in a blend. They are affected by polymer characteristics such as free volume (more free volume can increase S and D), shape and size of the diffusing molecules and the cohesive forces between polymer chains [41]. For example, in a highly crystalline polymer, the mobility of the components is less than in less crystalline or amorphous polymer, as the movement of the components is interrupted by the crystalline portions and occurs in the amorphous regions only [42].

In this study, we focus on the blending of PEG as a hydrophilic polymer with PET matrix and induce the migration of PEG molecules to the surface of the polymer film. The effect of the presence of PS as a third polymer in the PET-PEG blend is considered as a main cause of the phenomenon. PS forces the migration of PEG molecules towards the top surface layer due to its high M_w and higher immiscibility with PET. To our knowledge, this is the first investigation in which a second minor phase is added to a polymer PET-PEG blend to favor the migration of PEG molecules to the surface and impart hydrophilicity to PET films.

4.3 Experimental section

4.3.1 Materials and sample preparation

A low viscosity PET (commercial grade 9921W) obtained from Eastman, polyethylene glycols having molecular weights of 8, 20 and 35 kDa (supplied by Sigma Aldrich Co) and a general-purpose PS

Styron 663 with density 1.04 g/mL and molecular weight of 300 kDa (supplied by Dow Chemical) were used in this study. The used polystyrene is a common industrial polystyrene and is atactic PS with no order or regularity in the phenyl groups. This polystyrene's chains cannot pack very well so it is amorphous and does not crystallize. The PET and PEG were dried at 100 and 40 °C, respectively, in a vacuum oven for 24 h before blending. To prepare a benchmark PET film, the neat PET was extruded using a co-rotating twin-screw extruder (CICO-TSE) of Leistritz Corp. with an L/D ratio of 40 ($D=18$ mm), at a rotation speed of 100 rpm. The extruder was operated using a temperature profile set at 245, 255, 265, 265, 260 °C (for the different zones from the hopper to the die). The binary polymer blend films (PET-PEG and PET-PS) were prepared by direct solids mixing of the PET and 5wt% of the other component and then extruded under the conditions defined above. The ternary polymer blends films were prepared using direct solids mixing of the three components before feeding into the extruder and operated under the same conditions. After each processing, the polymer films were cooled using an air-knife right after the exit of the die.

4.3.2 Characterization

4.3.2.1 Contact angle measurements

Contact angle (θ) is a quantitative measurement of the wetting behavior of a solid surface by specific liquids at three-phase boundary when the liquid is brought into contact with the solid, liquid and gas interfaces. It determines the property of the very top surface of about 0.5 nm depth [43]. Basically, a low contact angle and a high contact angle mean high hydrophilicity and low hydrophilicity, respectively, of the substrate.

First, the prepared films for surface characterizations were washed with cyclohexane using an ultrasonic bath (USB) for 5 min and then washed with distilled water using USB to remove all

contamination and impurities and then dried in vacuum oven. Contact angles for two liquids (deionized water and formamide) on the polymer films were measured at constant temperature (20 °C) using a goniometer equipped with a system of drop shape analysis (DSA10, Krüss, Germany). A micro-syringe was used to place a liquid drop (2 µL) on the surface and a video camera took images of the drops every 10 s. Each contact angle result is the average of at least 15 measurements with a precision of $\pm 1^\circ$. The water contact angle was measured at different times up to 150 days after the first measurement.

4.3.2.2 XPS analysis

The samples were analyzed via X-ray photoelectron spectroscopy using a VG ESCALAB 3 MKII spectrometer. Electrons were excited using a non-monochromatic Mg K α x-ray source (1253.6 eV), with an experimentally determined spectral resolution of 0.7 eV and a standard error of the measurement of less than 0.1 eV. The pressure in the chamber was maintained at 10^{-9} Torr (1.333×10^{-7} Pa) and the main carbon peak was fixed to a binding energy of 284.7 eV. Relative concentrations were determined by dividing integrated intensity values by sensitivity factors taken from the Wagner table [44]. An area of approximately 5 mm in diameter on the sample surfaces was analyzed. Survey scans (0-1100 eV) and narrow scans of the C1s and O1s regions were obtained. Peak fitting of the C1s and O1s core levels was carried out using the Advantage V 4.12 software. Consequently, the O/C atom ratio was estimated from the relative peak intensities of the O1s and C1s spectra.

4.3.2.3 Time-of-flight secondary-ion mass spectrometry (TOF-SIMS)

TOF-SIMS studies were carried out on an ION-TOF SIMS IV (Munster, Germany) apparatus. The instrument has an operating pressure of 5×10^{-9} Torr (6.7×10^{-7} Pa). The sample was bombarded with a pulsed liquid metal ion source (Bi $_3^{++}$), at energy of 15 KeV in bunch mode. The gun was operated with a 100 ns pulse width, 0.3 pA pulsed ion current for a dosage lower than 5×10^{11} ions.cm $^{-2}$, well below

the threshold level of 10^{13} ions.cm⁻² for static SIMS. Charge neutralization was achieved with an electron flood gun. Secondary ion spectra were obtained from an area of 140 μ m x 140 μ m with 128x128 pixels (1 pulse per pixel) using at least 4 different positions per sample. A chemical mapping was done on the test surface area the same as for XPS.

4.3.2.4 Differential Scanning Calorimetry (DSC)

The crystallization and melting behavior of samples were studied via differential scanning calorimetry (DSC) using a DSCQ1000 (TA instruments, USA) under helium atmosphere. A scanning rate of 10 °C/min from 30 to 300 °C was used. To eliminate any initial thermal history, the samples were heated at a scanning rate of 10 °C /min from 30 to 300 °C, held for 2 min at 300 °C, then cooled to 30 °C at the same rate. The crystallization enthalpy (ΔH_c), melting enthalpy (ΔH_m), and degree of crystallinity were determined from the second heating cycle performed at the same heating rate.

4.4 Results and discussion

4.4.1 Effect of PEG molecular weight on migration

Three PEGs having different M_w (8, 20 and 35 kDa) were blended with PET to evaluate the effect of M_w on the PEG surface migration. Figure 4-1 shows the results of the contact angle measurements on the PET-PEG films. As expected, a lower contact angle is observed and decreases with time faster for the sample containing lower M_w PEG (8 kDa). This indicates that smaller molecules can move easier through the bulk of PET film than the longer chains (higher M_w). These results are in agreement with the previously mentioned thermodynamic theory about the large entropy penalty for higher M_w components in a polymer mixture, and thus higher M_w components are expected to be depleted from the surface. Consequently, the polymer surface layer will be enriched in the lower M_w polymer even for systems without substantial differences between the surface energies [51, 52]. This mechanism of

surface segregation has been reported for many polymer blends including polystyrene-PMMA for example [17].

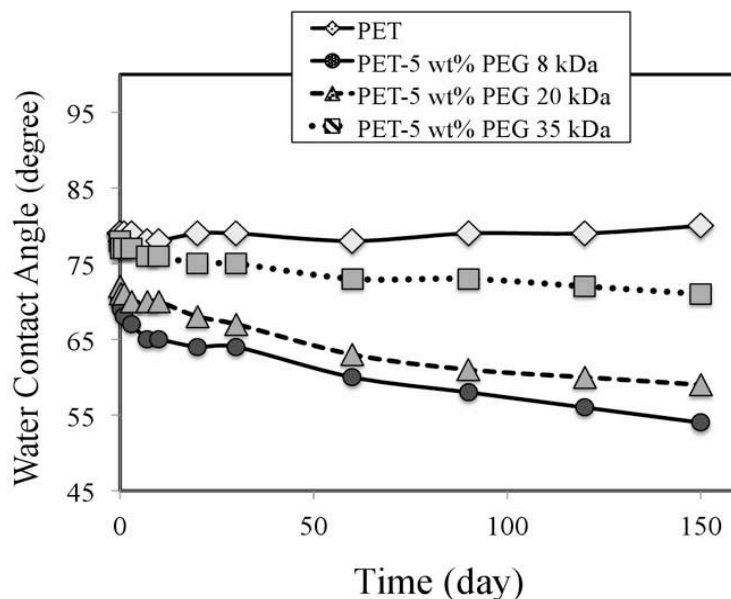


Figure 4-1: Water contact angle for the PET-PEG blends containing 5wt% of different M_w PEGs (35, 20, 8 kDa).

4.4.2 Binary blend

4.4.2.1 Contact angle analysis

Figure 4-2 reports the water contact angles of the neat PET and PET-5wt%PEG films. As can be seen in the graph, the water contact angle of the prepared PET film is 79° , which is in agreement with the reported values in the literature [45-49]. This value did not change over the period of 150 days. The addition of 5wt%PEG resulted in a reduction in the water contact angle from 79° to 72° , therefore, an increase of the hydrophilicity of the binary blend film compared to the original PET film. The results indicate a further improvement in the surface wettability with time, the contact angle decreasing to 58° after 150 days and keeping the samples in a vacuum oven at 40°C . This indicates that the most PEG molecules are located near the top surface layer and their migration to the surface due to moving the short chains of PEG through the free volume and considerably alter the surface composition and

contact angle with time. The contact angle values represent the property based on the polymer surface composition, which might be different from the bulk properties [50]. This reduction in water contact angle is accompanied by PEG surface enrichment due to the PEG molecules migration to the surface of the host polymer.

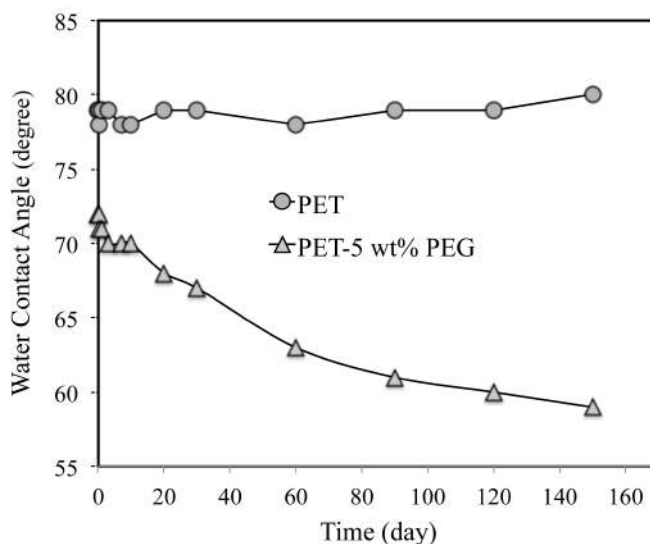


Figure 4-2: Water contact angle of the original PET and PET- 5wt%PEG films.

4.4.2.2 Surface characterization by XPS

The chemical compositions of the PET and PET-PEG films were determined via XPS analysis. XPS can be more accurate in determining and evaluating the alteration of the surface composition and the elements ratio than contact angle measurements. Figure 4-3 reports the XPS spectrum of the sample after blending with 5wt%PEG. The figure reveals that oxygen and carbon are the only existing elements on the surface of the sample. XPS results allow us to verify that the changes in PET surface properties are neither due to the presence of some other materials on the surface nor because of contamination during preparation. The changes are due to the alteration of the oxygen and carbon surface concentrations, which was obtained from enrichment of PEG on the PET-PEG film surface. Figure 4-4 reports the oxygen/carbon atom ratio obtained from XPS for the original PET and PET-PEG

film surface until 150 days after extrusion. The O/C atom ratio is observed to increase from 34.5% for the original PET film to 38% for the film of PET-PEG characterized immediately after extrusion. The determined O/C atom ratio of 34.5% for the original PET film is lower than the ratio of 40%, which is the value calculated from the repeating units of PET polymer chains. In addition, the O/C atom ratio of PEG calculated from the repeating units is 50%, which is a very high value for a polymer chain. Therefore, the results indicate the presence of PEG at the surface layer of the binary polymer blend film, and the concentration of PEG increases with time as the O/C ratio reaches almost 47 after 120 days. As we explained before, this can be due to the presence of the most PEG molecules near the top surface layer and they migrate to the surface gradually with time. The PEG chains are preferably located at the surface of the PET-PEG film since the O/C atom ratio is larger than 40%, (the theoretical value of original PET). By comparing Figures 4-2 and 4-4 it can be concluded that the contact angle trend is consistent with the XPS observations.

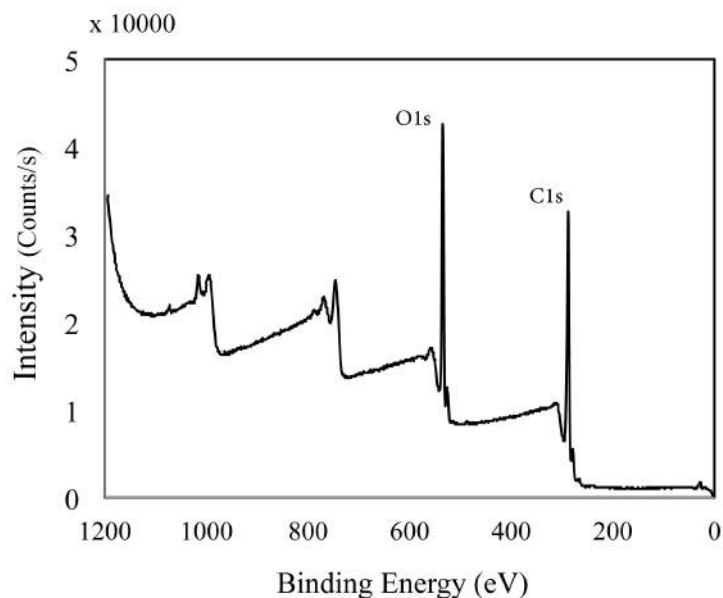


Figure 4-3: XPS survey spectra of the PET-5wt%PEG blend sample.

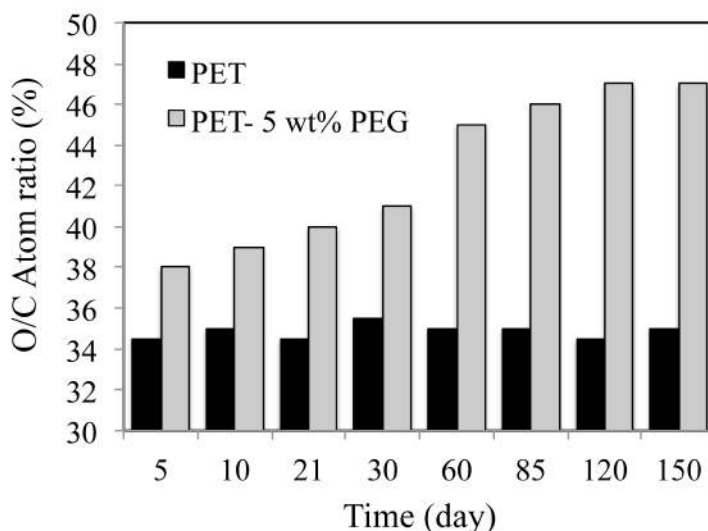


Figure 4-4: O/C atom ratio for the original PET and PET-5wt%PEG.

4.4.3 Ternary blend

4.4.3.1 A novel method to favor surface migration of a minor phase

In all cases so far investigated, the main concern was that the factors affecting the migration of additives in a host polymer strongly depend on externally applied conditions such as applied stresses, cooling and environment (the interfaces such as die-polymer interface and also the humidity). Hence, in this study, we have developed a method to force the migration of PEG molecules within the host polymer to the surface for any specific external conditions. Furthermore, the efficiency of the surface migration is increased, the cost is reduced and finally, outstanding surface properties of PET films are obtained. It was explored that a small amount of an immiscible polymer with PET of higher M_w than that of the minor component (PEG) could be effective in modifying the bulk properties of the blend. Dispersed droplets of this polymer having less affinity for PET would remain homogeneously distributed in the bulk of the polymer film and cannot be migrated to the surface as fast as PEG low M_w . Therefore, it will force the migration of PEG molecules towards the top surface layer due to its higher immiscibility and molecular weight.

Based on these hypotheses and from basic information on the properties of some polymers and their interactions with PET and PEG, PS was selected as the second minor phase in PET-PEG blend.

4.4.3.2 Contact angle

The extent of hydrophilicity of the samples was investigated by contact angle measurement. Figure 4-5 shows the variation of the contact angle as a function of time for PET-5wt%PEG, PET-5wt%PS and PET-5wt%PEG-5wt%PS films. In the figure, the result for the neat PET is included for comparison. The contact angle values are considerably reduced from 79° for the neat PET surface to 47° for the PET-PS-PEG film. Finally the contact angle value of the ternary polymer blend reaches 36° after 150 days, which is much lower than for the PET-PEG binary system. The trend observed is due to the more concentrated PEG molecules at the layer close to the surface of the PET-5wt%PEG-5wt%PS film and the migration of PEG molecules to the top surface layer with time.

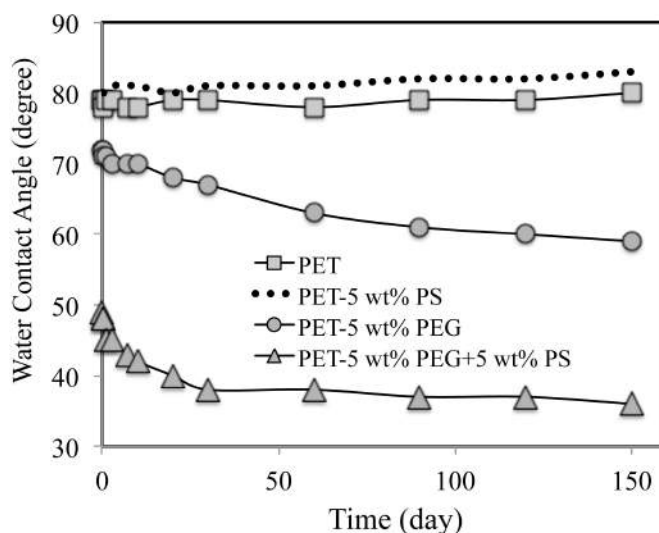


Figure 4-5: Water contact angles for PET, PET-5wt%PEG, PET-5wt%PS and PET-5wt%PS-5wt%PEG films.

4.4.3.3 Changes in surface chemical composition

XPS was used as previously to determine the composition of the neat PET and polymer blend film surfaces. From low resolution XPS data, the oxygen to carbon ratio was calculated and presented in Figure 4-6 after 150 days. The results indicate that addition of 5wt%PS to the binary blend increases the O/C atom ratio of the surface from 34.5% for the neat PET film to about 45.5% for the PET-5wt%PEG-5wt%PS. As mentioned earlier, the oxygen to carbon ratio value of PEG chains is larger than that for PET. Thus, the large shift in the O/C ratio is a clear indication that surface hydrophilicity improvement was induced in the ternary polymer blend and the amount of PEG on the film surface increased dramatically. Deconvoluted C1s peaks of PET chemical bonds (C=C, C=O, and C-O) are now analyzed in order to identify any new bonds and functional groups added after the modification. Figure 4-7 presents the high-resolution XPS C1s spectra of carbonyl functional groups for the neat PET, PET-PS, PET-PEG and PET-PS-PEG films. The intensity of the peak corresponding to the carbons in the C-O groups increases after blending of PS with the PET-PEG blend. The increase and broadening of the C-O peak is indicative of the formation of more carbonyl groups on the PET film surface. It is also obvious that the total area under the carbon peak belonging to the carbonyl groups in the ternary blend sample increases sharply, indicating that the PEG content on the surface of the ternary blend film has been increased considerably. The relative percentages of each component were analyzed by Gaussian and Lorentzian peak fitting algorithms and the results are summarized in Table 4.1 as differences in percentage between the surface functional groups for the ternary and binary blend film samples. It is observed that the surface of the ternary polymer blend film is covered by more carbonyl functional groups as indicated by the C2 results. Table 4.1 also shows significant differences in the surface composition for the ternary polymer blend film and the other samples.

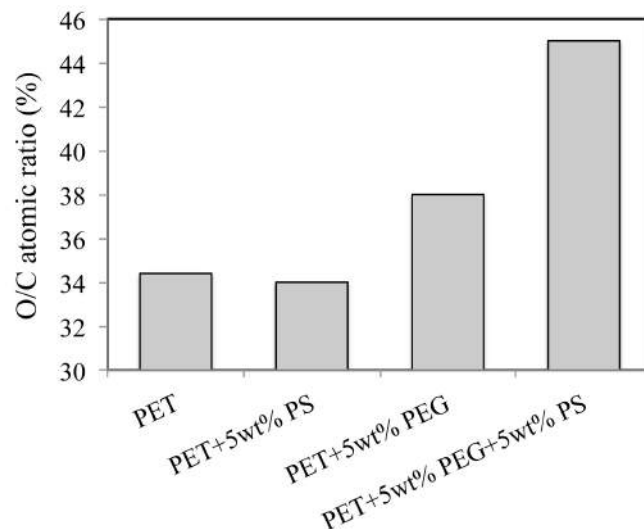


Figure 4-6: O/C atom ratio for PET, PET-5wt%PEG, PET-5wt%PS, PET-5wt%PS-5wt%PEG.

Table 4.1: Relative content (in %) of the carbon bonds and oxygen atoms at the surface of the neat PET, PET-PS, PET-PEG and PET-PS-PEG films. C1: C-C bonds, C2: Ether carbon atoms, C3: Ester carbon atoms, O1: Ester oxygen atoms, O2: Ether oxygen atoms.

	PET		PET- 5wt%PEG		PET- 5wt%PS		PET-5wt%PS-5wt%PEG	
Name	Binding energy (eV)	At. %	Binding energy (eV)	At. %	Binding energy (eV)	At. %	Binding energy (eV)	At. %
C1	284.7	47.61	284.76	43.21	284.73	47.92	284.73	18.11
C2	286.92	11.72	286.45	16.12	286.88	12.01	285.76	41.19
C3	288.19	9.57	288.71	8.69	288.54	10.31	289.18	6.95
O1	531.94	9.86	532.94	7.48	531.27	8.99	531.49	4.41
O2	534.1	21.23	534.26	24.5	534.49	20.77	533.58	29.14

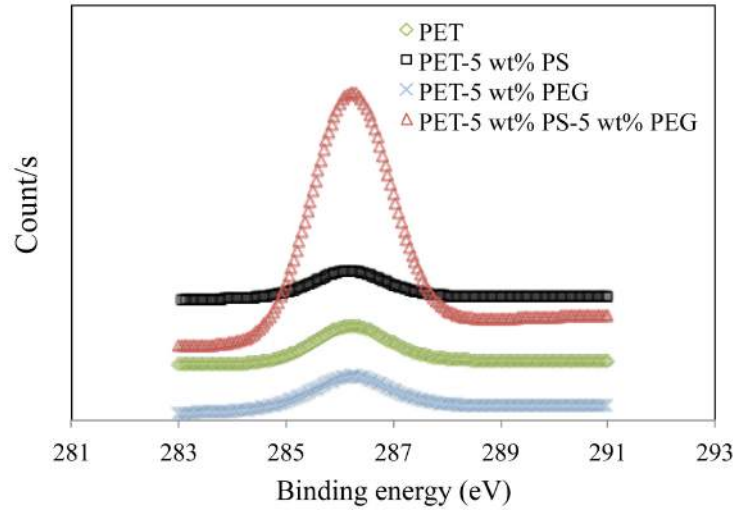


Figure 4-7: XPS high-resolution spectra of carbonyl groups on the surfaces of the neat PET, PET-5wt%PS, PET-5wt%PEG and PET-5wt%PS-5wt%PEG films.

4.4.3.4 Surface free energy

We compared three approaches to determine the surface free energy, namely the geometric mean approach according to Owens-Wendt [54], Wu's harmonic mean approach [53] and the estimation of the critical surface tension (γ_c) according to Zisman [55]. Wu [18] used a harmonic mean to combine the polar and dispersive components of the solid and liquid surface free energies and obtained Eq. (4.3) for surface energy calculation.

$$\gamma_{SL} = \gamma_S + \gamma_L - \frac{4\gamma_S^P \gamma_L^P}{\gamma_S^P + \gamma_L^P} + \frac{4\gamma_S^d \gamma_L^d}{\gamma_S^d + \gamma_L^d} \quad (4.3)$$

where γ_{SL} is the interfacial energy between polymer and liquid, γ_S is the surface tension of the solid, γ_L is the surface tension of the liquid, γ_S^d and γ_S^P are the dispersion and polar components of the surface tension of the solid and γ_L^d and γ_L^P are the dispersion and polar components of the surface tension of the liquid.

Combination of Eq. (4.3) and Young's equation ($\gamma_s = \gamma_{SL} + \gamma_L \cos \theta$) gives following relation between the contact angle and surface tensions:

$$\gamma_L (1 + \cos \theta) = \frac{4\gamma_S^P \cdot \gamma_L^P}{\gamma_S^P + \gamma_L^P} + \frac{4\gamma_S^d \cdot \gamma_L^d}{\gamma_S^d + \gamma_L^d} \quad (4.4)$$

$$\gamma_S = \gamma_S^P + \gamma_S^d \quad (4.5)$$

where θ is the contact angle between the solid (polymer film) and liquid (deionized water or formamide). Since some of the surface tension components ($\gamma_L, \gamma_L^d, \gamma_L^P$) are known, in order to obtain γ_S^d and γ_S^P , we just need to have contact angle results from two liquids (two equations with two unknowns) and then calculate γ_S from Eq. (4.5).

The surface free energy (γ_s) of the samples was calculated from the contact angle measurements. The calculated results using the three different approaches were almost the same and the results of the surface free energy are reported in Figure 4-8 for the neat PET, binary and ternary polymer blend films. The surface energies of the original PET, PET-5wt%PS and PET-5wt% PEG films are 41, 43 and 40.5 mN/m, respectively whereas the surface energy of the ternary polymer blend (PET-5wt%PS-5wt% PEG) reaches 51 mN/m. This is mainly due to the incorporation of C-O polar groups of PEG chain that has migrated to the surface of the film.

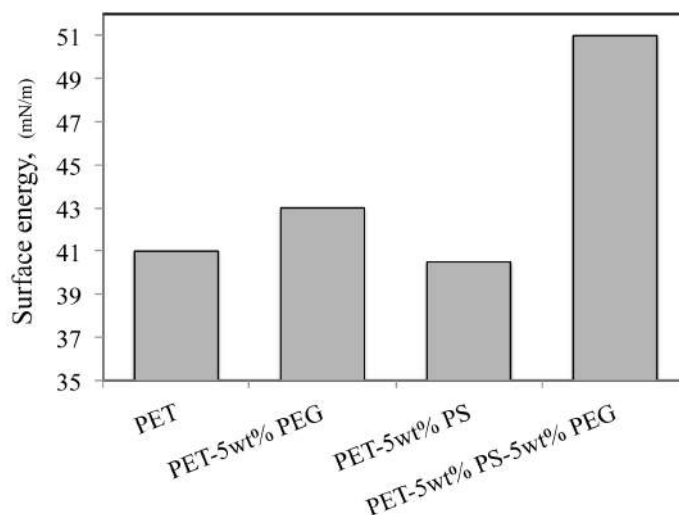


Figure 4-8: Surface energies of the neat PET, PET-5wt%PEG, PET-5wt%PS and PET-5wt%PEG-5wt%PS films.

4.4.3.5 Pattern characterization by TOF-SIMS

TOF-SIMS is an accurate and efficacious technique applicable to different types of system surfaces. The main advantages of TOF-SIMS are its high surface sensitivity (about 1nm) and spatial resolution. It provides useful information about the chemical composition of the surface. TOF-SIMS also probes very large areas (up to cm^2) compared to any other surface analysis method. It is the most reliable technique to analyze changes that occur in the chemical composition of a given surface associated with changes observed in water contact angle measurements.

Based on a preliminary analysis of the samples, four of them: PET, PET-PEG, PET-PS and PET-PS-PEG, exhibiting different results from XPS and SFE were selected for TOF-SIMS imaging. Figure 4-9 shows TOF-SIMS images of a $140\ \mu\text{m} \times 140\ \mu\text{m}$ area of the various films. The images provide information about the enrichment of the components on the surface of the films. The bright regions of the images represent the polymers (PET, PS and PEG) in the a, b and c images, respectively (left,

middle and right column). The spatial distribution of $C_7H_4O^+$, characteristic fragment of PET, is shown to have the largest intensity in Figure 4-9-a1 compared to the images of Figures 4-9-a2, a3 and a4. Figure 4-9-b image corresponds to the intensity of $C_7H_7^+$ ions, characteristic fragment of polystyrene. The images in the middle column (Figs. 4-9-a, b and c) are shown as shaded regions in all the images. These images indicate that PS is not present on the surface of the samples even for PET-PS and PET-PS-PEG films. Therefore, it can be concluded that the PS macromolecules have not significantly migrated to the surface of the binary and the ternary polymer blends films during the process or have moved back from the surface to the bulk of the blend during the cooling process. TOF-SIMS images further reveal the presence of a characteristic PEG molecular species ($C_2H_5O^+$) on the PET-PS-PEG sample (Figure 4-9-c). Considering the chosen atomic and molecular fragment ions, the bright feature all over Figure 4-9-c4 image presents the full coverage of the PEG at the surface layer of the PET-PS-PEG sample. This complementary information therefore demonstrates the effect of PS on the migration of PEG to the air-polymer interface. It implies also that for the PET-5wt%PEG blend without PS, PEG molecules cannot migrate sufficiently to the surface of the sample in order to change its surface properties. These results are in agreement with the XPS and contact angle results presented above.

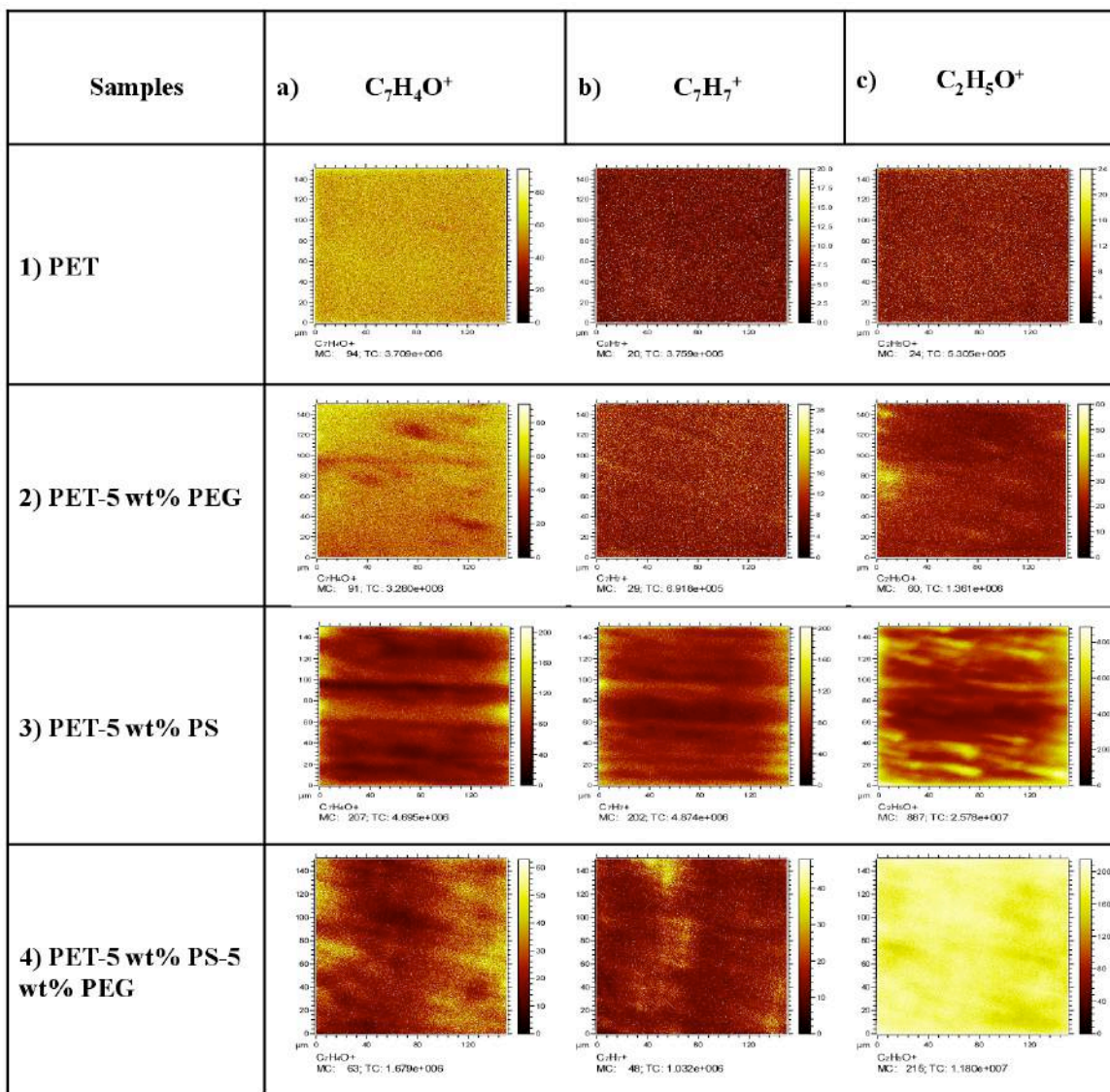


Figure 4-9: Results of TOF-SIMS imaging of the PET PET-5wt%PEG and PET-5wt%PS-5wt%PEG film surfaces.

4.4.3.6 SEM observations

To gain a view of the minor phase migration from the bulk to the surface, cross sections of films were prepared by embedding them in epoxy and microtomed using a diamond knife followed by SEM. The specimens containing PEG were immersed in water for 24h to extract the PEG particles. The SEM micrographs of the binary blend samples (PET-PS and PET-PEG) are shown in 4-10. The distribution of the PS droplets within the bulk of the PET matrix can be clearly observed in Figure 4-10-a and PEG droplets in the PET matrix are visible in the images of Figure 4-10-b (etched) and 4-10-c (non-etched) taken from the blend film cross-section. The dark regions in figure 4-10-b represent holes formed after PEG particles extraction. A comparison of the etched and non-etched samples clearly indicates that the bright regions within the surface of PET film are the PEG droplets. It is shown that most droplets are not located at the surface of the film, but are distributed within the bulk. A very strong evidence of PEG droplets surface migration is seen from the cross-section images of Figure 4-10-d (etched) and 10-e (non-etched) for the ternary blend film. It is obvious that the presence of PS droplets enhances the PEG droplet migration to the film surface. The images clearly show how the surface layers (polymer-epoxy interface) are covered by PEG droplets. This SEM image also exhibits that some PS droplets are located under the PEG covered surface. The droplets look like the observed droplets in Figure 4-10-a image and they have not extracted with water. Figure 4-10 confirms our interpretation and assumption of the role of PS in the ternary blend to induce migration of PEG droplets to the surface of the film.

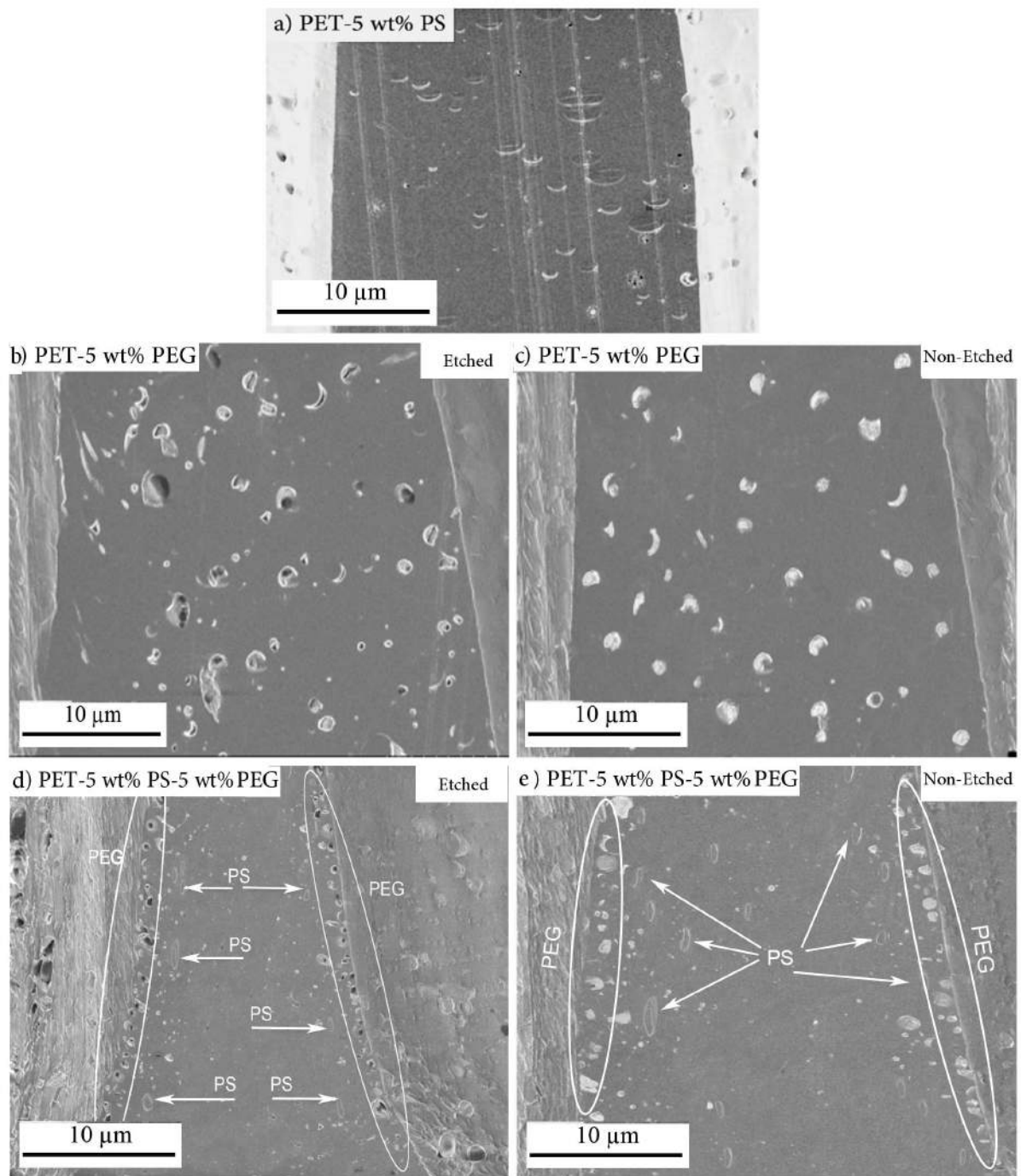


Figure 4-10: SEM cross-sectional images from (a) PET-5wt%PS and (b) PET-5wt%PEG (etched) (c) PET-5wt%PEG (non-etched) (d) PET-5wt%PS-5wt%PEG (etched) (e) PET-5wt%PS-5wt%PEG (non-etched)

4.4.3.7 Effect of PS and PEG on the crystallization of PET

The degree of crystallinity is one of the most important characteristics of a polymer and can affect significantly the mechanical properties. A good example is amorphous PET, which exhibits poor mechanical properties and low dimensional stability, whereas crystalline PET has higher strength and good dimensional stability [56]. Since PS and PEG have different mechanical properties and interfacial behavior in a PET matrix, the PET-PS-PEG crystallinity is an important parameter to be considered. The crystallinity of the samples was calculated according to the following equation:

$$\text{Crystallinity}\% = \frac{\Delta H_c}{\Delta H_0(1-X)} \quad (4.6)$$

where X indicates the total weight fraction of PEG and PS, subscript c stands for cold crystallization and ΔH_0 refers to the heat of fusion of a 100% crystalline PET, which is 115 J/g [57]. The crystallization of the samples during the cooling cycle is significant as illustrated by the DSC thermogram peaks of Figure 4-11. When PEG is added as one minor phase to the system, more PET crystals are formed and the PET film crystallinity increases from 23% for the original PET to 26% for the PET-PEG blend. This is believed to be due to the possibility that PEG crystalline structure can act as nucleation sites for the PET chain crystallization.

Shifting of the onset of the PET crystallinity temperature for the PET/PS sample to a lower temperature is indicative a decrease in the nucleation rate. In addition, the broaden crystallization peak for the PET/PS blend indicates a lower crystallization rate compared to the other samples, particularly the ternary blend. This may be due to reduced PET chain mobility in the presence of PS in the system.

For the ternary blend, both PEG and PS act synergistically and enhance PET crystallization. Figure 4-12 presents the crystallinity (in %) for all the samples. This figure demonstrates the remarkable

differences between the crystallinity of the system with three polymer components and binary ones.

The PET film crystallinity reaches 31% for PET-PEG-PS, much larger than the 23% observed for the original PET film.

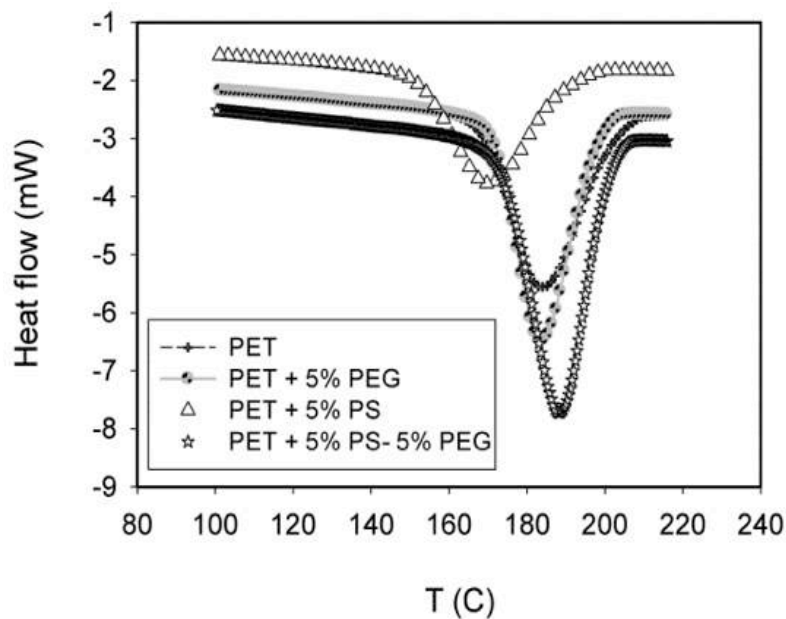


Figure 4-11 : DSC thermograms of the cooling cycle for the neat PET, PET-5wt%PEG, PET-5wt%PS and PET-5wt%PS-5wt% PEG films.

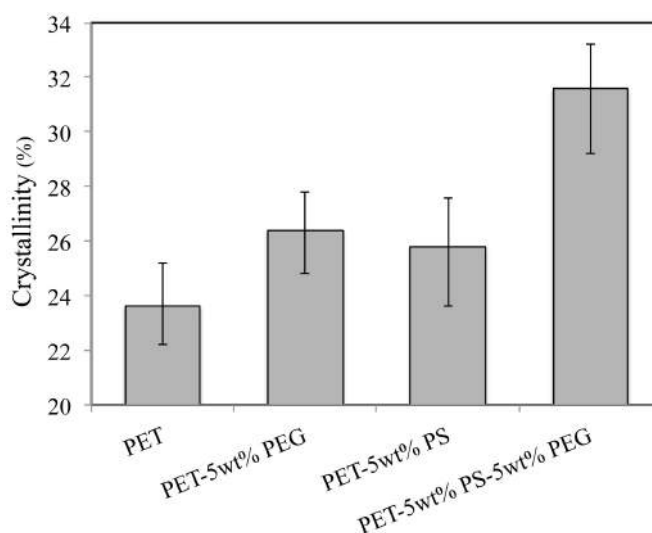


Figure 4-12: Crystallinity percentages calculated from DSC on the neat PET, PET-5wt%PEG, PET-5wt%PS and PET-5wt%PS-5wt%PEG DSC films

4.5 Conclusion

In this study, the surface of PET films was modified by blending with a PEG hydrophilic polymer via the extrusion process. It was shown that PET surface hydrophilicity could be enhanced by the addition of a third component in the blend. More specifically, the experimental results of this study for a ternary polymer blend (90wt%PET-5wt%PEG-5wt%PS) compared to the binary blends (95wt%PET-5wt%PEG and 95wt%PET-5wt%PS) showed that:

- The water contact angle of the PET film was significantly affected by adding 5wt%PS to the PET-PEG binary blend. The water contact angle decreased significantly from 79° for PET surface to 47° for the PET-PS-PEG. The surface energies of the ternary polymer blend, calculated from the contact angles, reached 51 mN/m from 41 for the original PET.
 - XPS revealed the enrichment of PEG on the PET-PEG-PS film surface, which led to a hydrophilic surface through the reduction of the water contact angle. The results indicated that the addition of 5wt%PS to the binary blend increased the O/C atom ratio of the surface from 34.5 for the neat PET film to about 45.5 for PET-5wt%PEG-5wt%PS
 - From TOF-SIMS analysis the identification of the component distribution on the top surface of the films could be made and the results showed that the surface was covered with PEG molecules when PS was added to the blend.
 - SEM images confirmed the surface segregation of PEG molecules to the film surface in the ternary blend.
-

- The PEG and PS addition to PET enhanced its crystallinity and a synergistic effect was observed for the ternary blend for which the PET film crystallinity reached 31% compared to 23% for the original PET film.

4.6 Acknowledgment

The authors wish to thank helpful support and discussions with A. Yaghoobi, F. Tofan, D. Davidescu. Financial support from NSERC (Natural Science and Engineering Research Council of Canada) and Lavergne Group Inc. is gratefully acknowledged.

4.7 References

1. C.M. Chan, T.M. Ko, and H. Hiraoka, *Surface Science Reports*, 24,1 (1996).
 2. N. Torres, J.J. Robin, and B. Boutevin, *European Polymer Journal*, 36, 2075 (2000).
 3. S. Lazare, and R. Srinivasan, *The Journal of Physical Chemistry*, 90, 2124 (1986).
 4. T.I. Croll, *Biomacromolecules*, 5, 463 (2004).
 5. P.K. Chu, *Materials Science and Engineering: R: Reports*, 36,143 (2002).
 6. J.M. Goddard, and J.H. Hotchkiss, *Progress in Polymer Science*, 32, 698 (2007).
 7. E.T. Kang, and K.G. Neoh, *Surface Modification of Polymers*, in *Encyclopedia of Polymer Science and Technology* (2002), John Wiley & Sons, Inc.
 8. B. Pukánszky, and E. Fekete, *Adhesion and Surface Modification Mineral Fillers in Thermoplastics I*, J. Jancar, Editors. (1999), Springer Berlin / Heidelberg. 109-153.
 9. P. Favia, M. Stendardo, and R. d'Agostino, *Plasmas and Polymers*, 1, 91 (1996).
 10. V. Datla, E. Shim, and B. Pourdeyhimi, *Polymer Engineering & Science*, (2012).
 11. M.X. Ramírez, D.E. Hirt, and L.L. Wright, *Nano Letters*, 2, 9 (2001).
 12. H. Lee, and L.A. Archer, *Macromolecules*, 34, 4572 (2001).
-

13. M. Strobel, *Journal of Adhesion Science and Technology*, 6, 429 (1992).
 14. J.F. Elman, *Macromolecules*, 27, 5341 (1994).
 15. W. Chen, and T.J. McCarthy, *Macromolecules*, 32, 2342 (1999).
 16. R.A.L. Jones, and E.J. Kramer, *Polymer*, 34, 115 (1993).
 17. K., A. Takahara, and T. Kajiyama, *Macromolecules*, 31, 863 (1998).
 18. H. Lee, and L.A. Archer, *Polymer*, 43, 2721 (2002).
 19. F. Zhang, *Biomaterials*, 23, 787 (2002).
 20. E.W. Merrill, and E.W. Salzman, *ASAIO Journal*, 6, 60 (1983).
 21. Z. Chen, *The Journal of Physical Chemistry B*, 103, 2935 (1999).
 22. S. Affrossman, *Macromolecules*, 26, 6251 (1993).
 23. H. Lee, and L.A. Archer, *Polymer Engineering & Science*, 42, 1568 (2002).
 24. R.M. Jendrejack, *The Journal of Chemical Physics*, 120, 2513 (2004).
 25. J.H. Glover, *Tappi Journal*, 71, 188 (1988).
 26. M.J. MacDonald, and S.J. Muller, *Journal of Rheology*, 40, 259 (1996).
 27. K.A. Dill, and B.H. Zimm, *Nucleic Acids Research*, 7, 735 (1979).
 28. S.H. Anastasiadis, *Macromolecules*, 36, 1994 (2003).
 29. J. Chen, and J.A. Gardella, *Macromolecules*, 31, 9328 (1998).
 30. H. Qian, *Applied Surface Science*, 253, 4659 (2007).
 31. P. Sakellariou, *Polymer*, 34, 3408 (1993).
 32. K.B. Walters, D.W. Schwark, and D.E. Hirt, *Langmuir*, 19, 5851 (2003).
 33. A.V. Bhave, R.C. Armstrong, and R.A. Brown, *The Journal of Chemical Physics*, 95, 2988 (1991).
 34. M.B. Khan, B.J. Briscoe, and S.M. Richardson, *A Review. Polymer-Plastics Technology and Engineering*, 33, 295 (1994).
 35. U.S. Agarwal, A. Dutta, and R.A. Mashelkar, *Chemical Engineering Science*, 49, 1693 (1994).
-

36. C. Raghunath, G.W. Roland, and G. Gerhard, *EPL (Europhysics Letters)*, 91, (2010).
 37. R. Drouot, and M. Berrajaa, *International Journal of Engineering Science*, 31, 1463 (1993).
 38. L.A. Miccio, *Polymer*, 51, 6219 (2010).
 39. C. Y. Lee, *Journal of Applied Polymer Science*, 86, 3702 (2002).
 40. Y. Tang, and M. Lewin, *Polymer Degradation and Stability*, 93, 1986 (2008).
 41. F. Fenouillot, P. Cassagnau, and J.C. Majesté, *Polymer*, 50, 1333 (2009).
 42. J. You, *Macromolecules*, 44, 5318 (2011).
 43. D.M. Choi, *Polymer*, 38, 6243 (1997).
 44. D. Briggs, J.T.G., *Practical Surface Analysis by Auger and X-Ray Photoelectron Spectroscopy* (1983), Chichester: Wiley.
 45. H.Y. Erbil, *Langmuir*, 15, 7378 (1999).
 46. A. Kamińska, H. Kaczmarek, and J. Kowalonek, *European Polymer Journal*, 38, 1915 (2002).
 47. R. Morent, N. De Geyter, and C. Leys, *Nuclear Instruments and Methods in Physics Research Section B: Beam Interactions with Materials and Atoms*, 266, 3081 (2008).
 48. D. Praschak, T. Bahners, and E. Schollmeyer, *Applied Physics A*, 66, 69 (1998).
 49. Q. Wei, *Journal of Materials Processing Technology*, 194, 89 (2007).
 50. D.Y. Kwok, and A.W. Neumann, *Advances in Colloid and Interface Science*, 81, 167 (1999).
 51. S.K. Kumar, and T.P. Russell, *Macromolecules*, 24, 3816 (1991).
 52. V.S. Minnikanti, and L.A. Archer, *Macromolecules*, 39, 7718 (2006).
 53. S. Wu, *J. Polym. Sci., Part C: Polym. Symp*, 19 (1971).
 54. D.K. Owens, R. C Wendt. *J. Appl. Polym. Sci*, 13, 1741 (1969).
 55. W.A. Zisman, *Advances in Chemistry*, 1, 1 (1964).
 56. Y. Kong, J.N.H., *polymer*, 43, 6 (2002).
 57. L. Mandelkern, *Crystallization of Polymers* (1964), New York: McGraw-Hill.
-

CHAPTER 5

ARTICLE 2: SURFACE MORPHOLOGY AND PROPERTIES OF TERNARY POLYMER BLENDS: EFFECT OF THE MIGRATION OF MINOR COMPONENTS⁸

Ahmad Rezaei Kolahchi, Abdellah Ajji*, Pierre J. Carreau

5.1 Abstract

In this work, the surface morphology and properties of ternary polymer blends and the migration of minor component molecules to the top surface layer of the films were studied. We used polystyrene (PS), poly (butylene adipate-co-terephthalate) (PBAT), polycaprolactone (PCL), polymethyl methacrylate (PMMA) and polylactide (PLA) as second minor phases in a blend of polyethylene terephthalate-polyethylene glycol (PET-PEG). The morphology of the ternary systems predicted using the spreading coefficient and relative interfacial energy concepts was confirmed by scanning electron microscopy (SEM) images. The surface characterization results showed a higher migration rate of PEG to the polymer/air interface in the systems with a non-wetting morphology and the highest in the PET-PS-PEG blend. Atomic force microscopy (AFM) images suggested that the high surface hydrophilicity of the PET-PS-PEG blend is due to a dendritic pattern of PEG crystals on the film surface, which were not observed for the other samples.

⁸ Submitted to The Journal of Physical Chemistry, February 2014

5.2 Introduction

Polymer blending is an inexpensive method to modify properties of polymers. Due to its simplicity, flexibility and effectiveness, polymer blending is currently attracting considerable attention as a feasible method for improving polymer surface properties [1-4]. Polymer surface modification can be performed through the migration of a polymer or small molecules to provide suitable functional groups at the surface of the film. The selective migration of one component to the surface of a solid product is usually driven by a reduction in the surface energy of the system at the polymer/air interface [3, 5-8].

It has been observed that blend morphology depends upon composition, molecular weight, and also it is influenced by the preparation method (extrusion conditions) [1, 3, 18-21]. Furthermore, the morphology can be affected by polymer/polymer interactions, determined by interfacial tensions [22-24] and many other factors. In addition, the morphology of a polymer blend near the surface layer can differ from that of the bulk, a phenomenon, which has been exploited in order to control surface properties [25, 26]. Molecular weight has a significant effect on both the final morphology of polymer blends [32] as well as the mobility of constituent molecules [27-31]. The mobility of components is also a function of concentration, since droplets and dissolved molecules are governed by different driving forces. A lower molecular weight (M_w) component can migrate faster than a higher M_w component towards the polymer/air interface to locate at the region of higher shear rates [8, 9, 32]. A good example of surface modification via polymer blending is the migration of a low M_w polymethyl methacrylate (PMMA) to the surface of a PS-PMMA blend having a relatively high M_w PS [14, 33, 34]. Moreover, it has been suggested that the migration mechanism is based on surface tension gradient and polymer-additive miscibility [35, 36].

When the system consists of two minor components, the complex morphology of ternary polymer blends may facilitate the migration of the minor components. In addition, it is reported that the morphology of ternary polymer blends is influenced by thermodynamics and kinetic factors [5-7, 37, 38]. The phase behavior and blend morphology of ternary systems can be predicted by the calculation of the interfacial tensions between the components [20, 39]. The use of spreading coefficients to predict the morphology was successfully demonstrated by Hobbs et al. [21] who used an alternate form of the Harkin equation. Each spreading coefficient shows the possibility of one phase to locate at the interface of another one [18, 19, 40]. This method is effective in predicting the position of each component between pairs of polymers. The spreading coefficient is calculated from:

$$\lambda_{ijk} = \gamma_{ij} - (\gamma_{ik} + \gamma_{jk}) \quad (5.1)$$

where γ_{ij} represents the interfacial tension for each pair of components. In the case of a ternary blend with one continuous phase, the spreading coefficient calculated via Eq. (5.1) identifies which of three possible types of phase morphology should occur at equilibrium, as illustrated in Figure 5-1: non-wetting, partial wetting and core-shell morphology. Figures 5-1a, b and c show three possible morphologies corresponding to complete wetting, in which one minor phase shares its area only with one of the others. The complete wetting morphology can take one of two forms: either as two separated droplets (Figure 5-1b), or as a core-shell structure (Figure 5-1c and a).

For example, λ_{ABC} gives the tendency of phase B to form a layer at the interface of other phases (A and C). If λ_{ABC} is positive, phase B spreads between A and C and completely wets the AC interface, while the other two will be negative. In each case of Figure 5-1a–c, one of the spreading coefficients is positive, while the other two are negative. Figure 5-1d shows the fourth

possible morphology when the three spreading coefficients are negative. In that case, none of the three polymers spreads and forms a complete layer at the interface of the other two and each polymer phase is adjacent to the other two and shares its surface area with other both components.

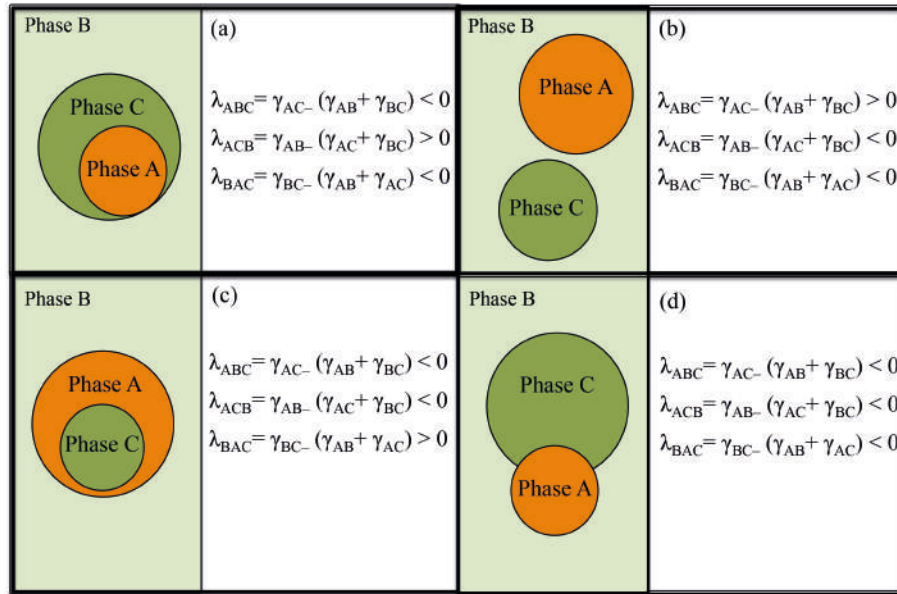


Figure 0-1: Possible morphologies in a ternary polymer blend composed of two minor phases A and C and one major phase B, as predicted by the spreading coefficient. a) Polymer A encapsulated by polymer C. b) A and C are two polymers dispersed in matrix B. c) Polymer C encapsulated by polymer A. d) Partial wetting morphology of polymer A and C.

Some useful techniques for measuring interfacial tension between immiscible polymer phases are the pendant drop [22, 24, 41], breaking thread method [23, 25, 42], deduced from the rheological behavior of the blend [43] and the geometric mean theory using Fowkes' equations, which assumes that the interfacial energies are composed of dispersion and polar components [27, 28].

A novel idea is proposed in this study to enhance the migration of one desired minor component to the surface of a polymer blend using a second high molecular weight minor polymer

component. Its role is to reduce interactions between the polymer matrix and the surface-active polymer (polymers with high energy functional groups). This method can allow the achievement of very interesting results in terms of the enhancement of polyethylene terephthalate (PET) film surface hydrophilicity via the migration of a hydrophilic polymer such as polyethylene glycol (PEG) to the film surface. Polystyrene (PS) as an immiscible polymer with PET with M_w of 300 kg/mole can be used in the PET-PEG blend. The PEG short chains ($M_w=8$ kg/mole) do not allow PS molecules to be localized at the surface layer since PEG molecules move very fast and locate at the highest stress region (extruder wall). Since it is clear that PET and PS are immiscible and have poor interfacial adhesion [44, 45], the relationship between the components of the blend is not intuitively clear, but is of practical interest due to the migration of PEG to the surface. The chemical structure of polymers, molecular weight, differences between their surface tension and crystallinity influence the migration of the minor component to the surface [8-11]. In addition the surface morphology is an important parameter that should be controlled for systems containing three polymer components [12-14]. Further, important parts of the PEG surface enrichment steps are affected by processing. The high surface tension of metal sheet die and cooling device following extrusion influence the migration as well [15-17]. Besides, the results of this study showed that the higher surface crystallinity of the PET-PEG-PS film hinders the mobility at the surface of PEG chains, and consequently they cannot easily migrate back to the bulk of the polymer blend.

The main objective of this work is to increase the hydrophilicity of PET films. In this part, the aim is to determine how the localization of hydrophilic minor components affects the surface properties of blends films. After establishing the relationship between the blend morphology and surface properties, it is hoped that novel conclusions about the relation between the surface

morphology and near-surface molecular arrangement and the migration of the components in the blends can be drawn. Therefore, the present approach consists in examining the minor component migration to the film surface of binary polymer blends and extending the analysis to ternary blends composed of PET, PEG and a second minor phase. The polymers investigated as a second minor phase are: PBAT, PCL, PS, PLA and PMMA, a set of components, which should result in a range of different morphologies.

5.3 Experimental section

5.3.1 Materials

The materials used in this study are listed according to type and manufacturer in Table 5.1.

Table 0.1: List of the materials and their characteristics

Material	Characteristics	Company
Recycled PET (R-PET)	15 mm ² thin flakes, crystalline portion of about 5% \pm 1 by weight	Lavergne Group Inc.
PEG	M _w = 8 kg/mole	Sigma Aldrich Co.
PS	Density = 1.04 g/cm ³ , M _w = 300 kg/mole, PDI = 1.06	Dow Chemical.
PLA	PLA 4032D – M _w = 210 kg/mole, PDI=1.7	Nature Works LLC, USA.
PBAT	Ecoflex, M _w = 145 kg/mole, PDI=2.6	BASF, Brazil.
PMMA	M _w = 180 kg/mole, PDI=1.4	Sigma–Aldrich.
PCL	Capa 6800, M _w =224.5 kg/mole	Perstorp Co. Ltd, Sweden.

5.3.2 Samples preparation

Before compounding, the PET, PEG, PS, PLA, PBAT, PCL and PMMA were dried at 100, 40, 70, 100, 50, 50 and 80 °C, respectively in a vacuum oven for 24 h. As a basis of comparison, dried PET was extruded using a co-rotating twin-screw extruder (CICO-TSE) of Leistritz Corp. with an *L/D* ratio of 40 (*L* = 720 mm), at a rotation speed of 100 rpm. The extruder was operated using the temperature profile set at 245, 250, 255, 255, 255 and 250 °C (from the hopper to the die).

Binary polymer blend films of PET with PS and PET with PEG were prepared by dry mixing of the polymers at the minor phase weight fraction of 5% and then fed to the extruder operating at the conditions outlined previously for the PET films. Ternary polymer blends were prepared using a master batch approach: first a binary blend of PEG and PET was produced as outlined above. The obtained master batch was dried in a vacuum oven at 60 °C for 24 h and then it was used to prepare ternary blends by dry mixing with a third component (PS, PBAT, PCL, PLA or PMMA) and then fed to the extruder. After each extrusion, the material was cooled using an air-knife placed at the exit of the sheet die.

5.3.3 Characterization

5.3.3.1 Contact angle measurements

Contact angle is a quantitative measurement of the wetting of a solid surface, defined geometrically as the angle formed by a liquid at the three-phase boundary where a solid, liquid and gas intersect. It is used to characterize the surface to a depth of approximately 0.5 nm. If the liquid is water, a low contact angle indicates a hydrophilic surface, whereas a high contact angle is the characteristic of low hydrophilicity. The contact angles were measured via a goniometer with a system of drop shape analysis, manufactured by DSA10, Krüss, Germany, using two liquids with known surface energy components on polymer film surfaces at constant temperature (20 °C). Deionized water and formamide were used to represent both polar and non-polar characteristics respectively.

A micro-syringe was used to place a liquid drop (2 μ L) on the surface and a video camera took images from the drop every 10 s. Each contact angle result is the average of a minimum of 15 measurements with a precision of $\pm 1^\circ$ from different locations of the polymer films to eliminate the errors associated with the surface heterogeneity. The measurements were carried out at

different times up to 150 days after the first measurement. The total surface energy and surface energy components were also obtained using the harmonic mean equation [45] from contact angle measurements for both liquids.

5.3.3.2 XPS analysis

The surface of samples was analyzed using a VG ESCALAB 3 MKII spectrometer manufactured by Thermo Scientific. Electrons were excited using non-monochromated Mg K α radiation at 1253.6 eV, with an experimentally determined spectral resolution of 0.7 eV and a standard error of less than 0.1 eV. The pressure in the analysis chamber was maintained at 10^{-9} Torr (1.333×10^{-7} Pa). The binding energy scale was calibrated by setting the lowest component of carbon 1s as 284.7 eV, which is the binding energy of carbon in an aromatic compound. Relative concentrations were determined by dividing the integrated intensity values by sensitivity factors taken from the Wagner Table [46]. First, the prepared films were washed with cyclohexane using an ultrasonic bath (USB) for 5 min and then washed with distilled water using USB to remove all contamination and impurities and then dried in vacuum oven. Areas of sample surfaces approximately 5 mm in diameter were analyzed. Peak fitting of the C1s and O1s core levels was carried out using the Avantage V 4.12 software. Consequently, the O/C atom ratio was estimated from the relative peak intensity of the O1s and C1s spectra.

5.3.3.3 Surface morphology

The surface and bulk morphology and also topography of the films was studied via scanning electron microscopy (SEM) and atomic force microscopy (AFM). To see the cross-section of the samples, the films were ultra-microtomed and cut with a diamond knife under cryogenic conditions. SEM observations were conducted using a Hitachi S-4700 operated at 10 kV and the samples were coated prior to the test with gold–palladium alloy by plasma sputtering for 15 s.

AFM were performed on a Dimension 3100 Nanoscope V controller from Digital Instruments Inc. (Santa Barbara, CA) in the tapping mode. ACTA Cantilevers from Applied Nano Inc. with spring constant of 42 N/m, resonance frequency of 300-400 kHz and medium oscillation damping with the set point of 75% Amplitude were used.

5.4 Results and discussion

5.4.1 Surface free energy

The surface free energy of the samples (γ_S) was obtained from Eq. (5.2), which is the combination of harmonic mean equation and Young's equation ($\gamma_S = \gamma_{SL} + \gamma_L \cos \theta$) and Eq. (5.3) [18] through measuring the contact angle of two liquids on the solid surfaces (water and Formamide in this experiment).

$$\gamma_L (1 + \cos \theta) = \frac{4\gamma_S^P \cdot \gamma_L^P}{\gamma_S^P + \gamma_L^P} + \frac{4\gamma_S^d \cdot \gamma_L^d}{\gamma_S^d + \gamma_L^d} \quad (5.2)$$

$$\gamma_S = \gamma_S^P + \gamma_S^d \quad (5.3)$$

where θ is the contact angle between liquid and solid, γ_L is the surface tension of the liquid. γ_S^d and γ_S^P are the dispersion and polar components of the surface energy of the solid and γ_L^d and γ_L^P are the dispersion and polar components of the surface tension of the liquid.

Experimentally determined surface free energies for the films of ternary blends are presented in Figure 5-2. γ_S values of samples containing PS, PBAT or PCL as the second minor phase in PET-PEG blends are the best in terms of wettability and hydrophilicity. The γ_S value of the PET film containing 5wt%PBAT and 5wt%PEG is larger than that of the PET film with 5wt%PCL and 5wt%PEG. Such a result is consistent with the larger surface tension of PBAT (see Table 5.2). Since the surface tension of PS is much less than that of PCL and PBAT, the use of PS as the second minor phase is expected to result in a lower γ_S . Surprisingly, the γ_S value of PET-

5wt%PS-5wt%PEG film is remarkably high. This indicates that another parameter besides surface energy affects the surface properties of the film.

Surface energy characterization of the samples indicates that the PET-5wt%PS-5wt%PEG film has the largest surface concentration of PEG, suggesting that the PS-containing ternary blends should have improved hydrophilicity. These desirable properties are likely to be related to composition, and consequently an attempt was made to optimize the composition of this ternary blend to maximize PEG surface coverage. To this end, blends were prepared with 3, 5 and 7wt% of PS while keeping PEG concentration constant. Blends with a constant PS concentration while similarly varying the concentration of PEG (3, 5 and 7wt%) were also prepared. As shown in Figure 5-3, the variation of either the PS or PEG content did not significantly change the contact angle, with the exception of the blend containing 5wt% PS. The PET-5wt% PS-7wt% PEG film surface presents the lowest water contact angle, around 45° . This is a remarkable result since the contact angle for the neat PET film is 79° , a 43% improvement. The contact angle of the PET film also displays a significant change of about 20 degrees when blended with 3wt%PS and 3wt%PEG. The system containing 5wt%PS was found to be very sensitive to the PEG concentration. Ultimately, 7wt% was found to be the optimum concentration for both PEG and PS in the PET-PS-PEG blends with respect to hydrophilicity as measured by water contact angle. Figure 5-3 also presents the surface energies calculated from the contact angle values for films prepared with a range of PEG and PS compositions. The highest surface energy is 54 mN/m, for the PET-5wt%PS-7wt%PEG film and the optimum concentration of PS with respect to PEG concentration at the surface is 7wt%. We also observe significant differences between the surface properties of the samples containing 3wt% and 5wt%PEG when the PS concentration is 5wt%. We conclude that a minimum PEG concentration of 5 to 7wt% is required to maximize the

surface coverage of PEG in ternary PET-PS-PEG blends containing 5wt%PS. Otherwise PEG will migrate back to the bulk from the surface layer as demonstrated by contact angle and the following XPS results.

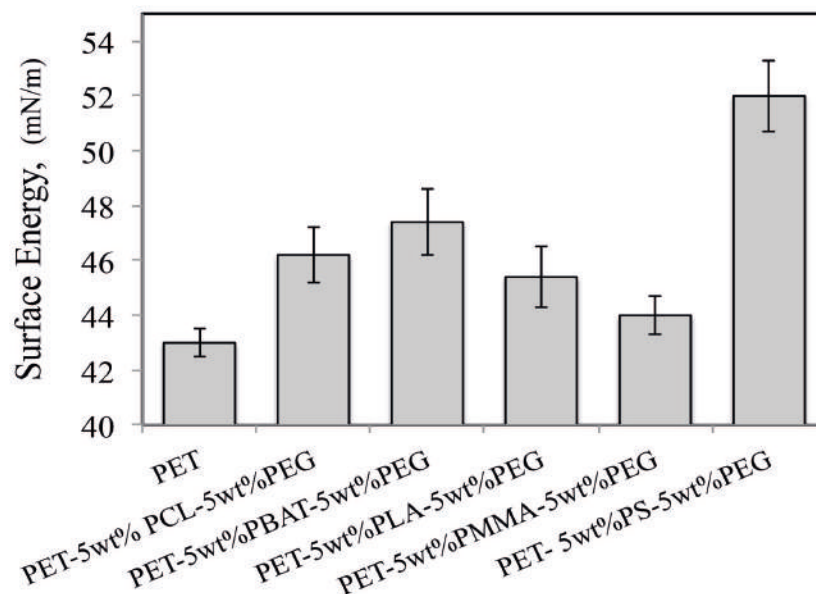


Figure 0-2: Surface free energy of samples of the neat PET and PET containing 5wt%PEG and 5wt% of a different second minor phase (PCL, PBAT or PLA, PMMA and PS).

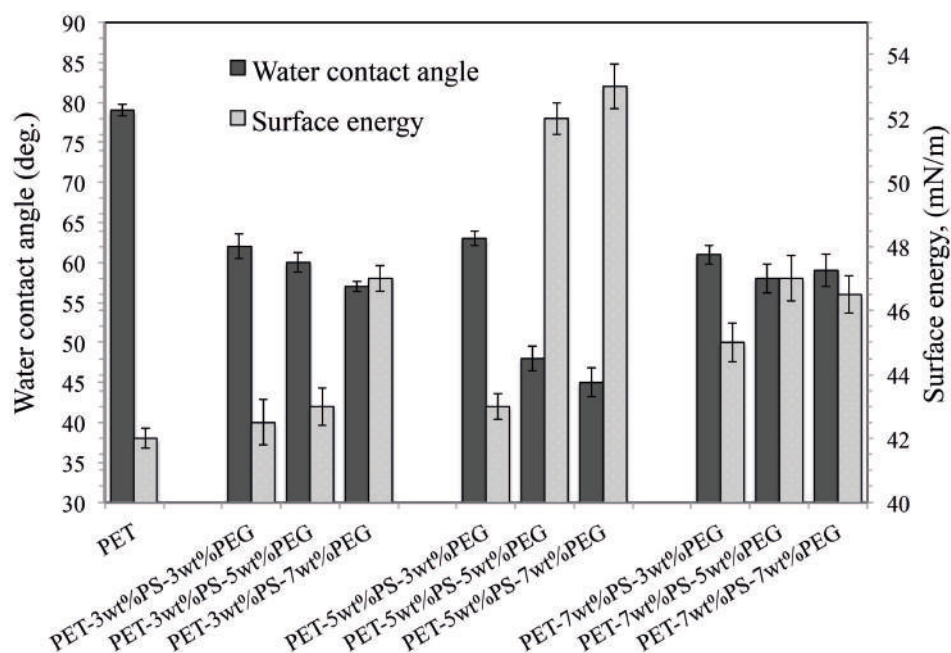


Figure 0-3: Water contact angle and surface energy of the neat PET film and prepared films with different concentrations of PET, PS or PEG.

5.4.2 Film surface morphology

Five polymers were selected (PS, PLA, PMMA, PCL and PBAT) as the second minor phase based on the calculations of the interfacial tension, which predicted that these polymers would result in all three possible morphologies (non-wetting, partial wetting and core-shell) depending on the polymer combinations. They are high molecular weight polymers in the same order of magnitude. Table 5.2 reports the interfacial tension of every pair of polymers and the spreading coefficient at the processing temperature of 255 °C. The interfacial tension between PET and other blended polymers, with the exception of PS, is quite small, varying between 0.4 ± 0.2 mN/m for PET-PCL and 1.4 ± 0.6 mN/m for PET-PLA based on our calculations. Conversely, the interfacial tension of 4.2 ± 0.3 mN/m between PET and PS is relatively high. This indicates the incompatibility of PET with PS [41,42]. With respect to PEG, good compatibility is expected with PMMA and PLA, based on interfacial tensions of 0.1 ± 0.1 and 0.7 ± 0.2 mN/m, respectively and slightly less compatibility between PEG and PBAT ($\gamma_{\text{PBAT-PEG}} = 1.7 \pm 0.1$ mN/m) and between PEG and PCL ($\gamma_{\text{PCL-PEG}} = 1.6 \pm 0.3$ mN/m). As for PET, the interfacial tension of 5.1 ± 0.8 mN/m between PEG and PS is significantly higher than that between PEG and the other polymers mentioned. Based on these interfacial tension values, a non-wetting morphology is expected for the blends containing PET as the continuous phase with PEG and either PS, PCL or PBAT as the minor phase. In contrast, PET blends with PEG and PLA is expected to display a partial wetting behavior, while a system containing PMMA as the second minor phase is expected to have a core-shell morphology with PMMA encapsulated in a PEG shell.

Scanning electron microscopy was used to observe the sample morphology and confirm the predictions based on the spreading coefficient. Figure 5-4 presents cross-sectional SEM images of different ternary polymer blend films produced from PET, PEG and a various second minor

phase polymers. A non-wetting morphology, which is characterized by segregated droplets of the two minor phases, is observed in blends containing either PBAT, shown in Figures 5-4a and b, or PS, shown in Figures 5-4c and d. For the PET-PLA-PEG blend, separate PLA and PEG droplets are partially in contact, although they primarily contact the PET matrix, as shown in Figures 5-4g and h. Figures 5-4e and f confirm the encapsulation of PMMA by PEG droplets in the blend of PET-PEG-PMMA, in agreement with the result predicted by the spreading coefficient.

The surface morphology of samples was also examined using atomic force microscopy, with resulting images presented in Figure 5-5. Figure 5-5a presents the surface morphology of PET-5wt%PBAT-5wt%PEG blend for which the PEG droplets are well distributed over the surface of the film. The same observation can be made for the surface of the PET-5wt%PCL-5wt%PEG blend, shown in Figure 5-5b. PET-5wt%PS-5wt%PEG blend displays a completely different morphology, as shown in Figure 5-5c. PEG crystals in this image form a dendritic pattern, also seen in the work of Chen et al. [46] on ultrathin films of poly (ethylene oxide)-block-poly{2,5-bis[(4-methoxyphenyl)oxycarbonyl] styrene} (PEO-b-PMPCS) for which the presence of PEO (High M_w PEG) blocks led to the formation of dendritic crystals. Wang et al. [47,48] observed the crystallization of PEO-PMMA films and reported a variety of structures attributed to the environment and processing conditions and they reported in a vacuum, fractal-like branches of PEG crystals. They also observed dendritic growth during the crystallization of PEO in PEO-PMMA blends. In Figures 5-5d (image of the surface of the PET-5wt% PEG-5wt%PMMA film) and 5-5e (images of the surface of the PET-5wt%PLA-5wt%PEG blend), PEG droplets are poorly distributed and they probably have coalesced.

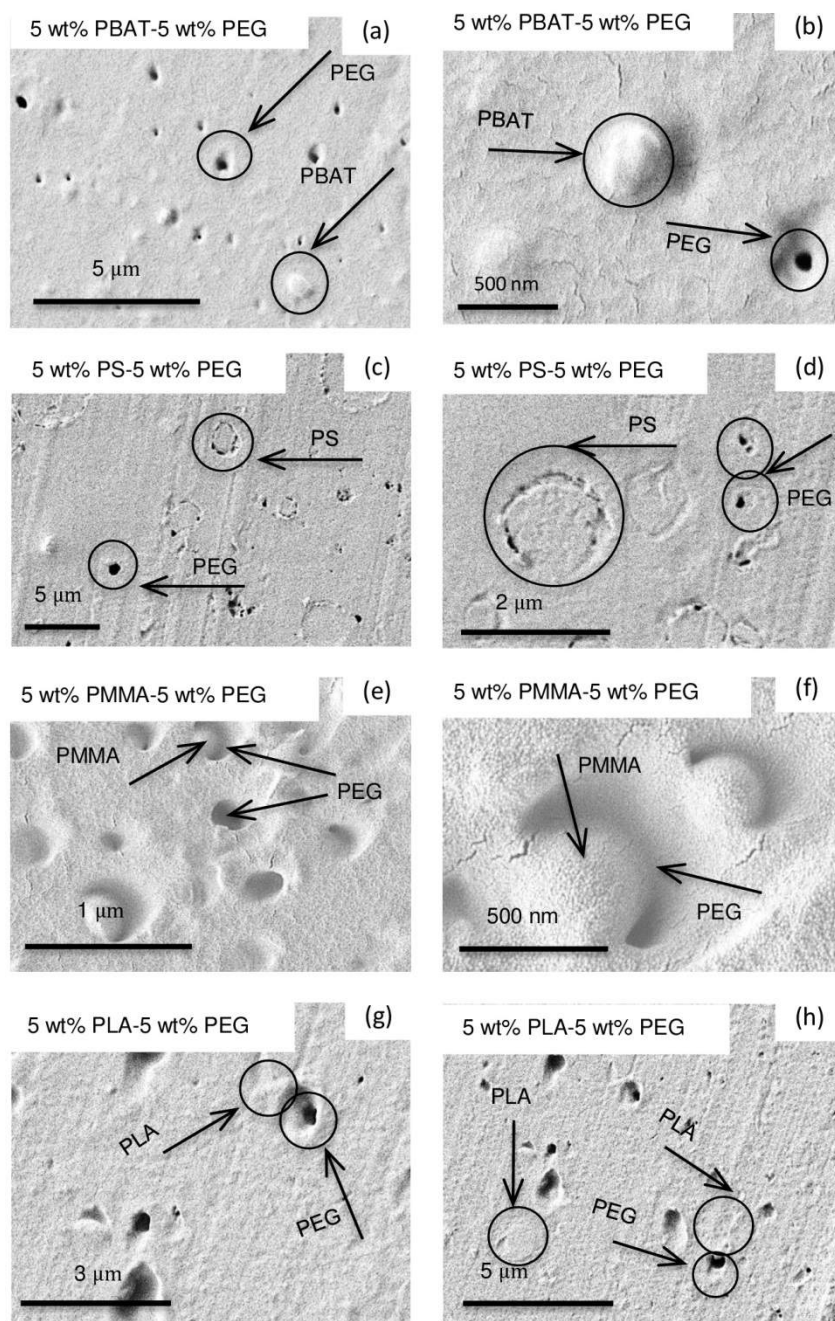


Figure 0-4: SEM cross-sectional images of the ternary polymer blend films composed of 90wt%PET, 5wt%PEG and 5wt% of the second minor phase. a,b) PET-PBAT-PEG. c,d) PET-PS-PEG. e,f) PET-PMMA-PEG. g,h) PET-PLA-PEG.

Table 0.2 : Interfacial tension of pairs of polymers in PET blends and spreading coefficient

Minor phases C	Surface tension, γ_s at 250°C (mN/m)	Interfacial tension (mN/m)		Spreading coefficient			Morphology type in Figure 1
		PET B	PEG A	λ_{ABC}	λ_{ACB}	λ_{BAC}	
PMMA	27.9	0.9 ± 0.3	0.1 ± 0.1	-1.6	PMMA	27.9	0.9 ± 0.3
PCL	37.8	0.4 ± 0.2	1.6 ± 0.3	0.4	PCL	37.8	0.4 ± 0.2
PBAT	39.8	0.7 ± 0.2	1.7 ± 0.1	0.3	PBAT	39.8	0.7 ± 0.2
PS	27.5	4.2 ± 0.3	5.1 ± 0.8	0.1	PS	27.5	4.2 ± 0.3
PLA	33.3	1.4 ± 0.6	0.7 ± 0.2	-1.5	PLA	33.3	1.4 ± 0.6
PEG	30.8	0.8 ± 0.1	---	---	PEG	30.8	0.8 ± 0.1

The variation of PEG crystal pattern between samples suggests that the selection of the second minor component influences the characteristics of the PEG crystals in the blend. When PEG crystals develop as a dendritic pattern, they could cover a greater portion of the film surface. Therefore, the film surface properties are closer to those of PEG surface and are more hydrophilic than PET film.

In order to explain trends in surface properties as a function of composition, the morphologies of film surfaces were characterized using AFM, with results presented in Figure 5-6. As can be seen in the graph, PEG developed a dendritic distribution, characteristic of the special PEG crystallization on the surface of ternary blend films. Unlike the images of blends containing 5 or 7wt%PEG, images of the PET-5wt%PS-3wt%PEG film surface only exhibit very small fractals accompanied by a relatively large number of PS droplets. At higher PEG concentrations, the surfaces have greater PEG coverage, consisting exclusively of dendrite shaped crystals.

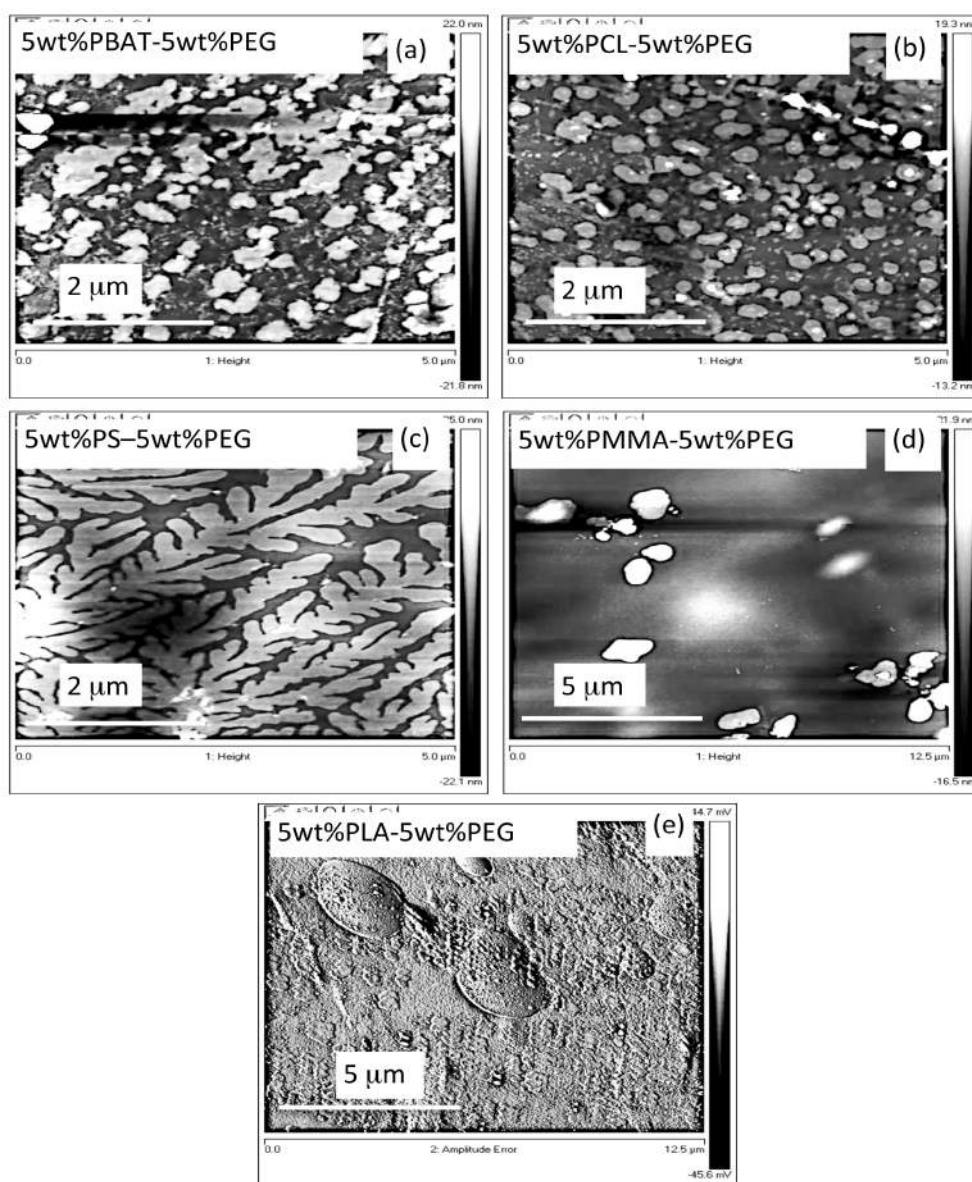


Figure 0-5: AFM images from the surface morphology of the samples containing PET, 5wt%PEG and 5w% of the second minor phase. a) PET-PBAT-PEG. b) PET-PCL-PEG. c) PET-PS-PEG. d) PET-PMMA-PEG. e) PET-PLA-PEG.

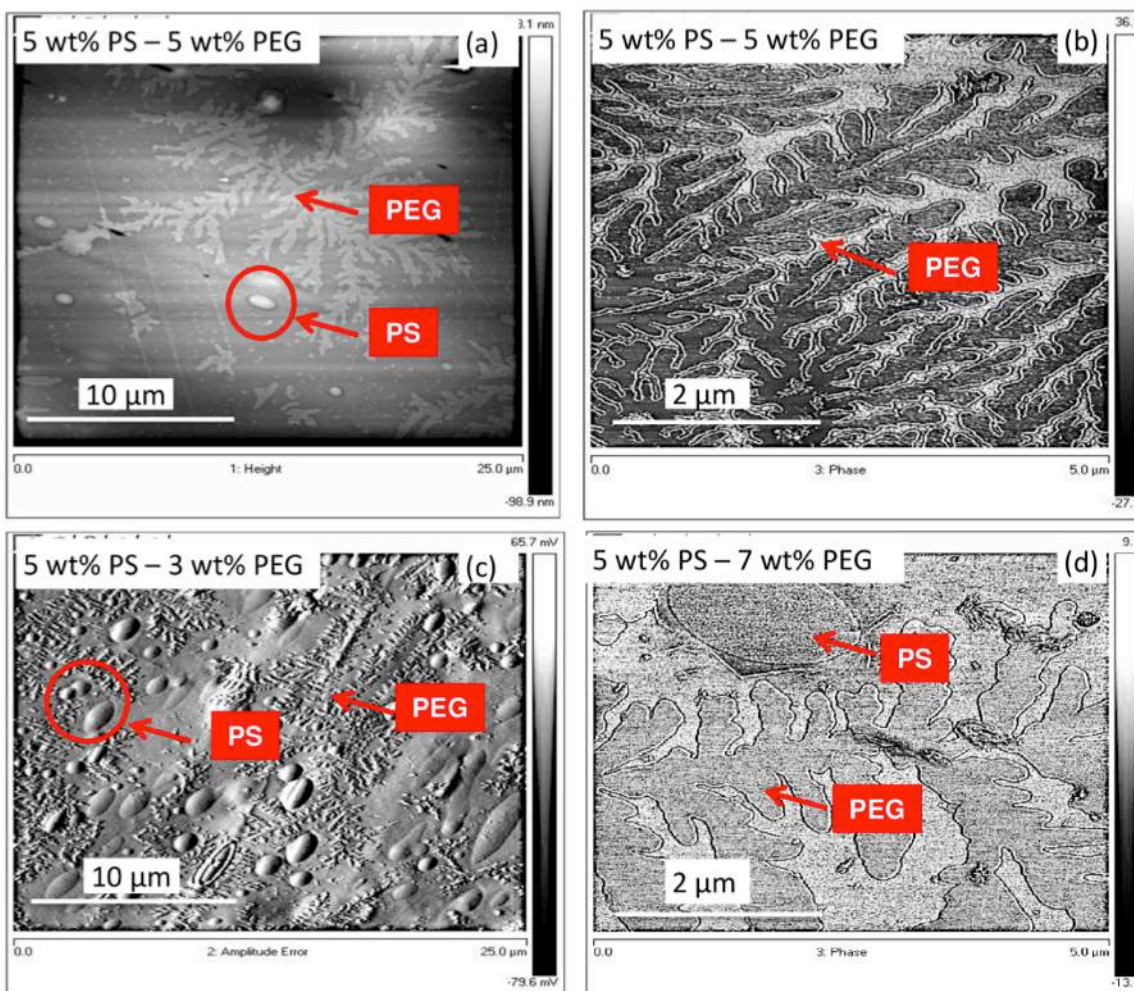


Figure 0-6: AFM images from the PET-PS-PEG film surfaces for different concentrations of PS and PEG. a,b) PET-5wt%PS-5wt%PEG. c) PET-5wt%PS-3wt%PEG. d) PET-5wt%PS-7wt%PEG.

5.4.3 Surface oxygen content

The atomic composition of the ternary blend film surfaces of different concentrations of PEG and PS were characterized using XPS to determine if a correlation existed between the surface free energy (contact angle) and the chemical composition of the surface. The O/C atom ratios present on the surfaces of ternary blend films as well as of the original PET film were calculated from the

XPS peak intensities and are reported in Figure 5-7. A higher O/C atom ratio is observed for the samples containing at least 5wt%PEG in the blend compared to samples containing less than 5wt%PEG, with PS concentration kept at 5wt%. The O/C atom ratio reaches a maximum of 33%, for the blend containing 5wt%PS and 7wt%PEG, increasing from 20% for the original PET film. The large increase in oxygen content at the surface after blending with PS and PEG is indicative of increasing PEG molecules on the polymer film. A large increase in O/C ratio is observed in the PET- 5wt%PS-7wt%PEG blend, supporting the conclusion that this blend is closest to the optimal composition. The top inset in the Figure 5-7 shows XPS survey spectra of PET (left side) and PET-5wt%PS-5wt%PEG (right side).

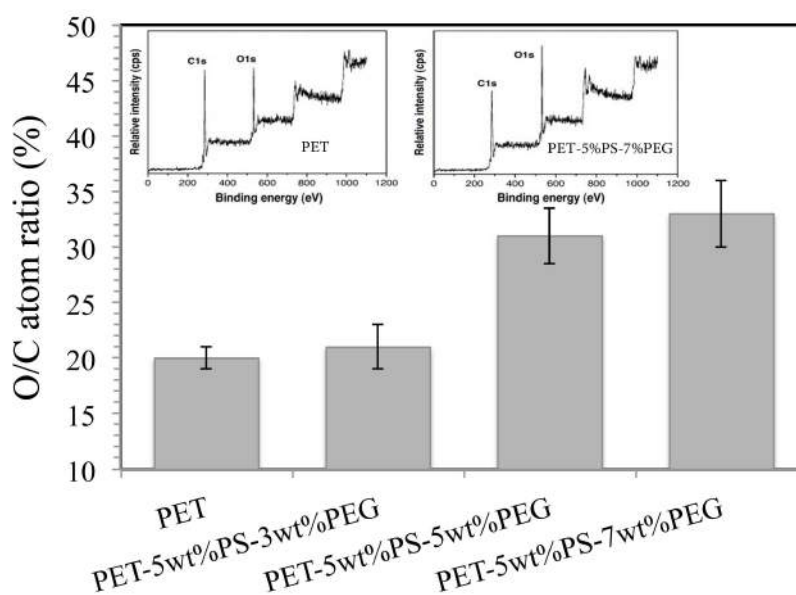


Figure 0-7: O/C atom ratio of the neat PET, PET-PS-PEG (92-5-3wt%), PET-PS-PEG (90-5-5wt%) and PET-PS-PEG (88-5-7wt%) film surfaces. The top inset shows XPS survey spectra of PET (left side) and PET-5wt%PS-5wt%PEG (right side).

5.5 Conclusion

In this work, we found that the incidence of non-wetting morphology (two separated dispersed droplets) in a ternary polymer blend promotes the migration of short chains of the minor phase

(PEG in this case) to the surface layer of the polymer. A ternary blend composed primarily of PET with 5wt%PMMA and 5wt%PEG, had a smaller surface concentration of PEG compared to other blends where the dispersed phases exhibited a core/shell morphology.

PEG was also found to have more surface coverage when its crystals formed dendritic patterns, as in the case of the PET-PS-PEG films. In addition, the calculated surface energy showed that the samples with higher surface free energy were those with the two separated droplets morphology of the minor phases in PET matrix, hence, of enhanced surface hydrophilicity. The PET-PS-PEG film had the largest surface energy value (52 mN/m) among all samples. This could be due to a special surface pattern of the PEG crystals as detected by AFM.

Finally, this study revealed that a minimum PEG concentration of 5wt% is necessary to maximize the surface crystallinity for blends containing 5wt% PS. The optimum concentration for both PEG and PS in the PET-PS-PEG blends was also 7wt%. Concentrations of PEG or PS larger than 5wt% would not change significantly the surface concentration.

5.6 Acknowledgment

The authors wish to thank helpful support and discussions with A. Yaghoobi, F. Tofan, D. Davidescu. Financial support from NSERC (Natural Science and Engineering Research Council of Canada) and Lavergne Group Inc. is gratefully acknowledged.

5.7 References

1. Khodabakhshi, A.R. *Separation and Purification Technology* **2012**, 90, 10-21.
2. Sionkowska, A. *Progress in Polymer Science* **2011**, 36, 9, 1254-1276.

3. Xue, M.L. *European Polymer Journal* **2007**, 43, 9, 3826-3837.
4. Xiaoying, L. *Biomedical Materials* **2009**, 4, 4, 44103.
5. Peña, G. *Polymer International* **2003**, 52, 9, 1444-1453.
6. Valera, T.S.; Morita, A.T.; Demarquette, N.R. *Macromolecules* **2006**, 39, 7, 2663-2675.
7. Li, L.P.; Yin, B.; Yang, M.-B. *Polymer Engineering & Science* **2011**, 51, 12, 2425-2433.
8. Reichart, G.C. *Macromolecules* **1997**, 30, 11, 3363-3368.
9. Almdal, K.; Hillmyer, M.A.; Bates, F.S. *Macromolecules* **2002**, 35, 20, 7685-7691.
10. Bousquet, A. *Macromolecules* **2008**, 41, 4, 1053-1056.
11. Lee, J.S.; Foster, M.D.; Wu, D.T. *Macromolecules* **2006**, 39, 15, 5113-5121.
12. Dadmun, M. *Macromolecules* **1996**, 29, 11, 3868-3874.
13. Landry, C.J.T.; Yang, H.; Machell, J.S. *Polymer*, **1991**, 32, 1, 44-52.
14. Luzinov, I.; Pagnouille, C.; Jérôme, R. *Polymer*, **2000**, 41, 19, 7099-7109.
15. Yekta-Fard, M.; Ponter, A.B. *Journal of Adhesion Science and Technology*, **1992**, 6, 2, 253-277.
16. Senshu, K. *Langmuir* **1999**, 15, 5, 1754-1762.
17. Shin, J.S. *Langmuir* **1999**, 16, 4, 1882-1888.
18. van Zyl, A.J.P. *Macromolecules* **2003**, 36, 23, 8621-8629.
19. Kwamena, N.O.A.; Buajarern, J.; Reid, J.P. *The Journal of Physical Chemistry A* **2010**, 114, 18, 5787-5795.
20. Reignier, J.I.; Favis, B.D. *Macromolecules* **2000**, 33, 19, 6998-7008.

21. Hobbs, S.Y.; Dekkers, M.E.J.; Watkins, V.H. *Journal of Materials Science* **1988**, 23, 4, 1219-1224.
22. Kamal, M.R.; Lai-Fook, R.; Demarquette, N.R. *Polym. Eng. Sci.* **1994**, 34, 24, 1834-1839.
23. Elmendorp, J.J. *Polymer Engineering and Science* **1986**, 26, 6, 418-426.
24. Demarquette, N.R.; Kamal, M.R. *Polymer Engineering & Science* **1994**, 34, 24, 1823-1833.
25. Son, Y. *Polymer* **2001**, 42, 3, 1287-1291.
26. Omonov, T.S.; Harrats, C.; Groeninckx, G. *Polymer* **2005**, 46, 26, 12322-12336.
27. Wu, S. *Journal of Polymer Science Part C: Polymer Symposia* **1971**, 34, 1, 19-30.
28. Fowkes, F.M. *Colloids and Surfaces* **1990**, 43, 2, 367-387.
29. Bell, J.R. *Macromolecules* **2010**, 43, 11, 5024-5032.
30. Geoghegan, M. *Journal of Polymer Science Part B: Polymer Physics* **1995**, 33, 8, 1307-1311.
31. Tanaka, T. *Langmuir* **2008**, 24, 21, 12267-12271.
32. Lee, H.; Archer, L.A. *Polymer* **2002**, 43, 9, 2721-2728.
33. Tchoudakov, R. *Polymer Engineering & Science* **1996**, 36, 10, 1336-1346.
34. Luo, Y.; Yu, W.; Xu, F. *Polymer-Plastics Technology and Engineering* **2011**, 50, 11, 1084-1090.
35. Lee, H.; Archer, L.A. *Macromolecules* **2001**, 34, 13, 8.
36. Chen, W.a.T.J.M. *Macromolecules* **1999**, 37, 7, 6.

37. Frank Curtis, W.; Zin, W.c. *Morphology in Miscible and Immiscible Polymer Blends*, in *Photophysics of Polymers* **1987**, American Chemical Society. p. 18-36.
38. Lin, C.C. *Macromolecules* **1996**, 29, 2, 661-669.
39. Guo, H.F. *Polymer* **1997**, 38, 4, 785-794.
40. Virgilio, N.; Marc-Aurèle C.; Favis,B.D. *Macromolecules* **2009**, 42, 9, 3405-3416.
41. Anastasiadis, S.H. *Journal of Colloid And Interface Science* **1987**, 119, 1, 55-66.
42. Cho, K., *Polymer* **1996**, 37, 7, 1117-1122.
43. Lacroix, C.B.; M; Carreau, PJ; Favis, BD; Michel, A. *Polymer* **1996**, 37, 14, 9.
44. Gauthier, F.; Goldsmith, H.L.; Mason,S.G. *Rheologica Acta*, **1971**, 10, 3, 344-364.
45. Elmendorp, J.J. *Polymer Engineering & Science*, **1986**, 26, 6, 418-426.
46. David Briggs, M.P.S. *Practical Surface Analysis by Auger and X-Ray Photoelectron Spectroscopy* **1990**: Wiley

CHAPTER 6

ARTICLE 3: SURFACE ROUGHENING OF PET FILMS THROUGH BLEND PHASE COARSENING⁹

Ahmad Rezaei Kolahchi, Pierre.J. Carreau, Abdellah Ajji*

6.1 Abstract

In this study, a novel method to increase the surface roughness of polyethylene terephthalate (PET) films is proposed. The mechanism of phase coarsening at the surface in extruded thin films of PET blended with low concentrations of polystyrene (PS) was investigated. A small amount of poly (hydroxyl ether) of bisphenol A (Phenoxy resin, PKHH) was found to significantly increase the surface roughness due to its effect on the PS-PET interfacial tension. X-ray photoelectron spectroscopy (XPS) results indicated that in the presence of PKHH, PS droplets migrated spontaneously towards the surface of the polymer film. An increased local concentration of PS near the surface took the form of encapsulated droplets. Above the flow temperature of the blend, the local concentration of PS eventually reached a level where a co-continuous morphology occurred, resulting in the instabilities on the surface of the film. The adhesion properties of films with various roughnesses were determined using a pull-off test and found to be significantly increased, which suggested that co-continuous morphology and the coarsening process increased the adhesive properties of the film.

⁹ Published in ACS Applied Materials & Interfaces, April 2014

6.2 Introduction

Despite the remarkable mechanical and physical properties of polyesters [1-4], poor wettability and surface energy means that this class of polymers does not adhere to most materials [5-8], precluding its use in applications such as printing and dyeing without previous surface treatment. Adhesion between two contacting surfaces depends on chemical bonds and mechanical interactions [9-11]. It increases in response to improved chemical and physical interactions based in part on an increase of surface energy [12-15] as well as roughness of solid surfaces [16-19, 68]. Many different theories and models have been proposed to measure adhesion between two surfaces based on bond formation and interface interactions [20-23]. One such model proposes that adhesion is a contribution of Lifshitz-van der Waals (LW) and acid-base (AB) interactions [22,23]. According to van Oss et al. [24], such interaction can be described in quantitative terms, using the work of adhesion:

$$W_a = W_a^{LW} + W_a^{AB} \quad (6.1)$$

where W_a is the work of adhesion while W_a^{LW} and W_a^{AB} represent the LW and AB contributions to the work of adhesion, respectively. In addition to LW and AB interactions, the work of adhesion was also shown to increase in rough surfaces due to increased surface contact [25-27]. The effect of roughness manifests itself in a number of ways. In the case of a liquid-solid interface, the liquid surface can anchor physically into the solid by penetrating into pores or by binding against concavities, a phenomenon referred to as mechanical interlocking (MI). Figure 6-1 shows a schematic of surface roughness and liquid anchoring in pores. Since MI increase the work of adhesion regardless of LW or AB contribution, Eq. (6.1) must be modified to account for this third factor:

$$Wa = Wa^{LW} + Wa^{AB} + Wa^{MI} \quad (6.2)$$

where Wa^{MI} is the MI contribution to the work of adhesion [28-30]. There are many examples of experimental work showing the effect of surface roughness on bonding area and adhesion [31-35].

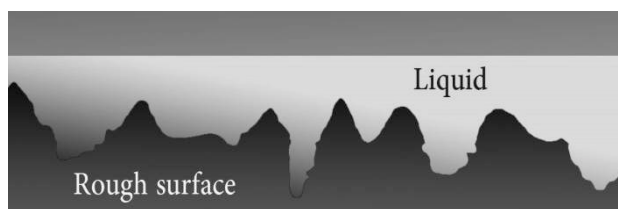


Figure 6-1: Schematic illustration of roughness and liquid anchoring on a solid surface

Several techniques exist for roughening polymer substrates, including but not restricted to: etching the polymer surface by dissolving some components from the surface [36-38], immersing in a reactive gas [39], bombardment by ions [40,41] and thermal and capillary fluctuations [42,43]. As yet, no roughening technique has been reported for use in conventional melt processing operations such as extrusion. Such a technique would be of interest due to its easy and cost-effective process.

Surface roughening can be achieved during melt processing if one of the components of a polymer blend naturally migrates toward the film surface, resulting in a composition gradient across the thickness of the film. This can occur for a number of reasons such as the buoyancy forces related to the density of the polymer components or due to segregation resulting from the applied shear developed by processing.

The surface roughening in polymer blends film occurs more efficiently through forming co-continuous network morphology of two phases at the surface of the film. It is found that under flow, coalescence of droplets and the formation of a co-continuous morphology are dependent on

viscoelastic parameters whereas under static conditions, the concentration controls the morphology (Utracki, L. 1991, Andradi, L. 1995). Dependent on the concentration of the phases, blends can evolve through different morphologies with their own characteristic wavelength ($\Lambda(t)$) (Sholten, E. 2005). Cahn and Hilliard (Cahn, J.W. 1958) proposed a theory describing the stage of the phase separation during which wavelengths grow in time. These wavelengths alteration can be obtained from radial average of a 2D fast Fourier transform (FFT) of the AFM topographical images or the intensity at different characteristic wavenumbers (q^*) using light scattering technique. The late stage coarsening of the phases is characterized by a power-law dependence of the domain size. The coarsening can be occur either by migration of droplets through the matrix or gradient in the capillary forces. In the former, coarsening of the domains is explained by $q^* \propto t^{1/3}$ and in the latter, it is described by $q^* \propto t^1$.

When a polymer blend with a co-continuous morphology is annealed above its flow temperature, the phase structure can become coarser to minimize the system free energy. For the case where one of the interfaces is air, the internal coarsening leads to roughening of the film at that surface. Surface roughening through phase coarsening in binary mixtures is a technique that has been widely studied, leading to rapid technological enhancements, particularly in thin polymer films [44-49].

In this study we investigate (1) the mechanisms for roughening polymer film surface and (2) the effect of induced roughness on polymer film surface adhesion and dyeability properties. We investigate the novel idea of roughening PET films based on the migration phenomenon that drives the system into a co-continuous morphology for a low concentration of the minor component. A method for the spontaneous migration of one desired minor component to the surface of a molten blend is applied. Then through annealing and by increasing concentration of

the minor component at the surface layer, a co-continuous morphology of the PET-PS at the surface of the blend is created. The coarsening of PS droplets occurs by coalescence through which the free energy of the blend is minimized by reducing the interfacial area between the phases.

In this work, PKHH and polystyrene (PS) were used as minor phases in blends with a PET matrix. PKHH can reduce the size of PS droplets and acts as a compatibilizer for PET due to its chemical structure. It tends to act as a hydrogen bond donor, which increases its interactions with the polyester, while the aromatic groups of the phenoxy resin probably coordinates with those of PS. Droplet size is an important variable, since small droplets are able to migrate more quickly to the surface layer in response to shear in the extruder.

Here, annealing was used to determine the kinetic behavior of the migration of PS to the subsurface layer of the film. We investigated the kinetics of phase segregation and coarsening by 2D fast Fourier transforms (FFT) of the AFM images. To quantitatively analyze the evolution of the surface roughness, the root-mean-square surface smoothness (RMS) of the binary polymer blend films at thin surface layer and the characteristic wavenumber were introduced. The FFT transformed data exhibit a maximum intensity at a characteristic wavenumber q_{\max} .

6.3 Experimental section

6.3.1 Materials and sample preparation

For the matrix, we used a recycled PET (R-PET) supplied by Lavergne Group Inc. in thin 15 mm² flakes. It contains a white crystalline portion of about 5% by weight. The other polymers were: PS Styron 663 with density 1.04 g/mL and molecular weight of 300 kDa and PDI=1.08 (supplied by Dow Chemical), PKHH phenoxy resin with M_w of 52 kDa (supplied by InChem

Corp.) and deuterated PS (dPS) with M_w of 298 kDa and PDI=1.06 (purchased from Scientific Polymer Products Inc.). For adhesion tests, a solvent borne alkyd paint (Brillant) was purchased from Timpe & Mock GmbH & co.

Before blending, PET, PS and PKHH were dried at 100, 80 and 100° C respectively in a vacuum oven for 24 h. To prepare a benchmark PET film, we extruded the dried PET using a co-rotating twin-screw extruder (CICO-TSE) manufactured by Leistritz Corp. with an L/D ratio of 40 ($L = 720$ mm), at a rotation speed of 100 rpm. The extruder was operated using a temperature profile of 245, 250, 255, 255, 250 ° C (for the different zones from the hopper to the die). Binary polymer films (PET/PS and PET/PKHH) were prepared by direct solid mixing of PET with 5wt% of the other component and then extruded under the conditions defined above. The ternary polymer blend film (90wt%PET-5wt%PKHH-5wt%PS) was prepared using direct solid mixing of the three components before feeding into the extruder and operated under the same conditions. After each processing, the polymer films were cooled using an air-knife right after the exit of the die. Annealing was performed isothermally in a vacuum oven at temperatures in the range of 240 to 260 °C for periods ranging from 20 to 1200 s followed immediately after by quenching to 0 ° C (into ice-water).

6.3.2 Characterization

6.3.2.1 X-ray photoelectron spectroscopy (XPS)

Blends films surfaces were analyzed via XPS using a VG ESCALAB 3 MKII spectrometer. Electrons were excited using a non-monochromatic Mg K α x-ray source (1253.6 eV), with an experimentally determined spectral resolution of 0.7 eV and a standard measurement error of less than 0.1 eV. Pressure in the chamber was maintained at 10^{-9} Torr ($1.333 \cdot 10^{-7}$ Pa) and the

main carbon peak was fixed to a binding energy of 284.7 eV. Relative concentrations were determined by dividing integrated intensity values by sensitivity factors taken from the Wagner table [50]. An area of approximately 5 mm in diameter of sample surface was analyzed. Survey scans (0-1100 eV) and narrow scans (high resolution) of the C1s and O1s regions were obtained. Peak fitting of the C1s and O1s core levels was carried out using the Advantage V 4.12 software. Consequently, the O/C atom ratio was estimated from the relative peak intensities of the O1s and C1s spectra.

6.3.2.2 Surface morphology

The surface morphology and topography of the films was studied via scanning electron microscopy (SEM) and atomic force microscopy (AFM). SEM observations were conducted using a Hitachi S-4700 operated at 10 kV and the samples were coated prior to the test with gold–palladium alloy by plasma sputtering for 15 s. AFM imaging was performed on a Dimension 3100 Nanoscope V controller from Digital Instruments Inc. (Santa Barbara, CA) in the tapping mode. ACTA Cantilevers from Applied Nano Inc. with a spring constant of 42 N/m, resonance frequency of 300-400 kHz and medium oscillation damping with the set point of 75% Amplitude were used. Samples were ultra-microtomed to observe morphology of the cross-section, using a diamond knife at room temperature.

6.3.2.3 Depth profiling

Depth profiling was used to determine the concentration of the components of a blend film as a function of depth when the information on the wetting properties of multicomponent polymer mixtures was required. It is a useful technique to analyze the segregation of the components in an unstable blend if this segregation corresponds to a wetting layer. By this technique the elements below the surface region, layer by layer are determined in the forward direction from a depth

ranging from 0 to 5000 Å. One of the direct depth profiling method is MeV ion beam scattering. A beam of ions produced by an accelerator is incident on the sample. The ions are scattered from the surface and the emitted particles due to fragments from collision or nuclear reaction are detected. Three MeV ion beam techniques are of particular importance including Rutherford backscattering, He nuclear reaction analysis (NRA) and forward recoil spectrometry (FRES), which is also referred to as elastic recoil detection (ERD) analysis.

In this study, FRES was performed on a model 5SDH Pelletron tandem accelerator (National Electrostatic Corporation, WI), interfaced with a scattering chamber. The technique has been described elsewhere [51]. Briefly, 1.51 MeV 4He^+ ions impinge on a target at an angle 78° with respect to the normal of the sample. The H and D atoms in the target surface are forward scattered and detected. The SIMNRA analysis program 30 version 5.02, was used to analyze the spectra [52].

6.3.2.4 Adhesion test

One of the aims of this work is to investigate the effect of roughness created through polymer blending on the adhesion of paint on the surface of the polymer. In this investigation, pull-off test can be used to measure the adhesion strength between coating layers. The pull-off adhesion test is a quantitative technique in which a metal surface called a dolly is bonded to the surface in question using an epoxy resin. The pull-off tests were performed with an automatic PosiTest® Pull-off Adhesion Tester (PosiTest At-A from DeFelsko Corp., USA) in accordance with ASTM D4541 and ISO 4624 under constant stress and fixed rate of loading of 1 MPa/s. A schematic of this test method is shown in Figure 6-2. In this method, an aluminum made dolly is glued to the specimen whose adhesion is to be tested, and a tensile load is applied until failure. The tensile force required breaking the bond between the dolly and the surface is then calculated. We used

aluminum dollies with a diameter of 10 and 25 mm and a two-component epoxy-based adhesive (Araldite 2011) to glue the dollies to the test specimens. This tester exerts tensile loads generated by an electrical hydraulic pump. In this experiment the PosiTest® pull-off adhesion tester was used to evaluate the adhesion of alkyd paint to the prepared film surfaces.

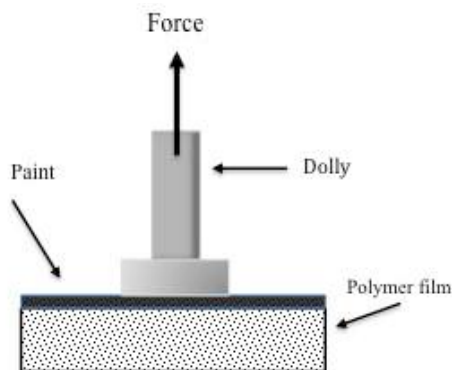


Figure 6-2: Schematic image of pull-off adhesion test

6.3.2.5 Measurement of interfacial tension

Films of PET of 0.5 mm thickness were pressed between two metal plates on a Carver laboratory press at 250°C. The PS and PKHH fibers were prepared manually. The fiber diameters ranged from 40 to 100 μm . The fibers were cut to 25 mm lengths and annealed at 60°C for about 24 h in a vacuum oven to remove any residual stress. The breaking thread technique was used to measure the interfacial tension between PET and PKHH and PS at 200 and 240°C. In the breaking thread method, the interfacial tension between two polymers can be measured by following the initial stages of breakup of a fiber of one of the polymers sandwiched in the other one to form small droplets as a function of time [63]. A Mettler hot-stage model FP 82 HT connected to a FP 90 central processor and to a Nikon transmission optical microscope was used. The tests were conducted for two PET films and a thread of PS or PKHH was sandwiched between the PET films mounted on glass slides and then placed under the microscope of a hot stage. The

temperature of the hot stage was raised to the desired temperatures and periodic digital images from the microscope were captured. At least 15 series of measurements were carried out. Details about the measurement and calculations of interfacial tension were reported elsewhere [54]. Figure 6-3 shows sinusoidal distortion on the PS thread embedded in the PET matrix.

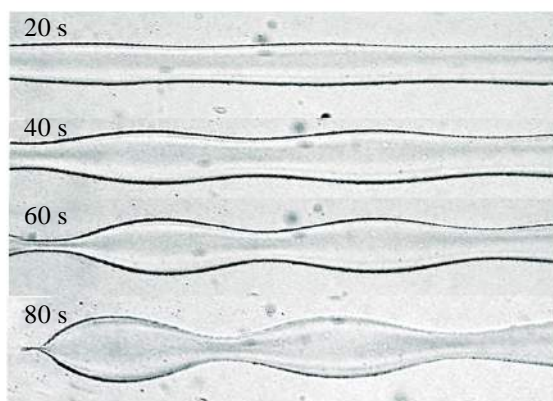


Figure 6-3: Sinusoidal distortions on the PS thread with diameter $55\ \mu\text{m}$, embedded in the PET matrix. The measurement was performed at $240\ ^\circ\text{C}$; the times at which subsequent photographs were taken are: $t=20, 40, 60, 80\ \text{s}$.

6.4 RESULTS AND DISCUSSION

6.4.1 XPS analysis

XPS measurements were performed with $0.1\ \text{eV}$ steps on the film samples to determine the relative content of carbon and oxygen atoms on their surfaces. The C1s spectrum has been fitted with three distinctly resolved peaks attributed to carbon atoms located in benzene rings (C marked with I in Figure 6-4-a), carbon bonded to oxygen (C marked with II in Figure 6-4-a) and ester atoms group (C marked with III in Figure 6-4-a) identified in the chemical structure of PET shown in Figure 6-4-a. The oxygen (O1s) spectrum was also fitted with two contributions: carbonyl oxygen (O marked with I in Figure 6-4-a) and singly bonded oxygen (O marked with II in Figure 6-4-a). The XPS spectra of C1s and O1s for neat PET film surface, polymer blend of

PET-5wt%PS-5wt%PKHH and the blend of PET-5wt%PS and also the XPS spectra of O1s for the samples are observed in Figure 6-4-b from 1 to 6 respectively. Relative abundance of carbon and oxygen atoms and the types of bonds they form were determined from the area of peaks corresponding to those identified previously. Table 6.1 shows the relative contents of the different types of oxygen and carbon for the neat PET and the blend films. The CI peak at a binding energy of 284.8 eV, which corresponds to carbon atoms in phenyl rings (C-H and C-C) for PET-5wt%PS-5wt%PKHH, changes significantly compared to the same spectrum for the neat PET film surface whereas for the binary blend, it is almost the same as for the neat one. Also, CII and CIII peaks remarkably decrease for the ternary blend while OI/OII ratio remains almost constant for all samples. Additionally, the total concentration of oxygen molecules decreases from 27.6 to 15.9% for PET-PS-PKHH blend, while there is no significant change for the binary one compare to neat PET film. Since PKHH chains contain two -C-O- and one -OH functional groups with almost 17% O/C ratio, the changes indicate the presence of more PS at the top layer of few nanometers (analytical depth of XPS) of the surface of the film. The results indicate that, at a given concentration of the minor phases, the surface layer of the film is enriched with PS, while PKHH is less apparent in this layer. No significant change in the surface concentration of carbon and oxygen of the PET-PS film indicates that there is no remarkable movement of PS molecules to the surface of the film. The solubility parameter of the phenoxy resin implies more compatibility with polar materials such as polyesters and nylons, but less compatibility with acrylics, olefins, and vinyls. Measurements of the interfacial tension between PKHH and PET (approximately 0.4 ± 0.2 mN/m) and between PET and PS (approximately 4.2 ± 0.8 mN/m) explain the tendency of PKHH to mix well with PET, and the tendency of PS to migrate from the bulk of the polymer to the surface layer during the extrusion process. It should be noted that the surface

free energy of PET and PS are 44.6 (mN/m) and 40.7 (mN/m) respectively at 20 °C [67]. Therefore, it can be concluded from XPS results that PS is preferentially present at the surface layer of the polymer blend.

Table 6.1: High-resolution XPS spectra of PET and PET-5wt% PS-5wt% PKHH film surfaces.

		C1s			O1s		C	O
		CI	CII	CIII	OI	OII		
PET	Peak BE (eV)	284.7	286.4	288.7	531.7	533.1	72	27.6
	At. %	47.7	12.9	11.8	14	13.6		
PET-5wt%PS- 5wt%PKHH	Peak BE (eV)	284.7	286.6	288.7	531.9	533.3	84.1	15.9
	At. %	68.5	8.7	6.9	8.1	7.8		
PET-5wt%PS	Peak BE (eV)	284.7	286.6	288.6	531.7	533.3	73.4	26.6
	At. %	48.3	13.7	11.4	13.5	13.1		

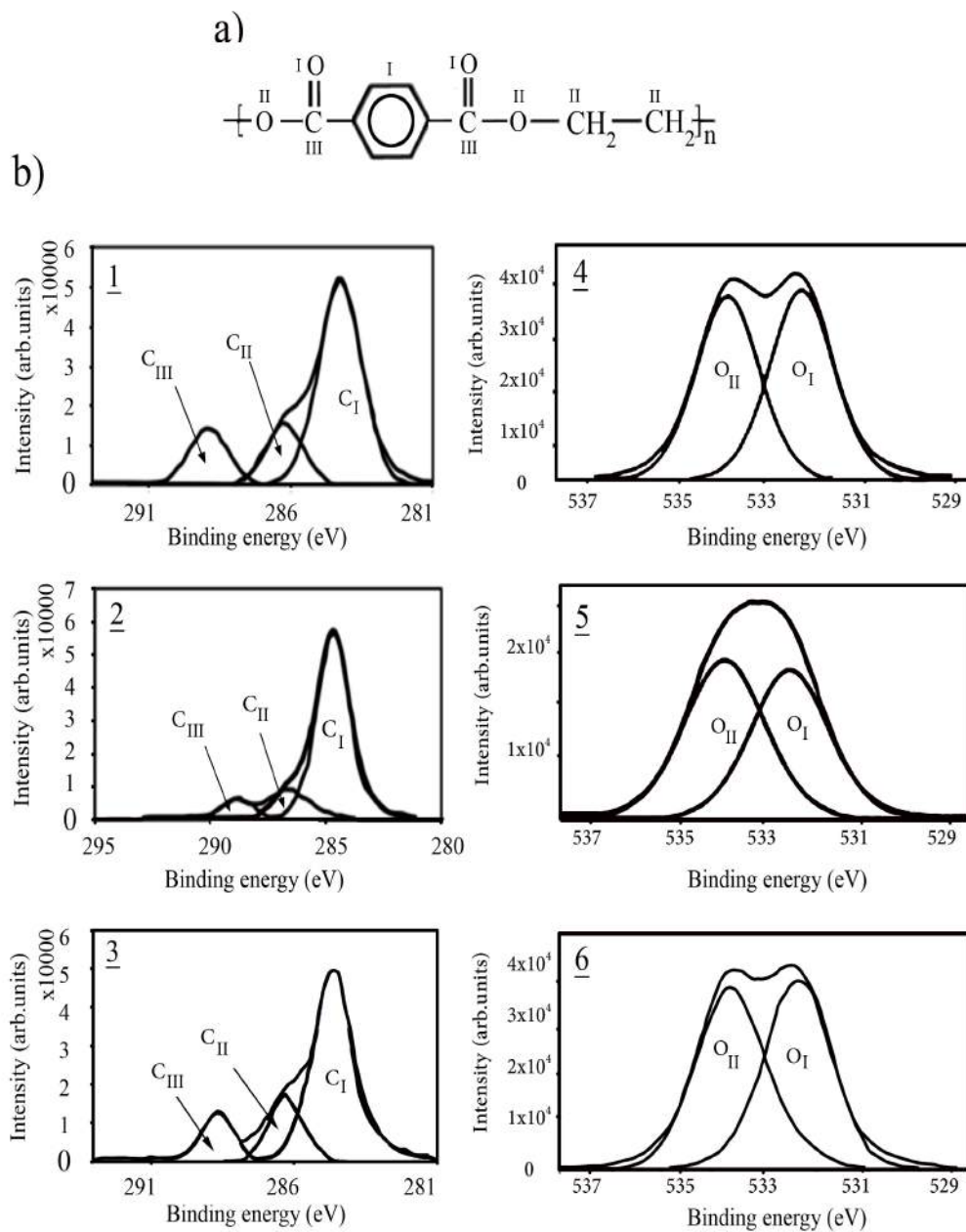


Figure 6-4: a) Chemical structure of PET. b) High-resolution XPS spectra of: 1 C1s PET, 2 C1s PET-5wt%PS-5wt%PKHH, 3 C1s PET-5wt%PS, 4 O1s PET, 5 O1s PET-5wt%PS-5wt%PKHH, 6 O1s PET-5wt%PS.

6.4.2 SEM results

Figure 6-5 exhibits SEM micrographs of the cross-section (b-1 and c-1) and surface (a, b-2 and c-2) of a PET film, a film of a binary blend of PET-PS and a film of a ternary polymer blend of PET-PS-PKHH, all for several magnifications. Because of the very low interfacial tension between PET and PKHH, they are almost miscible and PKHH cannot be observed as droplet in PET matrix. Therefore, the images of PET films containing 5wt%PS show a uniform distribution of PS droplets in the bulk of the film. Those presented in Figure 6-5b-1 show PS droplets well distributed regardless of the depth. Images of Figure 6-5b-2 present the size and shape of the PS droplets. They are oval-like droplets with a diameter of 4 μm on average with smooth interfaces. In the SEM images of the ternary polymer blend, the PS droplets are completely different in terms of distribution, size and shape. As can be observed from the Figure 6-5c-1 image, the distribution of the PS droplets within the film is not as homogenous as in the PET-PS film. Droplets of PS are abundant near the surfaces of the film and scarce in the bulk. Further, images of Figure 6-5c-2 show that PS droplet size has decreased significantly to an average of less than 2 μm in diameter in response to the addition of PKHH to the system. Another observation from these micrographs is that the addition of PKHH has resulted in a rougher interface between PET and PS.

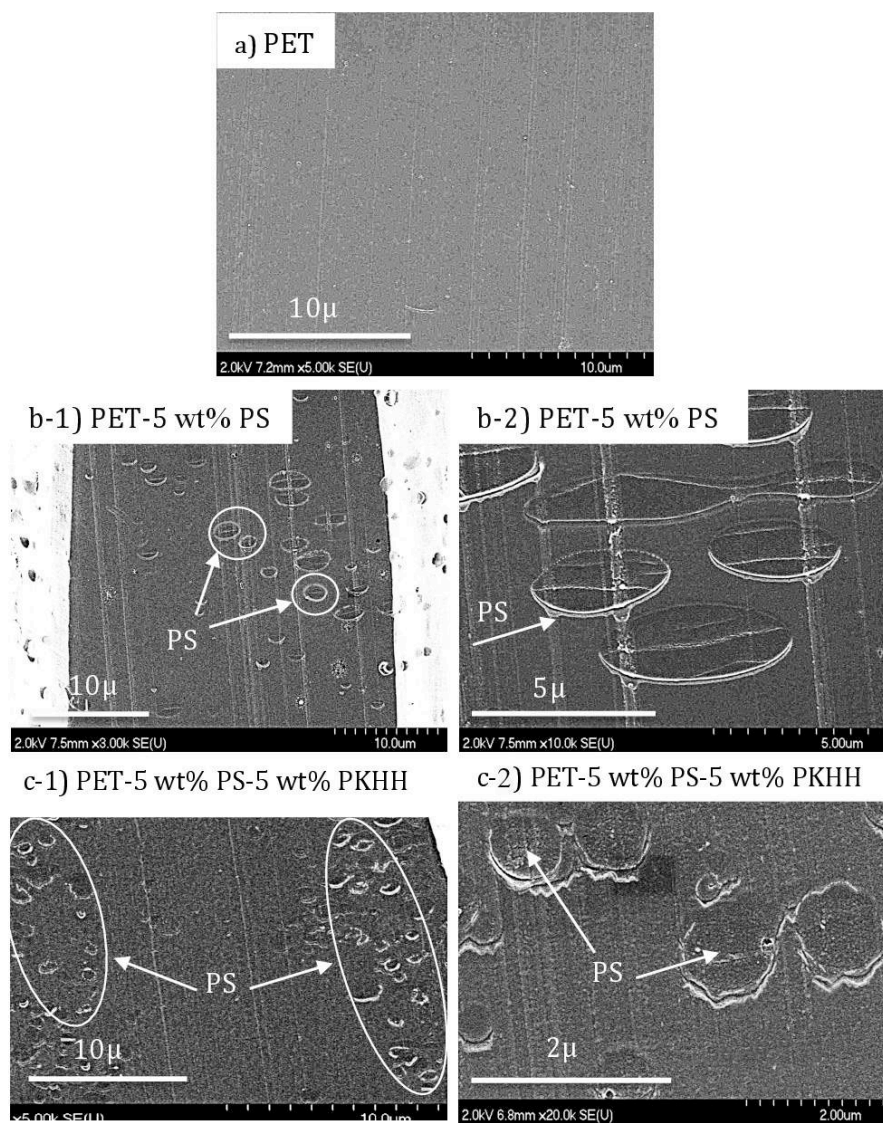


Figure 6-5: SEM images from a) PET film surface. b-1) Cross section of PET-5wt%PS. b-2) PET-5wt%PS film surface. c-1) Cross section of PET-5wt%PS-5wt%PKHH films. c-2) PET-5wt%PS-5wt%PKHH film surface.

6.4.3 Depth profiling and AFM results

Segregation in polymer blends can be observed by the variation of three parameters, namely temperature, composition and molecular weight. In this work, the temperature was modulated (annealing) while the other variables were kept constant in order to determine an ideal processing condition for extrusion. Therefore, we annealed the blend films at a controlled temperatures and characterized them using FRES technique.

FRES depth profiling was used to characterize the polymer/air interface of the ternary polymer blend. Figure 6-6 presents the FRES profile along with AFM images of the PET-dPS-PKHH film for different annealing times at 250 °C. Deuterated polystyrene (dPS) with the same characteristics of the PS was used in the blend to evaluate by depth profile technique whether the polystyrene chains change their locations at the surface layer during annealing. Deuterium and hydrogen from the film are elastically scattered and detected by a detector located at -75° . The surface depth resolution has a full-width half-maximum value of 80 nm. Figure 6-6-a reports the FRES profile for the PET-dPS-PKHH film without annealing. The graph indicates that dPS is located at the surface layer (the layer under the top surface) of the polymer film surface, which is consistent with the results of XPS. Although dPS makes up only 5wt% of the blend, the volume fraction of dPS at the layer close to the surface is about 35%. This indicates that most of the dPS droplets have segregated to the polymer/air interface during extrusion and film solidification. Annealing resulted in migration of more dPS molecules from the bulk to the surface layer. A comparison between Figure 6-6-a and Figures 6-6-b, c and d indicates that the concentration of dPS at the surface layer increases with annealing time. After 120 s annealing, the rate of migration is higher than what was initially expected based on the lower surface tension of dPS compared to PET. The average movement of PS molecules can be estimated using the Einstein

equation ($I^2 = 2Dt$)⁶⁶ where I^2 is the mean free quadratic displacement in one direction, D is the diffusion coefficient and t is the diffusion time. The typical diffusion coefficient of PS is $D = 2.8 \pm 0.07 \times 10^{-11} \text{ (cm}^2/\text{s)}$ ⁶⁶, so it was estimated that in the course of 1s, the average displacement of the PS molecules is 10 nm. Since the thickness of the prepared film is around 30 μm , the migration of PS molecules from the middle of film to the surface layer would take around 25 min if only the diffusion mechanism is involved. Therefore, the migration cannot be described only by diffusion and surface tension difference, while under this driving force more time (not in the scale of seconds) is needed for the migration of a component to the surface. Consequently, other factors such as density differences and viscosity ratio must also influence the migration of dPS droplets.

The right column of Figures 6-6-e, f, g and h shows the topography of dPS-rich layer at the surface. Phase imaging in tapping mode was used to obtain contrast based on surface hardness. The dark zones are associated with PET phase, whereas the brighter ones with PS. There is a sharp contrast between the PET and PS phases. It is suggested that phase contrast images of the samples are related to surface stiffness variations associated with changes in the elastic modulus. However the enhancement of the concentration of polystyrene in AFM images is correlated with the results from XPS and FRES. The PS phase could also be distinguished because of its higher elastic modulus (5.12 GPa) compared to the PET (3.05 GPa). According to the AFM images, the surface topography changes with time to exhibit a co-continuous surface pattern in the PET film. Figure 6-6-f shows the surface after 120 s. The co-continuous surface pattern visible in this image is similar to the pattern observed for spinodal decomposition in phase separation. The images show that phase coarsening starts to develop gradually with segregation of dPS in the blend. Thus, there are a dPS-rich unstable layer (about 500 nm from the top), and a PET-rich bulk

region. With further annealing, we observe an increasing concentration of dPS in the surface layer. By combining the depth profile and the surface topography of the films, the roughness evolution can be described in terms of phase coarsening of co-continuous morphology occurring on the polymer surface.

To conclude, segregated dPS droplets are present near the surface layer before annealing. Annealing at 250 °C for 120 s increases the polymer chains' mobility along with the dPS concentration in the surface layer, followed by the formation of a co-continuous structure. When annealing for 500 or 1200 s, the co-continuous structure coarsens, along with phase inversion.

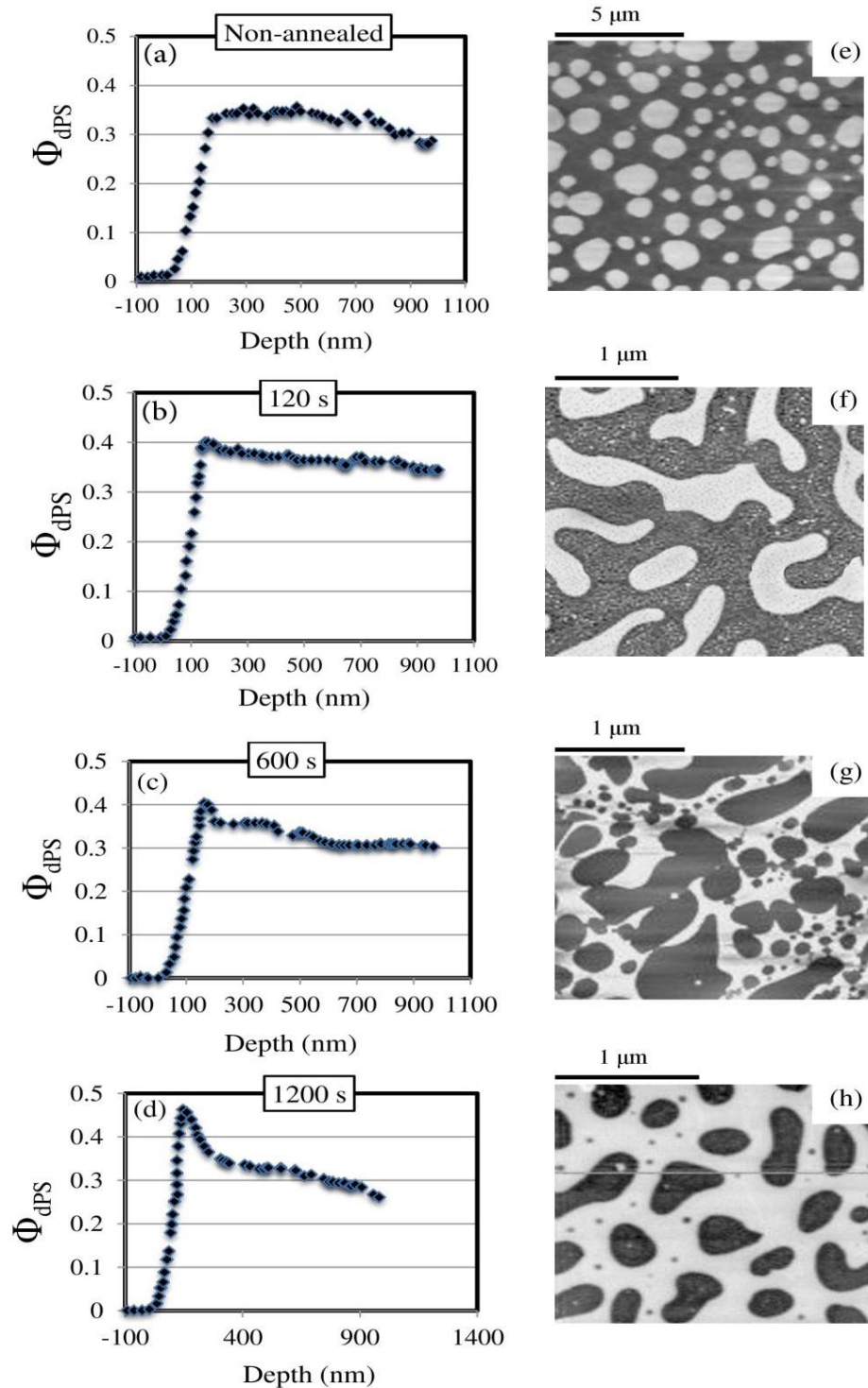


Figure 6-6: Volume fractions of dPS from FRES depth profiles of PET-5wt%dPS-5wt%PKHH film surface for a) Non-annealed sample, and annealed samples at 250 °C for b) 120 s c) 600 s, d) 1200 s, and AFM phase images of PET-5wt%dPS-5wt%PKHH film surfaces for e) Non-annealed sample and annealed samples at 250 °C for f) 120 s, g) 600 s, h) 1200 s. Scan sizes are 2.5 μm × 2.5 μm. (Dark region is PET and bright region is PS).

6.4.4 Phase coarsening kinetics

The phase coarsening kinetics was investigated by analyzing the evolution of the surface roughness correlation length $\lambda(t) = 2\pi/q_{\max(t)}$ on the polymer film surface, where $q_{\max(t)}$ is a characteristic wavenumber corresponding to peak maximum. $q_{\max(t)}$ can be obtained from the fast-Fourier transform (FFT) of AFM images. The two-dimensional FFT spectrum exhibits a maximum intensity at a characteristic wavenumber (q_{\max}). The first stage of phase coarsening identified in this process is consistent with the linearized theory developed by Cahn and Hilliard [55]. Later in the evolution of the coarsening, a different trend is identified, wherein the process is related to the peak wavenumber exponentially: $q(t) \approx t^{-n}$. Several articles have focused on this power-law behavior. Geoghegan has reviewed the phase behavior of polymer blend on polymer surface in detail [56].

The analysis of AFM images by 2D FFT over a square section of 512*512 pixels was performed. The intensity as a function of wavenumber for the PET-PS-PKHH film was obtained from the circular average of the 2D FFT from AFM images. The results achieved after annealing to find q_{\max} values and phase evolution kinetics. The right inset in Figure 6-7 shows 2D FFT image for this sample. The left inset in Figure 6-7 shows the PET-PS-PKHH film surface roughness as a function of time at different annealing temperatures. The RMS roughness increases with time for all samples. For samples annealed at 250 and 245 °C, the RMS roughness initially increases sharply whereas at 240 °C a plateau is reached after a slight increase. The q_{\max} value as a function of time is plotted in Figure 6-7 at different annealing temperatures on logarithmic scales. For the sample annealed at 240 °C, q_{\max} is constant over the entire experimental period, suggesting that coalescence did not occur at this temperature and the surface roughness at the beginning of the annealing (shown in left inset) could be due to the thermal fluctuations. For the samples annealed

at 245 and 250 °C, q_{\max} displays two distinct evolution stages. They are represented by two distinct linear trends in the plot of q_{\max} as a function of time. These two trends intersect after 132 s of annealing at 250 °C and after 237 s of annealing at 245 °C. The evolution of the characteristic wavenumber can be well approximated by a power-law dependence. As previously mentioned, each sample displayed two types of phases with different trends. The power-law exponents best representing these trends are 0.05 and 0.46 for the sample annealed at 245°C and 0.06 and 0.51 for the sample annealed at 250°C, in order of occurrence. These trends suggest that the characteristic wavenumber is initially independent of annealing time, consistent with Cahn's linearized theory for the early stage of spinodal decomposition [55]. Ultimately, the characteristic wavenumber does change according to a power-law behavior, a phenomenon frequently observed during phase coarsening of polymer blends.

In prior work kinetic models have been proposed for surface phase coarsening for a range of systems. Sung [58] modeled the coarsening kinetics of a PS/polybutadiene (PB) using two power-law trends, with the initial phase best modeled by the exponent 1/3 and the subsequent phase modeled by an exponent of 1. Phase coarsening and the phase behavior of polymer blends are much more complicated in thin films than in thick ones due to the significant effect of the substrate surface properties (the solid surface on which the thin film is located on) and film thickness. For example, the concentration gradient is a strong function of thickness [59].

In regards to the PET-PS system, annealing above the flow temperature allows droplets of the minor phase to migrate to the surface. This migration process is probably the first phase identified. This phase is not as visible with regard to a characteristic wavenumber because diffusion of this minor phase would be relatively slow and the subsurface concentration would not yet be sufficient for formation of co-continuous morphology and starting the phase

coarsening. Once the subsurface concentration of the minor phase reaches the critical concentration for phase coarsening, the co-continuous structure occurs. The effect of temperature on diffusion is clear from the fact that migration occurs faster for the sample annealed at 250 °C than for the one annealed at 245°C. This indicates that the critical subsurface minor phase concentration was reached more quickly for the former than for the latter. The model of phase coarsening derived for annealed films suggests that if the residence time of an extruded polymer film is sufficiently long (more than 3 min) in the sheet die at 250 °C, the film would be roughened to a similar degree as an annealed one of the same composition.

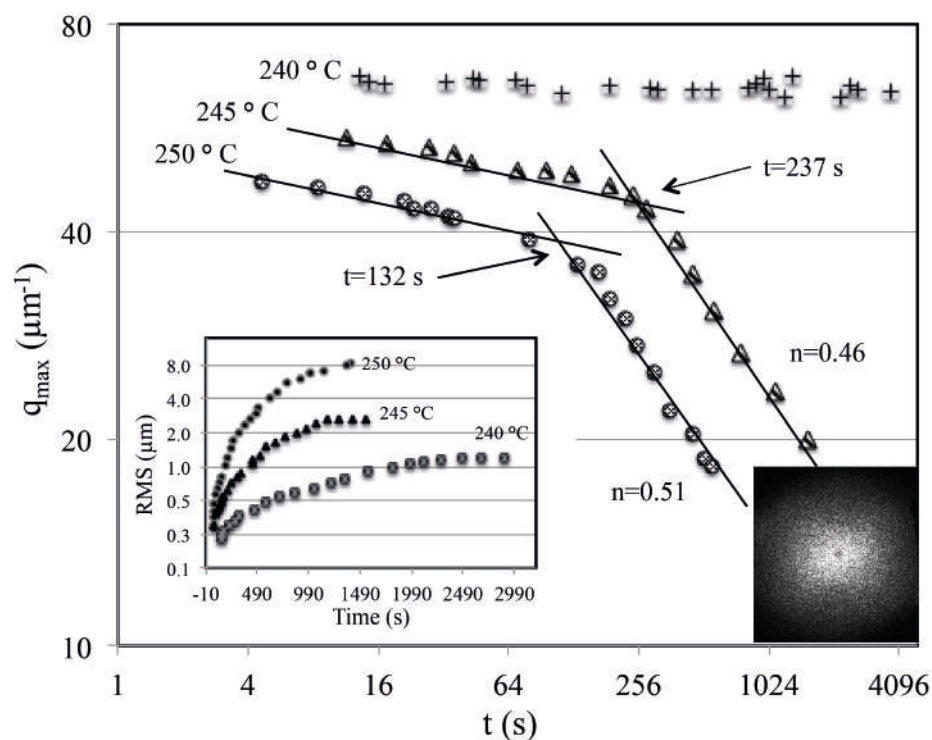


Figure 6-7: Characteristic wavenumber versus annealing time for the PET-PS-PKHH blend at three different temperatures (240, 245 and 250 °C). The left inset shows RMS surface roughness as a function of annealing time at different temperatures (240, 245 and 250 °C) and the right inset shows 2d FFT image of PET-5wt%PS-5wt%PKHH film.

6.4.5 Surface roughness

A profilometer was utilized to determine the average roughness of a 50mmx50mm square sample

surface. The technique allowed comparison of the surface topography of neat PET film with the topographies of aforementioned binary and ternary blends films. Average surface roughness was treated on two different length scales to represent the different scales of roughness. Average roughness for the two length scales, namely 472 and 5 μm , are shown in Figures 6-8a and b, respectively. The ternary polymer blend is significantly rougher than the other blends, with an RMS roughness of 481 nm and 10.5 μm for the 5 and 472 μm length scale measurements, respectively. These results can, in conjunction with SEM images, confirm the effect of PKHH on the surface roughening of the PET film for the two scale levels.

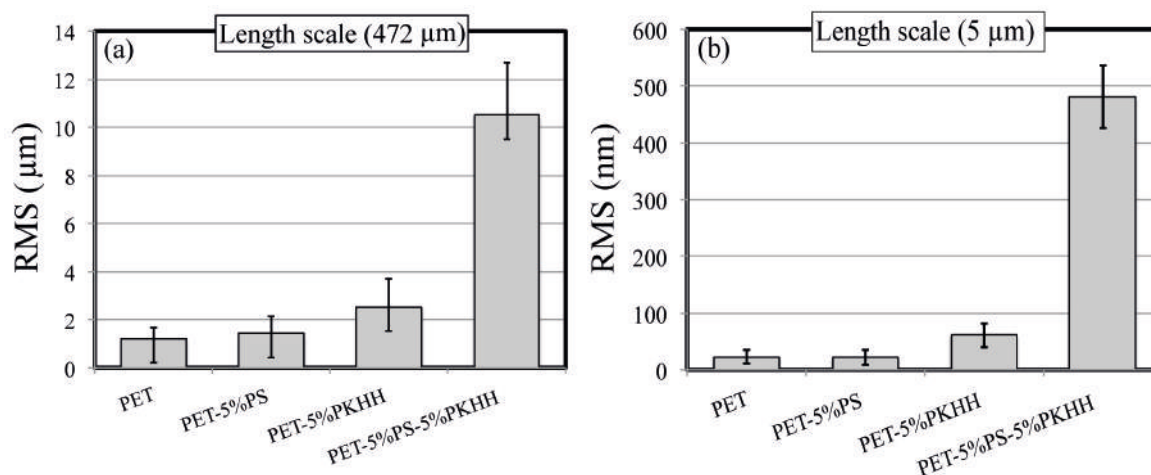


Figure 6-8: RMS surface roughness for the neat PET, PET-5wt%PS, PET-5wt%PKHH and PET-5wt%PS-5wt%PKHH films surfaces in a) 472 μm length scale and b) 5 μm length scale.

6.4.6 Adhesion test

The adhesion strength between the prepared films of PET, PET-5wt%PS, PET-5wt%PKHH and PET-5wt%PS-5wt%PKHH as measured by the pull-off test are reported in Figure 6-9. As expected, the surface of the ternary polymer blend adhered more strongly to the paint than the surface of films produced from the neat PET or from the binary blends. 7.8 MPa is the required

force to separate the paint from the surface of PET-PS-PKHH film whereas applying 4.6 MPa was enough for the neat PET film at room temperature. This observation is consistent with the results of profilometry of the same films, which showed in the previous section that the ternary polymer blend film is rougher than those produced from the binary blends or neat PET.

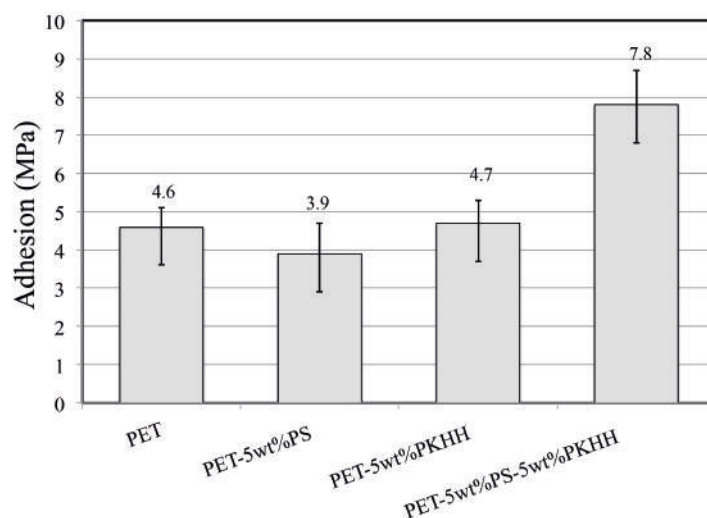


Figure 6-9: Adhesion test results on the surface of PET, PET-5wt%PS, PET-5wt%PKHH and PET-5wt%PS-5wt%PKHH film.

6.5 Conclusion

In conclusion, this study proposed a scenario for surface roughening of PET films through melt blending. In this particular work, 5wt%PS and 5wt%PKHH phenoxy resin were blended with PET in a twin-screw extruder. PS droplets were initially well distributed within the bulk PET. The size of these droplets was reduced by the presence of PKHH. The reduction in droplet size permitted more and faster migration of the droplets through the continuous phase, allowing segregation to the surface layer in response to the shear forces applied by the extruder. Despite the relatively low concentration of PS, migration of these droplets to a very thin layer just below the surface of the polymer resulted in a locally unstable concentration of PS, leading to phase coarsening.

XPS results confirmed a chemical modification of the PET film surface in response to the addition of PS and PKHH in the concentrations. Use of FRES demonstrated the high concentration of PS at the film surface. Also, a co-continuous pattern due to the high concentration of the PS molecules at the surface and their coalescence was observed in AFM images.

It was also found that the critical surface phase coarsening temperature for PET-PS polymer blend was around 245 °C. When the subsurface concentration of PS reached an unstable level, the characteristic wavenumber followed a power-law trend best fitted by an exponent of 0.42. The transition between PET and PS phases occurred after 132 s for the sample annealed at 250 °C.

Finally, pull-off tests indicated that the surface of PET-PS-PKHH film had better adhesive properties (7.8 MPa) than surfaces of the binary PET-PS blend, (4.6 MPa) and of the neat PET films (3.9 MPa).

6.6 Acknowledgments

The authors wish to thank helpful support and discussions with A. Yaghoobi, F. Tofan, D. Davidescu. Financial support from NSERC (Natural Science and Engineering Research Council of Canada) and Laverne Group Inc. are gratefully acknowledged.

6.7 References

- (1) Du, J. Z. Synthesis and Characterization of Photo-Cross-Linked Hydrogels Based on Biodegradable Polyphosphoesters and Poly(ethylene glycol) Copolymers. *Biomacromolecules* **2007**, 8, 3375-3381.
- (2) Lemmouchi, Y.; Schacht, E. Preparation and in Vitro Evaluation of Biodegradable Poly(ϵ -Caprolactone-Co-D,L Lactide)(X-Y) Devices Containing Trypanocidal Drugs. *J. Controlled Release* **1997**, 45, 227-233.
- (3) Park, J.H. Polymeric Nanomedicine for Cancer Therapy. *Prog. Polym. Sci.* **2008**, 33, 113-137.
- (4) Wu, J.; Chu, C. C. Block Copolymer of Poly(Ester Amide) and Polyesters: Synthesis, Characterization, and in Vitro Cellular Response. *Acta Biomater.* **2012**, 8, 4314-4323.
- (5) Bax, D. V. Directed Cell Attachment By Tropoelastin on Masked Plasma Immersion Ion Implantation Treated PTFE. *Biomaterials* **2011**, 32, 6710-6718.
- (6) Chan, C. M.; Ko, T. M.; Hiraoka, H. Polymer Surface Modification by Plasmas and Photons. *Surf. Sci. Rep.* **1996**, 24, 1-54.
- (7) Chu, P. K. Plasma-surface Modification of Biomaterials. *Mater. Sci. Eng.* **2002**, 36, 143-206.
- (8) Dargaville, T. R. High Energy Radiation Grafting of Fluoropolymers. *Prog. Polym. Sci.* **2003**, 28, 1355-1376.
- (9) Awaja, F. Adhesion of Polymers. *Prog. Polym. Sci.* **2009**, 34, 948-968.
- (10) Dubois, L. H.; Zegarski, B. R. High Energy Radiation Grafting of Fluoropolymers. *J. Phys. Chem.* **1993**, 97, 1665-1670.

- (11) Sheth, S. R.; Efremova, N.; Leckband, B. R. Interactions of Poly(ethylene oxide) Brushes with Chemically Selective Surfaces. *J. Phys. Chem. B*, **2000**, *104*, 7652-7662.
- (12) Patel, S. S.; Tirrell, M. Measurement of Forces Between Surfaces in Polymer Fluids. *Annu. Rev. Phys. Chem.* **1989**, *40*, 597-635.
- (13) Semenov, A.N. Interaction between Two Adsorbing Plates: The Effect of Polymer Chain Ends. *Macromolecules* **1997**, *30*, 1479-1489.
- (14) Katano, Y.; Tomono, H.; Nakajima, T. Surface Property of Polymer Films with Fluoroalkyl Side Chains. *Macromolecules* **1994**, *27*, 2342-2344.
- (15) Owens, D. K.; Wendt, R. C. Estimation of the Surface Free Energy of Polymers. *J. Appl. Polym. Sci.* **1969**, *13*, 1741-1747.
- (16) Gent, A. N.; Lin, C. W. Model Studies of the Effect of Surface Roughness and Mechanical Interlocking on Adhesion. *J. Adhes.* **1990**, *32*, 113-125.
- (17) Ramanathan, T. Functionalized Graphene Sheets for Polymer Nanocomposites. *Nat. Nanotechnol.* **2008**, *3*, 327-331.
- (18) Anastasiadis, S. H.; Hatzikiriakos, S.G. The Work of Adhesion of Polymer/Wall Interfaces and Its Association with the Onset of Wall Slip. *J. Rheol.* **1998**, *42*, 795-812.
- (19) Paiva, A. Study of the Surface Adhesion of Pressure-Sensitive Adhesives by Atomic Force Microscopy and Spherical Indenter Tests. *Macromolecules* **2000**, *33*, 1878-1881.
- (20) Ridgway, C. J.; Gane, P. A. C. Ink-Coating Adhesion: The Importance of Pore Size and Pigment Surface Chemistry. *J. Dispersion Sci. Technol.* **2005**, *25*, 469-480.

- (21) Baldan, A. Adhesively-Bonded Joints and Repairs in Metallic Alloys, Polymers and Composite Materials: Adhesives, Adhesion Theories and Surface Pretreatment. *J. Mater. Sci.* **2004**, *39*, 1-49.
- (22) Buckton, G.; Chandaria, B. Consideration of Adhesion to Modified Container Walls, by Use of Surface Energy and Polarity Data, and Lewis Acid-Lewis Base Interactions. *Int. J. Pharm.* **1993**, *94*, 223-229.
- (23) McCafferty, E. Acid-Base Effects in Polymer Adhesion at Metal Surfaces. *J. Adhes. Sci. Technol.* **2002**, *16*, 239-255.
- (24) Van Oss, C. J.; Good, R.J.; Chaudhury, M.K. Additive and Nonadditive Surface Tension Components and the Interpretation of Contact Angles. *Langmuir* **1988**, *4*, 884-891.
- (25) Miwa, M. Effects of the Surface Roughness on Sliding Angles of Water Droplets on Superhydrophobic Surfaces. *Langmuir* **2000**, *16*, 5754-5760.
- (26) Price, R. L. Nanometer Surface Roughness Increases Select Osteoblast Adhesion on Carbon Nanofiber Compacts. *J. Biomed. Mater. Res., Part A* **2004**, *70A*, 129-138.
- (27) Wenzel, R. N. Surface Roughness and Contact Angle. *J. Phys. Colloid Chem.* **1948**, *53*, 1466-1467.
- (28) Gent, A. N.; Lin, C.W. Model Studies of the Effect of Surface Roughness and Mechanical Interlocking on Adhesion. *J. Adhes.* **1990**, *32*, 113-125.
- (29) Kim, W. S. Evaluation of Mechanical Interlock Effect on Adhesion Strength of Polymer-Metal Interfaces Using Micro-Patterned Surface Topography. *Int. J. Adhes. Adhes.* **2010**, *30*, 408-417.

- (30) Packham, D. E. Work of Adhesion: Contact Angles and Contact Mechanics. *Int. J. Adhes. Adhes.* **1996**, *16*, 121-128.
- (31) Davis, C. S.; Crosby, A.J. Mechanics of Wrinkled Surface Adhesion. *Soft Matter* **2011**, *7*, 5373-5381.
- (32) Fuller, K. Effect of Surface Roughness on the Adhesion of Elastomers to Hard Surfaces. *Mater. Sci. Forum.* **2010**, *662*, 39-51.
- (33) Maugis, D. On the Contact and Adhesion of Rough Surfaces. *J. Adhes. Sci. Technol.* **1996**, *10*, 161-175.
- (34) Mazzitelli, C. Surface Roughness Analysis of Fiber Post Conditioning Processes. *J. Dent. Res.* **2008**, *87*, 186-190.
- (35) Peng, Z. L.; Chen, S. H. Effects of Surface Roughness and Film Thickness on the Adhesion of a Bioinspired Nanofilm. *Phys. Rev. E: Stat., Nonlinear, Soft Matter Phys.* **2011**, *83*, 051915.
- (36) Fu, X.; He, X. Fabrication of Super-hydrophobic Surfaces on Aluminum Alloy Substrates. *Applied Surface Science* **2008**, *255*, 1776-1781.
- (37) Qian, B.; Shen, Z. Fabrication of Superhydrophobic Surfaces by Dislocation-Selective Chemical Etching on Aluminum, Copper, and Zinc Substrates. *Langmuir* **2005**, *21*, 9007-9009.
- (38) Chun, Y. W. The Role of Polymer Nanosurface Roughness and Submicron Pores in Improving Bladder Urothelial Cell Density and Inhibiting Calcium Oxalate Stone Formation. *Nanotechnology* **2009**, *20*, 85104.
- (39) Lee, H. U. Surface Modification of and Selective Protein Attachment to a Flexible Microarray Pattern Using Atmospheric Plasma with a Reactive Gas. *Acta Biomater.* **2010**, *6*, 519-525.

- (40) Dai, W. Ion-Beam Induced Surface Roughening of Poly-(methyl methacrylate) (PMMA) Tuned by a Mixture of Ar and O₂ Ions. *Plasma Processes Polym.* **2012**, *9*, 975-983.
- (41) Ting, Y. H. Surface Roughening of Polystyrene and Poly(methyl methacrylate) in Ar/O₂ Plasma Etching. *Polymers* **2010**, *2*, 649-663.
- (42) Vrij, A.; Overbeek, J. T. G. Rupture of Thin Liquid Films due to Spontaneous Fluctuations in Thickness. *J. Am. Chem. Soc.* **1968**, *90*, 3074-3078.
- (43) Wyart, F. B.; Daillant, J. Drying of Solids Wetted by Thin Liquid Films. *Can. J. Phys.* **1990**, *68*, 1084-1088.
- (44) Boltau, M.; Walheim, S.; Mlynek, J.; Krausch, G.; Steiner, U. Surface-induced Structure Formation of Polymer Blends on Patterned Substrates. *Nature* **1998**, *391*, 877.
- (45) Karim, A. Phase-Separation-Induced Surface Patterns in Thin Polymer Blend Films. *Macromolecules* **1998**, *31*, 857-862.
- (46) Tanaka, H. Dynamic Interplay Between Phase Separation and Wetting in a Binary Mixture Confined in a One-Dimensional Capillary. *Phys. Rev. Lett.* **1993**, *70*, 53-56.
- (47) Tanaka, K. Ultrathinning-Induced Surface Phase Separation of Polystyrene/Poly(vinyl methyl ether) Blend Film. *Macromolecules* **1995**, *28*, 934-938.
- (48) Wang, H.; Composto, R. J. Understanding Morphology Evolution and Roughening in Phase-Separating Thin-film Polymer Blends. *EPL* **2000**, *50*, 622.
- (49) Wang, H.; Composto, R. J. Kinetics of Surface and Interfacial Fluctuations in Phase Separating Polymer Blend Films. *Macromolecules* **2002**, *35*, 2799-2809.

- (50) Briggs, D.; Seah, M. P., *Practical Surface Analysis by Auger and X-Ray Photoelectron Spectroscopy*; Wiley: New York, 1983; Appendix 4, pp 1716.
- (51) Composto, R. J.; Walters, R.M.; Genzer, J. Application of Ion Scattering Techniques to Characterize Polymer Surfaces and Interfaces. *Mater. Sci. Eng., R* **2002**, *38*, 107-180.
- (52) Mayer, M. Simnra User's Guide, *M.P.I.f. Plasmaphysik*, **1997**.
- (53) Cho, K.; Jeon. H. K.; Park, C. E.; Kim, J.; Kim, K. U. Plasma-Surface Modification of Biomaterials. *Polymer* **1996**, *37*, 143-206.
- (54) Elemans, P. H. M.; Janssen, J. M. H.; Meijer, H. E. H. The Measurement of Interfacial Tension in Polymer/Polymer Systems : The Breaking Thread Method. *J. Rheol.* **1990**, *34*, 1311-1325.
- (55) Cahn, J. W.; Hilliard, J. E. Free Energy of a Nonuniform System. I. Interfacial Free Energy. *J. Chem. Phys.* **1958**, *28*, 258-267.
- (56) Geoghegan, M.; Krausch, G. Wetting at Polymer Surfaces and Interfaces. *Prog. Polym. Sci.* **2003**, *28*, 261-302.
- (57) Wang, H.; Composto, R. J. Wetting and Phase Separation in Polymer Blend Films: Identification of Four Thickness Regimes with Distinct Morphological Pathways. *Interface Sci.* **2003**, *11*, 237--248.
- (58) Sung, L. Phase Separation Kinetics and Morphology in a Polymer Blend with Diblock. Copolymer Additive. *J. Polym. Res.* **1996**, *3*, 139-150.
- (59) Xue; L.; Han, Y. *Pattern*, Y. H. Pattern Formation by Dewetting of Polymer Thin Film. *Prog. Polym. Sci.* **2011**, *36*, 269-293.

- (60) Liao, Y.; You, J.; Shi, T.; An, L.; Dutta, P. K. Phase Behavior and Dewetting for Polymer Blend Films Studied by In Situ AFM and XPS: From Thin to Ultrathin Films. *Langmuir* **2007**, *23*, 11107-11111.
- (61) Wang, H.; Composto, R. J. Thin Film Polymer Blends Undergoing Phase Separation and Wetting: Identification of Early, Intermediate, and Late Stages. *J. Chem. Phys.* **2000**, *113*, 10386-10397.
- (62) Wu, S. *Polymer Interface and Adhesion*; Marcel Dekker Inc.: New York, 1982; pp 420-447.
- (63) Andradi, L. N.; Hellmann, G. P. Morphologies of Mechanically Mixed Amorphous Blends Before and after Annealing. *Polym. Eng. Sci.* **1995**, *35*, 693-702.
- (64) Utracki, L. A. On the Viscosity-Concentration Dependence of Immiscible Polymer Blends. *J. Rheol.* **1991**, *35*, 1615-1637.
- (65) Scholten, E.; Sagis, L. M. C.; Van der Linden, E. Bending Rigidity of Interfaces in Aqueous Phase-Separated Biopolymer Mixtures. *Macromolecules* **2005**, *38*, 3515-3518.
- (66) Stokes, R. J.; Evans D. F. *Fundamental of Interfacial Engineering*, 1st ed; Wiley-VCH: New York, 1997; pp 220-334.
- (67) Wu, S. Interfacial and Surface Tensions of Polymers. *J. Macromol. Sci., Polym. Rev.* 1974, *10*, 1-73.
- (68) Rezaei Kolahchi, A.; Ajji, A.; Carreau, Pierre. J. Enhancing Hydrophilicity of Polyethylene Terephthalate Surface through Melt Blending. *Polym. Eng. Sci.* **2014**, *10*, 2390-2499.

CHAPTER 7

GENERAL DISCUSSION

A proper control of the surface properties of polymers has drawn a lot of attention because of its advantages for various applications such as membranes, adhesion to the other surfaces, coating, patterning on the surface and many more. The excellent thermal and mechanical properties of polyethylene terephthalate (PET) give it a wide variety of uses for everyday items. Like most polymers, PET doesn't have suitable surface properties in terms of adhesion to the other materials such as inks and paints. Therefore, the surface treatment is needed before any coating process. However, current surface modification methods have many limitations and they cannot be applied for many applications. Some modifications lead to an immediate deterioration after the process and some of them are limited to treat complex shaped surfaces (such as automotive parts) where a uniform treatment cannot be achieved.

There is a longstanding need for alternative reliable methods for modification of polymer surfaces. Migration of additives or polymers dispersed in a host polymer to the host polymer's surface has long been recognized as a potential solution. The premise here is that if a surface active additive with desirable functional groups is blended in small amounts with the host polymer melt or solution, physical processes such as diffusion, surface segregation, and shear might be used to transport the additive to the surface during normal polymer processing. The key here is to get uniform modification all over the surface even for the objects with complex shape.

Due to the importance of surface properties of PET films, the main objective of this dissertation was to modify the surface properties of PET through blending. To achieve this goal, twin-screw extruder, along with several characterization techniques such as scanning electron microscopy (SEM) and atomic force microscopy (AFM), time of flight secondary ion mass spectroscopy

(TOF-SIMS), x-ray photoelectron spectroscopy and contact angle were employed. In the following paragraphs, a general discussion is provided to emphasize the essential role-played by various factors as determined by the mentioned characterization techniques.

The first part of this work was aimed at develop an effective method for imparting hydrophilicity to PET film surface to overcome the current limitation of the surface modification methods. We used PEG as a hydrophilic polymer with very high O/C ratio (50%) to blend with PET matrix and tried to induce the migration of PEG molecules to the surface of the polymer film.

It was explored that a small amount of an immiscible polymer with PET of higher M_w than that of the minor component (PEG) could be effective in localizing the PEG molecules at polymer/air interface. Dispersed droplets of this polymer having less affinity for PET would remain homogeneously distributed in the bulk of the polymer film and cannot be migrated to the surface as fast as PEG low M_w under a shear field in extruder. In addition, the immiscibility of this polymer causes forming big droplets in PET matrix that move to the high-field region. Therefore, it will force the migration of PEG molecules towards the top surface layer. We started blending of the minor phases with the same concentration with PET. The contact angle for PET-5wt%PEG-5wt%PS films considerably reduced compared to the binary blends (PET-PS and PET-PEG).

XPS analysis and SEM images revealed the migration of the PEG molecules to the surface layer. It demonstrated that most PEG droplets have been localized at the two side interfaces of the polymer film with air and some PS droplets are located under the PEG droplets.

When the system consists of two minor components, the type of the morphology of ternary polymer blends may influence the migration of the minor components. AFM microscopy

provided a comprehensive picture of how the localization of minor components affects the surface properties of blends films. Therefore, the present approach consisted in examining the minor component migration to the film surface of ternary blends composed of PET, PEG and a second minor phase. PBAT, PCL, PS, PLA and PMMA were chosen to use as a second minor phase, which should result in a range of different morphologies. The results from calculation of the surface free energy (γ_s) of samples showed that the blend films containing PS, PBAT or PCL in PET-PEG blends, those with separated droplets morphology were more hydrophilic surfaces compared to the other samples.

The dendritic-shaped crystals are formed throughout the whole surface of the PET-PS-PEG film. This pattern suggests that PS influences the characteristics of the PEG crystals in the blend and the dendritic pattern could cover a greater portion of the film surface resulted in more hydrophilicity. It could be also the main reason of very high surface energy of PET-PS-PEG sample.

In the last part of this work, a novel method to increase the surface roughness of polyethylene terephthalate films was proposed. Surface roughening of the PET film with a minimum content of some minor phases was the objective of the study. The same concept as mentioned hereinabove was applied for surface migration of the component to have a rich layer of an immiscible polymer with PET at the film surface and make distortion resulting in roughness amplitude on the surface. In this regard, PKHH and polystyrene (PS) were used as minor phases in a blend with a PET matrix. The chemical structure of PKHH has tendency to act as a hydrogen bond donor, which increases its interactions with the polyester, while the aromatic groups of the phenoxy resin probably coordinates with those of PS.

SEM images confirmed the idea to break the PS droplets down to the smaller size by adding PKHH in the system. The smaller droplets could migrate to the surface layer in response to shear in the extruder.

FRES determines the concentration of the components of a blend film as a function of depth when the information on the wetting properties of multicomponent polymer mixtures is required. It analyzes the segregation of the components in an unstable blend if this segregation corresponds to a surface layer. By this technique the elements below the surface region, layer by layer are determined in the forward direction from a depth ranging from 0 to 5000 Å. Accordingly in this study, the blend films annealed at an extrusion temperature to determine an ideal processing condition and then cooled to freeze the morphologies. AFM phase morphologies obtained from samples frozen at different annealing times provided numerous valuable information. It appeared that most of the PS droplets have segregated to the polymer/air interface during the extrusion and film solidification. It was observed that annealing increases the concentration of PS at the surface layer. The rate of migration indicated that many factors such as density fluctuation, viscosity ratio and incompatibility with PET (high interfacial tension) have influenced the migration of PS droplets besides the surface tension difference. The AFM phase morphologies further revealed the phase coarsening resulted in continuous morphology in PET film during annealing and after 120 s.

Fast-Fourier transform (FFT) of AFM images can investigate the kinetics phase coarsening by analyzing the evolution of the surface roughness correlation length $\lambda(t) = 2\pi/q_{\max(t)}$ on the polymer film surface. FFT revealed that there is an evolution of the characteristic wavenumber well approximated by a power-law dependence.

CHAPTER 8

CONCLUDING REMARKS AND RECOMMENDATIONS

8.1 Conclusions

In this dissertation, the surface of PET film was successfully modified in terms of surface hydrophilicity and roughness through blending. Blending of two polymers as minor components in a PET matrix showed strong influences on the surface formation, surface compositions, surface roughness and some other surface properties of the PET film. Type and nature of the additives (minor components), surface tension of the polymers, miscibility and compatibility of the minor components as well as the bulk and surface morphologies can influence the migration of the minor phases to the polymer/air interface.

All of the above-mentioned parameters showed significant effect on the surface properties as observed by their migration behavior, surface hydrophilicity, roughness and finally printability. More specifically, the following conclusions were drawn from the experimental results:

- XPS analyses revealed surface enrichment of PEG in PET film by adding PS as a second minor component in the blend and this mostly led to a hydrophilic surface by reducing the water contact angle over time.
- PEG surface concentration changes as a function of time indicated migration of minor components after extrusion. Surface activity of the minor component molecules and the extent of PET surface modification were interpreted in terms of additive molecular characteristics.

- PEG with lower molecular weight led to more migration to the surface than higher molecular weight PEG
- Quantitative XPS alone couldn't fully describe hydrophilicity of the surface due to the differences in the analytical depth. TOF-SIMS analysis enabled identification of the melt additive distribution on the top surface, and contact angle showed alteration of surface structures after blending with the minor phases.
- The migration of PEG molecules to the film surface was observed by SEM images from the cross section of the embedded PET film in epoxy.
- The PEG and PS addition to PET enhanced its crystallinity synergistically from 23% for the original PET film to 31% for the ternary system.
- Two separated dispersed droplets morphology in a ternary polymer blend promoted the migration of short chains of the minor component to the surface layer of the polymer.
- Surface pattern and morphology of the surface-active additive was considered as the main factor for more surface coverage. PEG crystals formed dendritic patterns, as in the case of the PET-PS-PEG films resulting in a larger surface free energy.
- The optimum PEG and PS concentration to affect changes in the surface properties was 7wt% and 5wt% respectively. To be more specific a minimum PEG concentration of 5wt% is necessary to maximize the surface crystallinity when the blend contained 5wt%PS.

- Blending of 5wt% PKHH phenoxy resin in the blend of PET-5wt%PS reduced the PS droplet size and favored the migration of the droplets through the continuous phase, allowing segregation to the surface layer in response to the shear forces applied by the extruder.
- Annealing of the PET-PKHH-PS revealed the phase behaviour of PET-PS blend by depth profile analysis and AFM images at the film surface layer. At 250° C, the phase coarsening following by co-continuous morphology progressed when the concentration of PS reached around 40%.
- The kinetics of phase coarsening was analyzed by 2D FFT of AFM images for annealed samples. The transition to co-continuous morphology occurred at 132 s for the sample annealed at 250 °C.
- The adhesion of the polymer film surface can be estimated by pull-off test.

8.2 Recommendations

The following unexplored topics are recommended for future research:

- In addition to what has been studied in this work, it would be interesting to study the effect of PS molecular weight on the surface migration of PEG.
- It is recommended to explore the efficiency of other polymers containing very active functional groups such as poly (ethylene glycol) diacetylene, Methoxypolyethylene glycol maleimide instead of using PEG on the surface properties of PET. Using a copolymer with a hydrophilic block would be interesting as well.

- Concerning providing hydrophilicity and roughness simultaneously on the PET film surface, it would be recommended to study the effect of blending of an immiscible hydrophilic polymer with PET and PKHH.
- As for the case of PET-PS-PEG blend, it would be recommended to alter the processing condition (screw speed, temperature, die and etc.) and consequently to investigate their effect on the migration rate.
- To study the possibility of applying the method (using two minor phases) in fibers and electro-spinning technique to get specific properties on the surface of fibers.
- It is recommended to explore the effect of the PET film thickness on the surface properties either for the system containing PEG-PS or PKHH-PS.
- Concerning the stability of the migrated minor components at the surface of the film, it would be useful to do some specific test such as thermal and solvent stability (water immersion) test.
- It would be interesting to find the optimum concentration of PKHH in the system based on minimum PS size droplets and PS surface concentration.

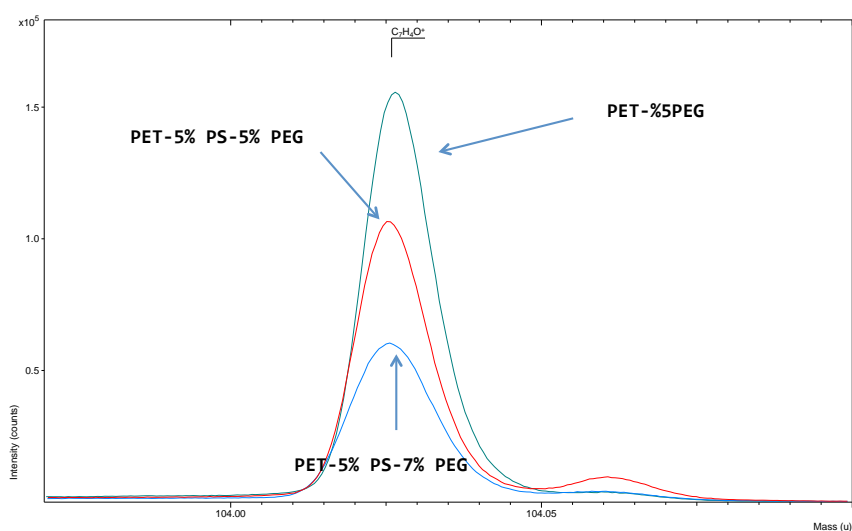
CHAPTER 9

INDEX

9.1 Index A

TOF-SISM spectra for the samples corresponding to the intensities of $C_7H_4^+$ and $C_2H_5^+$ ions.

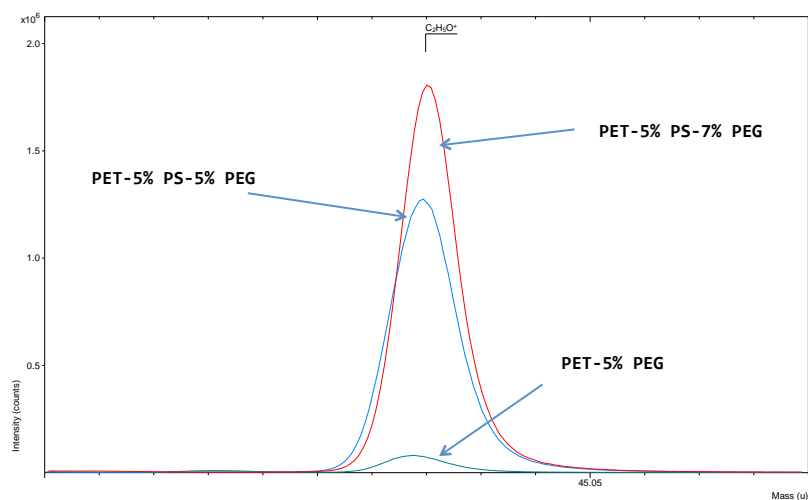
PET



PET content : PET-5%PEG > PET-5% PS-5% PEG > PET-5% PS-7% PEG

1

PEG

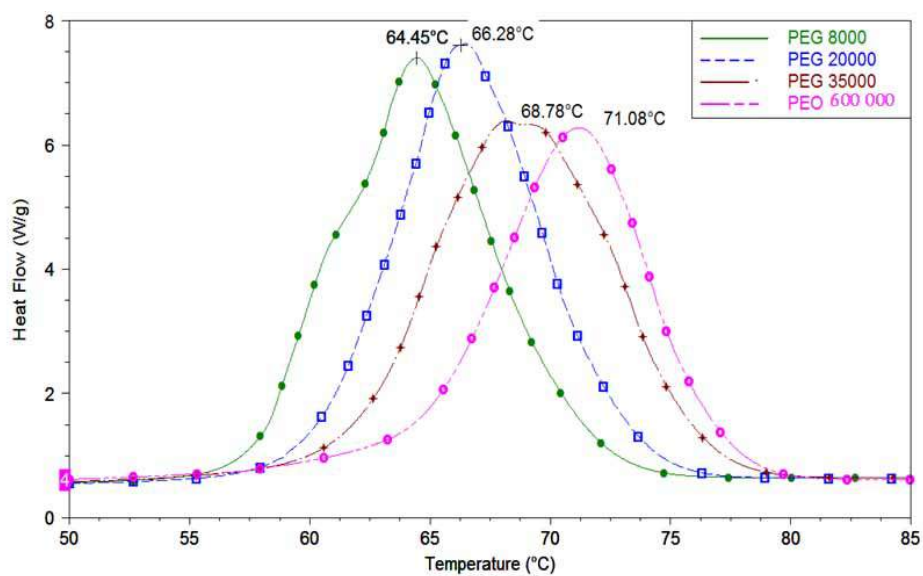
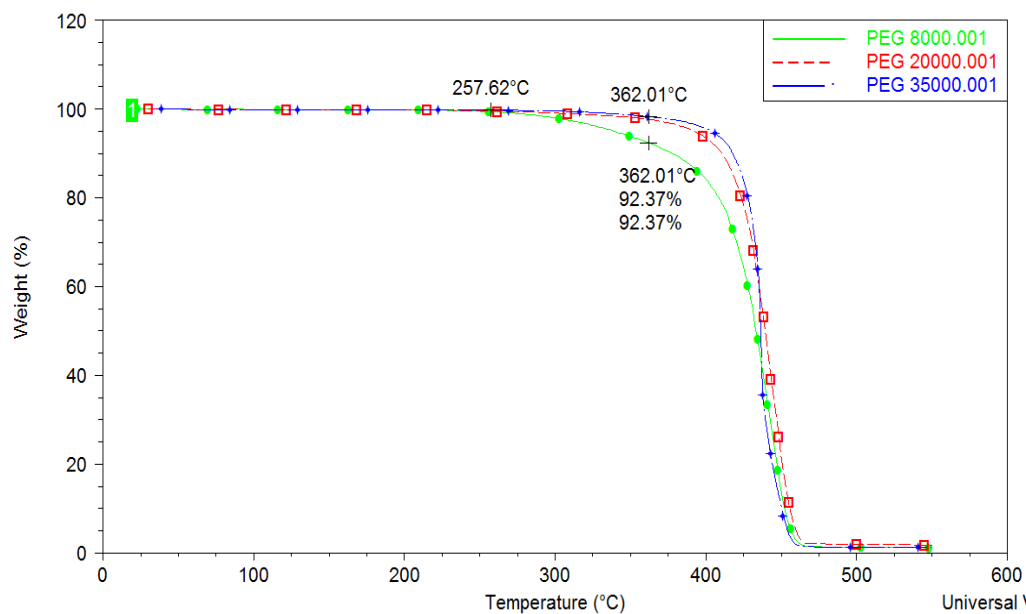


PEG content: PET-5% PS-7% PEG > PET-5% PS-5% PEG > PET-5% PEG

2

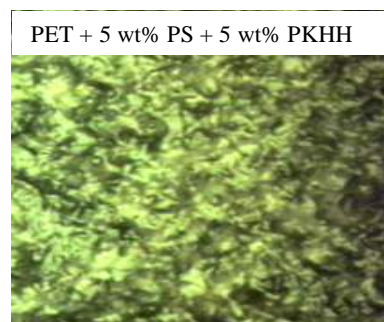
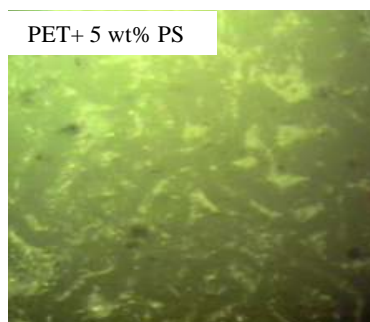
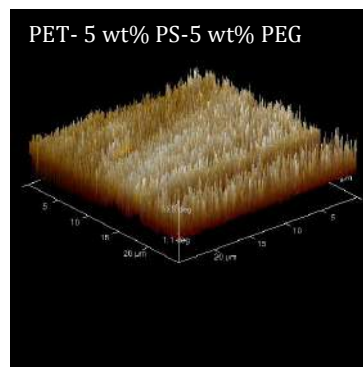
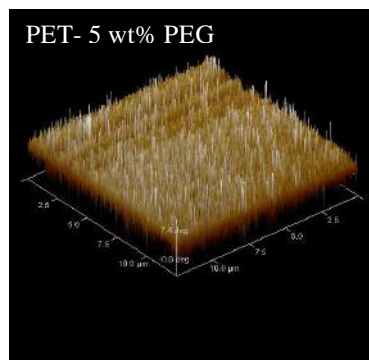
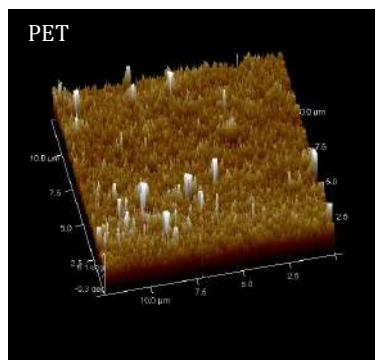
9.2 Index B

Thermal analysis of different molecular weights of PEG polymer.



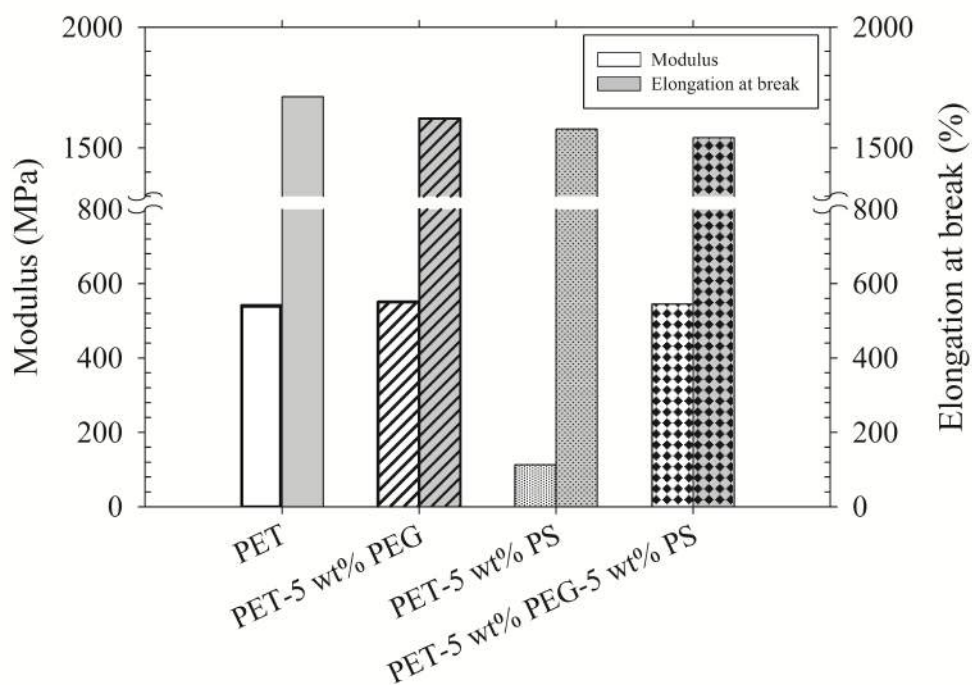
9.3 Index C

Roughness of the film surfaces by AFM.

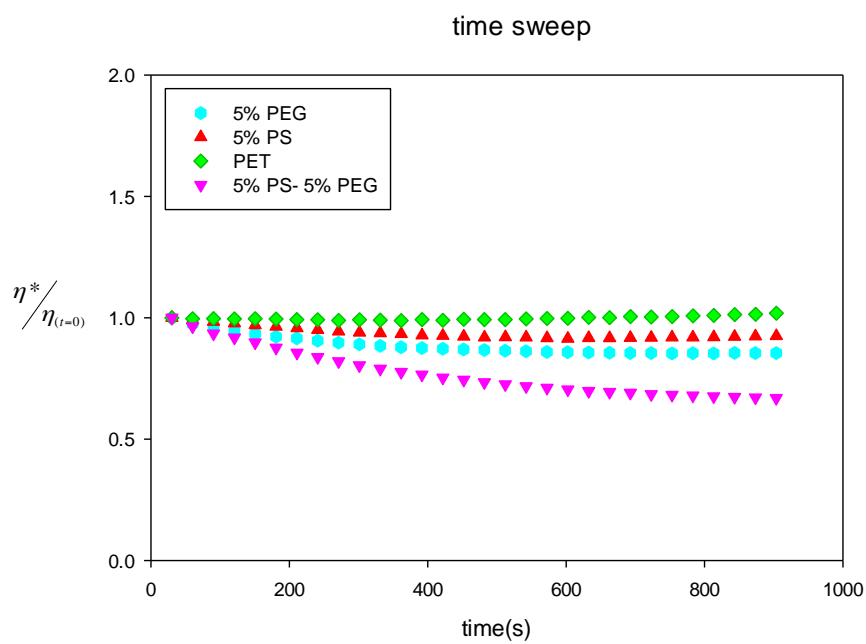


9.4 Index D

Mechanical properties of the PET, binaries and ternary blend films containing PET, PS and PEG.



9.5 Index E



REFERENCES

- Abbasi, F., H. Mirzadeh and A.-A. Katbab (2001). "Modification of polysiloxane polymers for biomedical applications: a review." Polymer International **50**(12): 1279-1287.
- Affrossman, S., M. Hartshorne, R. Jerome, R. A. Pethrick, S. Petitjean and M. R. Vilar (1993). "Surface concentration of chain ends in polystyrene determined by static secondary ion mass spectroscopy." Macromolecules **26**(23): 6251-6254.
- Agarwal, U. S., A. Dutta and R. A. Mashelkar (1994). "Migration of macromolecules under flow: the physical origin and engineering implications." Chemical Engineering Science **49**(11): 1693-1717.
- Al Ghatta, H., S. Cobror and T. Severini (1997). "New Technology for Solid-state Polymerization of Polymers: Polyethylene terephthalate–Solid-state Polyaddition." Polymers for Advanced Technologies **8**(4): 161-168.
- Allen, K. W. (2000). "Formation and failure of adhesive bonds." Surface Coatings International **83**(1): 20-26.
- Allen, N. S., J. Segurola, M. Edge, A. McMahon and I. Roberts (1999). "A comparative kinetic study of UV-curable resins the relationship between structure and rheology." Surface Coatings International **82**(6): 285-292.
- Almdal, K., M. A. Hillmyer and F. S. Bates (2002). "Influence of Conformational Asymmetry on Polymer, à Polymer Interactions:, ÄÄ An Entropic or Enthalpic Effect?" Macromolecules **35**(20): 7685-7691.
- Anastasiadis, S. H., J. K. Chen, J. T. Koberstein, A. F. Siegel, J. E. Sohn and J. A. Emerson (1987). "The determination of interfacial tension by video image processing of pendant fluid drops." Journal of Colloid And Interface Science **119**(1): 55-66.
- Anastasiadis, S. H. and S. G. Hatzikiriakos (1998). "The work of adhesion of polymer/wall interfaces and its association with the onset of wall slip." Journal of Rheology **42**(4): 795--812.
- Anastasiadis, S. H., H. Retsos, S. Pispas, N. Hadjichristidis and S. Neophytides (2003). "Smart Polymer Surfaces." Macromolecules **36**(6): 1994-1999.

- Andruzzi, L., A. Hexemer, X. Li, C. K. Ober, E. J. Kramer, G. Galli, E. Chiellini and D. A. Fischer (2004). "Control of Surface Properties Using Fluorinated Polymer Brushes Produced by Surface-Initiated Controlled Radical Polymerization." Langmuir **20**(24): 10498-10506.
- Aouinti, M., P. Bertrand and F. Poncin-Epaillard (2003). "Characterization of Polypropylene Surface Treated in a CO₂ Plasma." Plasmas and Polymers **8**(4): 225-236.
- Awaja, F., M. Gilbert, G. Kelly, B. Fox and P. J. Pigram (2009). "Adhesion of polymers." Progress in Polymer Science **34**(9): 948-968.
- Baldan, A. (2004). "Adhesively-bonded joints and repairs in metallic alloys, polymers and composite materials: Adhesives, adhesion theories and surface pretreatment." Journal of Materials Science **39**(1): 1-49.
- Ballara, A. and J. Verdu (1989). "Physical aspects of the hydrolysis of polyethylene terephthalate." Polymer Degradation and Stability **26**(4): 361-374.
- Bax, D. V., D. R. McKenzie, M. M. M. Bilek and A. S. Weiss (2011). "Directed cell attachment by tropoelastin on masked plasma immersion ion implantation treated PTFE." Biomaterials **32**(28): 6710-6718.
- Bell, J. R., K. Chang, C. R. Lopez-Barron, C. W. Macosko and D. C. Morse (2010). "Annealing of Cocontinuous Polymer Blends: Effect of Block Copolymer Molecular Weight and Architecture." Macromolecules **43**(11): 5024-5032.
- Bhadane, P. A., A. H. Tsou, J. Cheng, M. Ellul and B. D. Favis (2011). "Morphology and continuity development in highly reactive nanoscale polymer blends." Polymer **52**(22): 5107-5117.
- Bhave, A. V., R. C. Armstrong and R. A. Brown (1991). "Kinetic theory and rheology of dilute, nonhomogeneous polymer solutions." The Journal of Chemical Physics **95**(4): 2988-3000.
- Biresaw, G. and C. J. Carriere (2001). "Correlation between mechanical adhesion and interfacial properties of starch/biodegradable polyester blends." Journal of Polymer Science Part B: Polymer Physics **39**(9): 920-930.
- Biscardi, D., S. Monarca, R. De Fusco, F. Senatore, P. Poli, A. Buschini, C. Rossi and C. Zani (2003). "Evaluation of the migration of mutagens/carcinogens from PET bottles into

mineral water by Tradescantia/micronuclei test, Comet assay on leukocytes and GC/MS." Science of The Total Environment **302**(1–3): 101-108.

Blythe, A. R., D. Briggs, C. R. Kendall, D. G. Rance and V. J. I. Zichy (1978). "Surface modification of polyethylene by electrical discharge treatment and the mechanism of autoadhesion." Polymer **19**(11): 1273-1278.

Bodas, D. S., S. J. Patil, A. B. Mandale and S. A. Gangal (2004). "RF sputter deposition of poly(tetrafluoroethylene) films as masking materials for silicon micromachining." Journal of Applied Polymer Science **91**(2): 1183-1192.

Bordereau, V., M. Carrega, Z. H. Shi, L. A. Utracki and P. Sammut (1992). "Development of polymer blend morphology during compounding in a twin-screw extruder. Part III: Experimental procedure and preliminary results." Polymer Engineering & Science **32**(24): 1846-1856.

Bousquet, A., E. Ibarboure, C. Drummond, C. Labrugere, E. Papon and J. Rodriguez-Hernandez (2008). "Design of Stimuli-Responsive Surfaces Prepared by Surface Segregation of Polypeptide-b-polystyrene Diblock Copolymers." Macromolecules **41**(4): 1053-1056.

Brewis, M. (2002). Adhesion and Bonding to Polyolefins, Shrewsbury.

Bruder, F. and R. Brenn (1992). "Spinodal decomposition in thin films of a polymer blend." Physical Review Letters **69**(4): 624-627.

Brunn, P. O. and S. Chi (1984). "Macromolecules in non-homogeneous flow fields: A general study for dumbbell model macromolecules." Rheologica Acta **23**, 163.

Buckton, G. and B. Chandaria (1993). "Consideration of adhesion to modified container walls, by use of surface energy and polarity data, and Lewis acid-Lewis base interactions." International Journal of Pharmaceutics **94**: 223-229.

Cahn, J. W. and J. E. Hilliard (1958). "Free Energy of a Nonuniform System. I. Interfacial Free Energy." The Journal of Chemical Physics **28**(2): 258-267.

Cantu, A. A. (2009). Ink Analysis. Wiley Encyclopedia of Forensic Science, John Wiley & Sons, Ltd.

- Cerclé, C., P. Sarazin and B. D. Favis (2013). "High performance polyethylene/thermoplastic starch blends through controlled emulsification phenomena." Carbohydrate Polymers **92**(1): 138-148.
- Chan, C. M., T. M. Ko and H. Hiraoka (1996). "Polymer surface modification by plasmas and photons." Surface Science Reports **24**: 1-54.
- Chen, C. C. and J. L. White (1993). "Compatibilizing agents in polymer blends: Interfacial tension, phase morphology, and mechanical properties." Polymer Engineering & Science **33**(14): 923-930.
- Chen, J. and J. A. Gardella (1998). "Solvent Effects on the Surface Composition of Poly(dimethylsiloxane)-co-Polystyrene/Polystyrene Blends." Macromolecules **31**(26): 9328-9336.
- Chen, W. and T. J. McCarthy (1999). "Adsorption/Migration of a Perfluorohexylated Fullerene from the Bulk to the Polymer/Air Interface." Macromolecules **32**(7): 2342-2347.
- Chen, Z., R. Ward, Y. Tian, A. S. Eppler, Y. R. Shen and G. A. Somorjai (1999). "Surface Composition of Biopolymer Blends Biospan-SP/Phenoxy and Biospan-F/Phenoxy Observed with SFG, XPS, and Contact Angle Goniometry." The Journal of Physical Chemistry B **103**(15): 2935-2942.
- Cho, K., H. K. Jeon, C. E. Park, J. Kim and K. U. Kim (1996). "The effect of end-sulfonated polystyrene on the interfacial tension of nylon-6/polystyrene blends." Polymer **37**(7): 1117-1122.
- Choi, D. M., C. K. Park, K. Cho and C. E. Park (1997). "Adhesion improvement of epoxy resin/polyethylene joints by plasma treatment of polyethylene." Polymer **38**(25): 6243-6249.
- Chu, P. K., J. Y. Chen, L. P. Wang and N. Huang (2002). "Plasma-surface modification of biomaterials." Materials Science and Engineering: R: Reports **36**: 143-206.
- Coad, B. R., Y. Lu and L. Meagher (2012). "A substrate-independent method for surface grafting polymer layers by atom transfer radical polymerization: Reduction of protein adsorption." Acta Biomaterialia **8**(2): 608-618.

- Composto, R. J. and H. J. Chung (2005). Nanolithography and patterning techniques in microelectronics Surface-induced structure formation of polymer blends. D. Bucknall. Woodhead Publishing: 39-75.
- Composto, R. J., R. M. Walters and J. Genzer (2002). "Application of ion scattering techniques to characterize polymer surfaces and interfaces." Materials Science and Engineering: R: Reports **38**: 107-180.
- Croll, T. I., A. J. OConnor, G. W. Stevens and J. J. Cooper-White (2004). "Controllable Surface Modification of Poly(lactic-co-glycolic acid) (PLGA) by Hydrolysis or Aminolysis I: Physical, Chemical, and Theoretical Aspects." Biomacromolecules **5**(2): 463-473.
- Curtiss, C. F. and R. B. Bird (1996). "Statistical mechanics of transport phenomena: Polymeric liquid mixtures" Adv. Polym. Sci. **125**, 1.
- D. Briggs, J. T. G. (1983). Practical Surface Analysis by Auger and X-Ray Photoelectron Spectroscopy. Chichester, Wiley.
- Dadmun, M. (1996). "Effect of Copolymer Architecture on the Interfacial Structure and Miscibility of a Ternary Polymer Blend Containing a Copolymer and Two Homopolymers." Macromolecules **29**(11): 3868-3874.
- Dai, W., T. J. Ko, K. H. Oh, K. R. Lee and M.-W. Moon (2012). "Ion-Beam Induced Surface Roughening of Poly-(methyl methacrylate) (PMMA) Tuned by a Mixture of Ar and O₂ Ions." Plasma Processes and Polymers **9**(10): 975-983.
- Dargaville, T. R., G. A. George, D. J. T. Hill and A. K. Whittaker (2003). "High energy radiation grafting of fluoropolymers." Progress in Polymer Science **28**(9): 1355-1376.
- Dastjerdi, R., M. R. M. Mojtahedi and N. Heidari (2012). "Developing chromic dyeable PET nanocomposites: The dye absorption and complex formation mechanisms." Journal of Applied Polymer Science **125**(5): 3688-3694.
- Datla, V., E. Shim and B. Pourdeyhimi (2012). "Surface modifications of polypropylene with nonylphenol ethoxylates melt additives." Polymer Engineering & Science **52**: 1920.
- David Briggs, M. P. S. (1990). Practical Surface Analysis by Auger and X-Ray Photoelectron Spectroscopy. New York, Wiley: 553.

- David, R. and A. W. Neumann (2013). "Contact Angle Hysteresis on Randomly Rough Surfaces: A Computational Study." Langmuir **29**(14): 4551-4558.
- Davis, C. S. and A. J. Crosby (2011). "Mechanics of wrinkled surface adhesion." Soft Matter **7**(11): 5373-5381.
- Demarquette, N. R. and M. R. Kamal (1994). "Interfacial tension in polymer melts. I: An improved pendant drop apparatus." Polymer Engineering & Science **34**(24): 1823-1833.
- Desai, S. and R. P. Singh (2004). Surface Modification of Polyethylene. Long Term Properties of Polyolefins. A. C. Albertsson, Springer Berlin Heidelberg. **169**: 231-294.
- Desie, G., G. Deroover, F. De Voeght and A. Soucemarianadin (2004). "Printing of Dye and Pigment-Based Aqueous Inks Onto Porous Substrates." Journal of Imaging Science and Technology **48**(5): 389-397.
- Dill, K. A. and B. H. Zimm (1979). "A rheological separator for very large DNA molecules." Nucleic Acids Research **7**(3): 735-749.
- Dong, Y., W. Lyoo and J. Jang (2010). "Union dyeing of the photografted PET/wool blend fabrics with dimethylaminopropyl methacrylamide." Fibers and Polymers **11**(2): 213-217.
- Drouot, R. and M. Berrajaa (1993). "A thermodynamical approach of wall effects on the rheology of dilute polymer solutions." International Journal of Engineering Science **31**(11): 1463-1474.
- Du, J. Z., T. M. Sun, S. Q. Weng, X. S. Chen and J. Wang (2007). "Synthesis and Characterization of Photo-Cross-Linked Hydrogels Based on Biodegradable Polyphosphoesters and Poly(ethylene glycol) Copolymers." Biomacromolecules **8**(11): 3375-3381.
- Dubois, L. H. and B. R. Zegarski (1993). "Bonding of alkoxysilanes to dehydroxylated silica surfaces: a new adhesion mechanism." The Journal of Physical Chemistry **97**(8): 1665-1670.
- DuPont. (2008). "A new Additive for Solvent-Based Printing Inks." from http://www2.dupont.com/Tyzor/es_MX/assets/downloads/K16107_tyzor_iam_final.pdf.

- Elman, J. F., B. D. Johs, T. E. Long and J. T. Koberstein (1994). "A neutron reflectivity investigation of surface and interface segregation of polymer functional end groups." Macromolecules **27**(19): 5341-5349.
- Elmendorp, J. J. (1986). "Study on polymer blending microrheology." Polymer Engineering and Science **26**(6): 418-426.
- Erbil, H. Y., G. McHale, S. M. Rowan and M. I. Newton (1999). "Determination of the Receding Contact Angle of Sessile Drops on Polymer Surfaces by Evaporation." Langmuir **15**(21): 7378-7385.
- Esteves, A. C. C., K. Lyakhova, L. G. J. van der Ven, R. A. T. M. van Benthem and G. de With (2013). "Surface Segregation of Low Surface Energy Polymeric Dangling Chains in a Cross-Linked Polymer Network Investigated by a Combined Experimental–Simulation Approach." Macromolecules **46**(5): 1993-2002.
- Favaro, S. L., A. F. Rubira, E. C. Muniz and E. Radovanovic (2007). "Surface modification of HDPE, PP, and PET films with KMnO₄/HCl solutions." Polymer Degradation and Stability **92**(7): 1219-1226.
- Favia, P., M. Stendardo and R. d'Agostino (1996). "Selective grafting of amine groups on polyethylene by means of NH₃-H₂ RF glow discharges." Plasmas and Polymers **1**(2): 91-112.
- Favis, B. D. and J. P. Chalifoux (1988). "Influence of composition on the morphology of polypropylene/polycarbonate blends." Polymer **29**(10): 1761-1767.
- Fenouillot, F., P. Cassagnau and J. C. Majeste (2009). "Uneven distribution of nanoparticles in immiscible fluids: Morphology development in polymer blends." Polymer **50**(6): 1333-1350.
- Flory, P. J., R. A. Orwoll and A. Vrij (1964). "Statistical Thermodynamics of Chain Molecule Liquids. II. Liquid Mixtures of Normal Paraffin Hydrocarbons." Journal of the American Chemical Society **86**(17): 3515-3520.
- Fodor, J., D. A. Hill, (1992). "On the detection of flow-induced fractionation in melts of homopolymers by normal-mode microdielectrometry." Macromolecules **25**, 3511–3520.

- Fortelny, I., J. Juza, T. Vacková and M. Šlouf (2011). "The effect of anisometry of dispersed droplets on their coalescence during annealing of polymer blends." Colloid and Polymer Science **289**(17-18): 1895-1903.
- Foulc, M. P., A. Bergeret, L. Ferry, P. Ienny and A. Crespy (2005). "Study of hygrothermal ageing of glass fibre reinforced PET composites." Polymer Degradation and Stability **89**(3): 461-470.
- Fourche, G. (1995). "An overview of the basic aspects of polymer adhesion. Part I: Fundamentals." Polymer Engineering & Science **35**(12): 957-967.
- Fowkes, F. M. (1968). "Calculation of work of adhesion by pair potential summation." Journal of Colloid and Interface Science **28**(3-4): 493-505.
- Fowkes, F. M., F. L. Riddle Jr, W. E. Pastore and A. A. Weber (1990). "Interfacial interactions between self-associated polar liquids and squalane used to test equations for solid, liquid interfacial interactions." Colloids and Surfaces **43**(2): 367-387.
- Frank Curtis, W. and W. Zin (1987). Morphology in Miscible and Immiscible Polymer Blends. Photophysics of Polymers, American Chemical Society. **358**: 18-36.
- Fraunhofer, J. (2012). "Adhesion and Cohesion." International Journal of Dentistry, 2012, from <http://dx.doi.org/10.1155/2012/951324>.
- Fu, X. and X. He (2008). "Fabrication of super-hydrophobic surfaces on aluminum alloy substrates." Applied Surface Science **255**(5, Part 1): 1776-1781.
- Fuller, K. (2011). "Effect of surface roughness on the adhesion of elastomers to hard surfaces." Materials Science Forum. SEP 25, 2009, Trans tech Publications Ltd. **662**: 39--51.
- Garner F. and A. Nissan (1946). "Rheological properties of high viscosity solutions of long molecules." Nature **158**, 634.
- Gao, L., T. J. McCarthy and X. Zhang (2009). "Wetting and Superhydrophobicity†." Langmuir **25**(24): 14100-14104.
- Gauthier, F., H. L. Goldsmith and S. G. Mason (1971). "Particle motions in non-Newtonian media." Rheologica Acta **10**(3): 344-364.

- Gent, A. N. and C. W. Lin (1990). "Model Studies of the Effect of Surface Roughness and Mechanical Interlocking on Adhesion." The Journal of Adhesion **32**(2-3): 113-125.
- Gent, A. N. and C. W. Lin (1990). "Model studies of the effect of surface-roughness and mechanical interlocking on adhesion." Journal of Adhesion **32**(2-3): 113-125.
- Geoghegan, M., R. A. L. Jones, A. S. Clough and J. Penfold (1995). "The morphology of as-cast films of a polymer blend: Dependence on polymer molecular weight." Journal of Polymer Science Part B: Polymer Physics **33**(8): 1307-1311.
- Geoghegan, M. and G. Krausch (2003). "Wetting at polymer surfaces and interfaces." Progress in Polymer Science **28**(2): 261-302.
- Glover, J. H. (1988). "Slip migration in extrusion coatings." Tappi Journal **71**(3)(1988): 188-192.
- Goddard, J. M. and J. H. Hotchkiss (2007). "Polymer surface modification for the attachment of bioactive compounds." Progress in Polymer Science **32**(7): 698-725.
- Good, R. J. (1993). Contact Angle, Wettability and Adhesion. Utrecht, VSP.
- Guerrica-Echevarría, G. and J. I. Eguiazábal (2009). "Structure and mechanical properties of impact modified poly(butylene terephthalate)/poly(ethylene terephthalate) blends." Polymer Engineering & Science **49**(5): 1013-1021.
- Guo, H. F., S. Packirisamy, N. V. Gvozdic and D. J. Meier (1997). "Prediction and manipulation of the phase morphologies of multiphase polymer blends: 1. Ternary systems." Polymer **38**(4): 785-794.
- H. Lee, a. L. A. A. (2001). "Functionalizing Polymer Surfaces by Field-Induced Migration of Copolymer Additives. 1. Role of Surface Energy Gradients." Macromolecules **34**(13): 8.
- Hardman, S. J., L. R. Hutchings, N. Clarke, S. M. Kimani, L. L. E. Mears, E. F. Smith, J. R. P. Webster and R. L. Thompson (2012). "Surface Modification of Polyethylene with Multi-End-Functional Polyethylene Additives." Langmuir **28**(11): 5125-5137.
- Hardman, S. J., N. Muhamad-Sarih, H. J. Riggs, R. L. Thompson, J. Rigby, W. N. A. Bergius and L. R. Hutchings (2011). "Electrospinning Superhydrophobic Fibers Using Surface Segregating End-Functionalized Polymer Additives." Macromolecules **44**(16): 6461-6470.

- Hobbs, S. Y., M. E. J. Dekkers and V. H. Watkins (1988). "Toughened blends of poly(butylene terephthalate) and BPA polycarbonate." Journal of Materials Science **23**(4): 1219-1224.
- Hong, J., K. Ahn and S. Lee (2005). "Strain hardening behavior of polymer blends with fibril morphology." Rheologica Acta **45**(2): 202-208.
- Hong, S. J., F. M. Chang, T. H. Chou, S. H. Chan, Y. J. Sheng and H. K. Tsao (2011). "Anomalous Contact Angle Hysteresis of a Captive Bubble: Advancing Contact Line Pinning." Langmuir **27**(11): 6890-6896.
- Huneault, M. A., Z. H. Shi and L. A. Utracki (1995). "Development of polymer blend morphology during compounding in a twin-screw extruder. Part IV: A new computational model with coalescence." Polymer Engineering & Science **35**(1): 115-127.
- Inoue, T. (2003). Morphology of Polymer Blends. Polymer Blends Handbook. L. A. Utracki, Springer Netherlands: 547-576.
- Jendreck, R. M., D. C. Schwartz, J. J. de Pablo and M. D. Graham (2004). "Shear-induced migration in flowing polymer solutions: Simulation of long-chain DNA in microchannels." The Journal of Chemical Physics **120**(5): 2513-2529.
- Jones, R. A. L. and E. J. Kramer (1993). "The surface composition of miscible polymer blends." Polymer **34**(1): 115-118.
- K Cho, H. K. J., C.E Park (1996). "The effect of end-sulfonated polystyrene on the interfacial tension of nylon-6/polystyrene blends." polymer **37**.
- Kahn, B. E. and B. E. Kahn (2008). "Printing Methods for Printed Electronics." NIP & Digital Fabrication Conference **2008**(1): 15-20.
- Kamal, M. R., R. Lai-Fook and N. R. Demarquette (1994). "Interfacial tension in polymer melts. Part II: Effects of temperature and molecular weight on interfacial tension." Polym. Eng. Sci. **34**(24): 1834-1839.
- Kami, A., H. Kaczmarek and J. Kowalonek (2002). "The influence of side groups and polarity of polymers on the kind and effectiveness of their surface modification by air plasma action." European Polymer Journal **38**(9): 1915-1919.

- Kang, E. T. and K. G. Neoh (2002). Surface Modification of Polymers. Encyclopedia of Polymer Science and Technology, John Wiley & Sons, Inc.
- Karim, A., T. M. Slawacki, S. K. Kumar, J. F. Douglas, S. K. Satija, C. C. Han, T. P. Russell, Y. Liu, R. Overney, J. Sokolov and M. H. Rafailovich (1998). "Phase-Separation-Induced Surface Patterns in Thin Polymer Blend Films." Macromolecules **31**(3): 857-862.
- Katano, Y., H. Tomono and T. Nakajima (1994). "Surface Property of Polymer Films with Fluoroalkyl Side Chains." Macromolecules **27**(8): 2342-2344.
- Kato, K., E. Uchida, E. T. Kang, Y. Uyama and Y. Ikada (2003). "Polymer surface with graft chains." Progress in Polymer Science **28**(2): 209-259.
- Katzen, D. and S. Reich (1993). "Image Analysis of Phase Separation in Polymers Blends." EPL (Europhysics Letters) **21**(1): 55.
- Khan, M. B., B. J. Briscoe and S. M. Richardson (1994). "Field-Induced Phase Fractionation in Multiphase Polymer Flow Systems: A Review." Polymer-Plastics Technology and Engineering **33**(3): 295-322.
- Khodabakhshi, A. R., S. S. Madaeni, T. W. Xu, L. Wu, C. Wu, C. Li, W. Na, S. A. Zolanvari, A. Babayi, J. Ghasemi, S. M. Hosseini and A. Khaledi (2012). "Preparation, optimization and characterization of novel ion exchange membranes by blending of chemically modified PVDF and SPPO." Separation and Purification Technology **90**(0): 10-21.
- Kim, E. Y., W. K. Lee, M. J. Moon, S. S. Hong, K. T. Lim and S. Y. Yoon (2009). "Critical Value and Control of Complexation of Polylactide Blends Using Optical Purity." Composite Interfaces **16**(4-6): 307-317.
- Kim, W. S., I. H. Yun, J. J. Lee and H. T. Jung (2010). "Evaluation of mechanical interlock effect on adhesion strength of polymer-metal interfaces using micro-patterned surface topography." International Journal of Adhesion and Adhesives **30**(6): 408--417.
- Kinloch, A. J. (1980). "The science of adhesion." Journal of Materials Science **15**(9): 2141-2166.
- Kinloch, A. J. (1987). Adhesion and Adhesives Science and Technology. New York, Chapman & Hall.

- Koberstein, J. T. J., D. E. D. Duch, W. Hu, T. J. Lenk, R. Bhatia, H. R. Brown, J. P. Lingelser and Y. Gallot (1998). "Creating Smart Polymer Surfaces with Selective Adhesion Properties." The Journal of Adhesion **66**(1-4): 229-249.
- Koningsveld, R. (1994). "Thermodynamics of polymer blends." Macromolecular Symposia **78**(1): 1-13.
- Kroschwitz, J. I. (1999). Kirk-Othmer concise encyclopedia of chemical technology. New York, Wiley.
- Kumar, S. K. and T. P. Russell (1991). "Behavior of isotopic, binary polymer blends in the vicinity of neutral surfaces: the effects of chain-length disparity." Macromolecules **24**(13): 3816-3820.
- Kwamena, N. O. A., J. Buajarern and J. P. Reid (2010). "Equilibrium Morphology of Mixed Organic/Inorganic/Aqueous Aerosol Droplets: Investigating the Effect of Relative Humidity and Surfactants." The Journal of Physical Chemistry A **114**(18): 5787-5795.
- Kwok, D. Y. and A. W. Neumann (1999). "Contact angle measurement and contact angle interpretation." Advances in Colloid and Interface Science **81**(3): 167-249.
- Lacroix, C. B., M; Carreau, PJ; Favis, BD; Michel, A. (1996). "Properties of PETG/EVA blends .1. Viscoelastic, morphological and interfacial properties." Polymer **37**(14): 9.
- Landry, C. J. T., H. Yang and J. S. Machell (1991). "Miscibility and mechanical properties of a ternary polymer blend: polystyrene/polycarbonate/tetramethyl polycarbonate." Polymer **32**(1): 44-52.
- Lazare, S. and R. Srinivasan (1986). "Surface properties of poly(ethylene terephthalate) films modified by far-ultraviolet radiation at 193nm (laser) and 185nm (low intensity)." The Journal of Physical Chemistry **90**(10): 2124-2131.
- Leach, R. H. and R. J. Pierce (1993). The nature of printing ink. The Printing Ink Manual. R. H. Leach, R. J. Pierce, E. P. Hickman, M. J. Mackenzie and H. G. Smith, Springer Netherlands: 1-13.

- Lee, C. Y., J. W. Ha, I. Jun Park and S. B. Lee (2002). "Surface characteristics of water-soluble cationic fluoro copolymers containing perfluoroalkyl, quaternized amino, and hydroxyl groups." Journal of Applied Polymer Science **86**(14): 3702-3707.
- Lee, H. and L. A. Archer (2001). "Functionalizing Polymer Surfaces by Field-Induced Migration of Copolymer Additives. 1. Role of Surface Energy Gradients." Macromolecules **34**(13): 4572-4579.
- Lee, H. and L. A. Archer (2002). "Functionalizing polymer surfaces by field-induced migration of copolymer additives—role of shear fields." Polymer Engineering & Science **42**(7): 1568-1579.
- Lee, H. and L. A. Archer (2002). "Functionalizing polymer surfaces by surface migration of copolymer additives: role of additive molecular weight." Polymer **43**(9): 2721-2728.
- Lee, H. U., S. Y. Park, Y. H. Kang, S. Y. Jeong, S. H. Choi, K. Y. Jahng and C. R. Cho (2010). "Surface modification of and selective protein attachment to a flexible microarray pattern using atmospheric plasma with a reactive gas." Acta Biomaterialia **6**(2): 519-525.
- Lee, J. K., C. S. Ha and W. K. Lee (2004). "Surface Analysis and Modification of Fluorocarbon-End Capped Polyester Ultrathin Films." Molecular Crystals and Liquid Crystals **425**(1): 69-75.
- Lee, J. K. and C. D. Han (1999). "Evolution of polymer blend morphology during compounding in an internal mixer." Polymer **40**(23): 6277-6296.
- Lee, J. K. and C. D. Han (2000). "Evolution of polymer blend morphology during compounding in a twin-screw extruder." Polymer **41**(5): 1799-1815.
- Lee, J. S., M. D. Foster and D. T. Wu (2006). "Effects of Branch Points and Chain Ends on the Thermodynamic Interaction Parameter in Binary Blends of Regularly Branched and Linear Polymers." Macromolecules **39**(15): 5113-5121.
- Lee, S. J., G. Khang, Y. M. Lee and H. B. Lee (2003). "The effect of surface wettability on induction and growth of neurites from the PC-12 cell on a polymer surface." Journal of Colloid and Interface Science **259**(2): 228-235.

- Lee, W. K., I. Losito, J. A. Gardella and W. L. Hicks (2001). "Synthesis and Surface Properties of Fluorocarbon End-Capped Biodegradable Polyesters." Macromolecules **34**(9): 3000-3006.
- Lemmouchi, Y. and E. Schacht (1997). "Preparation and in vitro evaluation of biodegradable poly(α -caprolactone-co-d,l lactide)(X-Y) devices containing trypanocidal drugs." Journal of Controlled Release **45**(3): 227-233.
- Li, L. P., B. Yin and M.-B. Yang (2011). "Morphology prediction and the effect of core-shell structure on the rheological behavior of PP/EPDM/HDPE ternary blends." Polymer Engineering & Science **51**(12): 2425-2433.
- Li, X., L. Andruzzi, E. Chiellini, G. Galli, C. K. Ober, A. Hexemer, E. J. Kramer and D. A. Fischer (2002). "Semifluorinated Aromatic Side-Group Polystyrene-Based Block Copolymers: Bulk Structure and Surface Orientation Studies." Macromolecules **35**(21): 8078-8087.
- Lin, C. C., S. V. Jonnalagadda, N. P. Balsara, C. C. Han and R. Krishnamoorti (1996). "Thermodynamic Interactions in Multicomponent Polymer Blends." Macromolecules **29**(2): 661-669.
- Lin, J. W. (1990). Ink compositions containing modified pigment particles. **5281261**.
- Liu, X. D., D. K. Sheng, X. M. Gao, T.-B. Li and Y. M. Yang (2013). "UV-assisted surface modification of PET fiber for adhesion improvement." Applied Surface Science **264**(0): 61-69.
- Longjian Xue, Y. H. (2011). "Pattern formation by dewetting of polymer thin film." Progress in Polymer Science **36**(2): 25.
- Loopez-Santos, C., F. Yubero, J. Cotrino and A. n. R. Gonzaaez-Elipe (2010). "Surface Functionalization, Oxygen Depth Profiles, and Wetting Behavior of PET Treated with Different Nitrogen Plasmas." ACS Applied Materials & Interfaces **2**(4): 980-990.
- Luo, Y., W. Yu and F. Xu (2011). "Surface Modification and Vapor-Induced Response of Poly(Vinylidene Fluoride)/Carbon Black Composite Conductive Thin Films." Polymer-Plastics Technology and Engineering **50**(11): 1084-1090.

- Luzinov, I. and C. Pagnouille (2000). "Ternary polymer blend with core-shell dispersed phases: effect of the core-forming polymer on phase morphology and mechanical properties." Polymer **41**(19): 7099-7109.
- MacDonald, M. J. and S. J. Muller (1996). "Experimental study of shear-induced migration of polymers in dilute solutions." Journal of Rheology **40**(2): 259-283.
- Mandelkern, L. (1964). Crystallization of Polymers. New York, McGraw-Hill.
- Marmur, A. (2003). "Wetting on Hydrophobic Rough Surfaces: To Be Heterogeneous or Not To Be?" Langmuir **19**(20): 8343-8348.
- Marshall, S. J., S. C. Bayne, R. Baier, A. P. Tomsia and G. W. Marshall (2010). "A review of adhesion science." Dental Materials **26**(2): e11-e16.
- Maugis, D. (1996). "On the contact and adhesion of rough surfaces." Journal of Adhesion Science and Technology **10**(2): 161--175.
- Mayer, M. (1997). SIMNRA User's Guide. M. P. I. f. Plasmaphysik.
- Mazzitelli, C., M. Ferrari, M. Toledano, E. Osorio, F. Monticelli and R. Osorio (2008). "Surface Roughness Analysis of Fiber Post Conditioning Processes." Journal of Dental Research **87**(2): 186-190.
- McCafferty, E. (2002). "Acid-base effects in polymer adhesion at metal surfaces." Journal of Adhesion Science and Technology **16**(3): 239-255.
- McMaster, L. P. (1973). "Aspects of Polymer-Polymer Thermodynamics." Macromolecules **6**(5): 760-773.
- Medard, N., J. C. Soutif and F. Poncin-Epaillard (2002). "Characterization of CO₂ plasma-treated polyethylene surface bearing carboxylic groups." Surface and Coatings Technology **160**(2-3): 197-205.
- Mekhilef, N., B. D. Favis and P. J. Carreau (1997). "Morphological stability, interfacial tension, and dual-phase continuity in polystyrene-polyethylene blends." Journal of Polymer Science Part B: Polymer Physics **35**(2): 293-308.
- Mendel, J., D. Bugner and A. D. Bermel (1999). "Particle Generation and Ink Particle Size Effects in Pigmented Inkjet Inks – Part II." Journal of Nanoparticle Research **1**(3): 421-424.

- Merrill, E. W. and E. W. Salzman (1983). "Polyethylene oxide as a biomaterial." ASAIO Journal **6**(2): 60-64.
- Miccio, L. A., R. Liao, W. H. Schreiner, P. E. Montemartini and P. A. Oyanguren (2010). "Partially fluorinated polymer networks: Surface and tribological properties." Polymer **51**(26): 6219-6226.
- Micheli, P. (2000). "Pigment wetting characteristics of radiation curing systems." Surface Coatings International **83**(9): 455-459.
- Migdal, A. and H. P. Schreiber (1995). "Specific Interactions, Initial and Equilibrium Bond Strength in Polymer/Polymer Assemblies." The Journal of Adhesion **52**(1-4): 1-11.
- Minnikanti, V. S. and L. A. Archer (2006). "Entropic Attraction of Polymers toward Surfaces and Its Relationship to Surface Tension." Macromolecules **39**(22): 7718-7728.
- Miwa, M., A. Nakajima, A. Fujishima, K. Hashimoto and T. Watanabe (2000). "Effects of the Surface Roughness on Sliding Angles of Water Droplets on Superhydrophobic Surfaces." Langmuir **16**(13): 5754-5760.
- Moore (2012). 2011 Postconsumer Plastics Recycling in Canada, Moore Recycling Associates.
- Morent, R., N. De Geyter and C. Leys (2008). "Effects of operating parameters on plasma-induced PET surface treatment." Nuclear Instruments and Methods in Physics Research Section B: Beam Interactions with Materials and Atoms **266**(12,Ä13): 3081-3085.
- Morisada, Y., H. Fujii, T. Nagaoka and M. Fukusumi (2006). "MWCNTs/AZ31 surface composites fabricated by friction stir processing." Materials Science and Engineering: A **419**(1-2): 344-348.
- Nahar, P., A. Naqvi and S. F. Basir (2004). "Sunlight-mediated activation of an inert polymer surface for covalent immobilization of a protein." Analytical Biochemistry **327**(2): 162-164.
- Noeske, M., J. Degenhardt, S. Strudthoff and U. Lommatzsch (2004). "Plasma jet treatment of five polymers at atmospheric pressure: surface modifications and the relevance for adhesion." International Journal of Adhesion and Adhesives **24**(2): 171-177.

- Omonov, T. S., C. Harrats and G. Groeninckx (2005). "Co-continuous and encapsulated three phase morphologies in uncompatibilized and reactively compatibilized polyamide 6/polypropylene/polystyrene ternary blends using two reactive precursors." Polymer **46**(26): 12322-12336.
- Owens, D. K. (1969). "R. C Wendt." Journal of Applied Polymer Science. **13**: 1741.
- Owens, D. K. and R. C. Wendt (1969). "Estimation of the surface free energy of polymers." Journal of Applied Polymer Science **13**(8): 1741-1747.
- Ozdemir, M., C. U. Yurteri and H. Sadikoglu (1999). "Physical Polymer Surface Modification Methods and Applications in Food Packaging Polymers." Critical Reviews in Food Science and Nutrition **39**(5): 457-477.
- OZMAN, A. (2008). Health and Safety Considerations in Printing, Dokuz Eylul University
- P.H.M Elemans, J. M. H. J., H.E.H Meijer (1990). "The measurement of interfacial tension in polymer/polymer systems: The breaking thread method." Journal of Rheology **34**: 1311.
- Packham, D. E. (1992). "The Mechanical Theory of Adhesion-Changing Perceptions 1925-1991." The Journal of Adhesion **39**(2-3): 137-144.
- Packham, D. E. (1996). "Work of adhesion: Contact angles and contact mechanics." International Journal of Adhesion and Adhesives **16**(2): 121-128.
- Packham, D. E. and C. Johnston (1994). "Mechanical adhesion: were McBain and Hopkins right? An empirical study." International Journal of Adhesion and Adhesives **14**(2): 131-135.
- Paiva, A., N. Sheller, M. D. Foster, A. J. Crosby and K. R. Shull (2000). "Study of the Surface Adhesion of Pressure-Sensitive Adhesives by Atomic Force Microscopy and Spherical Indenter Tests." Macromolecules **33**(5): 1878-1881.
- Pandiyaraj, K. N., V. Selvarajan and R. R. Deshmukh (2010). "Effects of operating parameters on DC glow discharge plasma induced PET film surface." Journal of Physics: Conference Series **208**(1): 12100.
- Pangelina, A. B., R.L. McCullough, M.J. Kelley (1994). "Analytic model for surface induced molecular weight segregation in thermoplastic composites. Journal of Polymer Science: Part B, **32**, 2383.

- Park, J. H., S. Lee, J. H. Kim, K. Park, K. Kim and I. C. Kwon (2008). "Polymeric nanomedicine for cancer therapy." Progress in Polymer Science **33**(1): 113-137.
- Parvinzadeh Gashti, M. and S. Moradian (2012). "Effect of nanoclay type on dyeability of polyethylene terephthalate/clay nanocomposites." Journal of Applied Polymer Science **125**(5): 4109-4120.
- Patel, S. S. and M. Tirrell (1989). "Measurement of Forces Between Surfaces in Polymer Fluids." Annual Review of Physical Chemistry **40**(1): 597-635.
- Pekarovicova, A., H. Bhide, P. Fleming and J. Pekarovic (2003). "Phase-Change Inks." Journal of Coatings Technology **75**(936): 65-72.
- Pena, G., A. Eceiza, A. Valea, P. Remiro, P. Oyanguren and I. Mondragon (2003). "Control of morphologies and mechanical properties of thermoplastic-modified epoxy matrices by addition of a second thermoplastic." Polymer International **52**(9): 1444-1453.
- Peng, Z. L. and S. H. Chen (2011). "Effects of surface roughness and film thickness on the adhesion of a bioinspired nanofilm." Physical Review E **83**(5): 051915.
- Praschak, D., T. Bahners and E. Schollmeyer (1998). "PET surface modifications by treatment with monochromatic excimer UV lamps." Applied Physics A **66**(1): 69-75.
- Price, R. L., K. Ellison, K. M. Haberstroh and T. J. Webster (2004). "Nanometer surface roughness increases select osteoblast adhesion on carbon nanofiber compacts." Journal of Biomedical Materials Research Part A **70A**(1): 129-138.
- Pukanszky, B. and E. Fekete (1999). Adhesion and Surface Modification Mineral Fillers in Thermoplastics I. J. Jancar, E. Fekete, P. Hornsby et al., Springer Berlin / Heidelberg. **139**: 109-153.
- Qian, B. and Z. Shen (2005). "Fabrication of Superhydrophobic Surfaces by Dislocation-Selective Chemical Etching on Aluminum, Copper, and Zinc Substrates." Langmuir **21**(20): 9007-9009.
- Qian, C., S. J. Mumby and B. E. Eichinger (1991). "Phase diagrams of binary polymer solutions and blends." Macromolecules **24**(7): 1655-1661.

- Qian, H., Y. X. Zhang, S. M. Huang and Z. Y. Lin (2007). "Effect of the surface-modifying macromolecules on the duration of the surface functionalization." Applied Surface Science **253**(10): 4659-4667.
- Raghunath, C., G. W. Roland and G. Gerhard (2010). "Migration of semiflexible polymers in microcapillary flow." EPL (Europhysics Letters) **91**(1): 14001.
- Ramanathan, T., A. A. Abdala, S. Stankovich, D. A. Dikin, M. Herrera-Alonso, R. D. Piner, D. H. Adamson, H. C. Schniepp, X. Chen, R. S. Ruoff, S. T. Nguyen, I. A. Aksay, R. K. Prud'homme and L. C. Brinson (2008). "Functionalized graphene sheets for polymer nanocomposites." Nature Nanotechnology **3**(6): 327--331.
- Ramírez, M. X., D. E. Hirt and L. L. Wright (2001). "AFM Characterization of Surface Segregated Erucamide and Behenamide in Linear Low Density Polyethylene Film." Nano Letters **2**(1): 9-12.
- Reichart, G. C., W. W. Graessley, R. A. Register, R. Krishnamoorti and D. J. Lohse (1997). "Measurement of Thermodynamic Interactions in Ternary Polymer Blends by Small-Angle Neutron Scattering." Macromolecules **30**(11): 3363-3368.
- Reignier, J. I. and B. D. Favis (2000). "Control of the Subinclusion Microstructure in HDPE/PS/PMMA Ternary Blends." Macromolecules **33**(19): 6998-7008.
- Ridgway, C. J. and P. A. C. Gane (2005). "Ink-Coating Adhesion: The Importance of Pore Size and Pigment Surface Chemistry." Journal of Dispersion Science and Technology **25**(4): 469-480.
- Saad, A. A. E. R. E. (2007). Environmental pollution reduction by using VOC-free water-based gravure inks and drying them with a new drying system based on dielectric heating, Universität Wuppertal.
- Sakellariou, P. (1993). "Effect of polymer compatibility on surface enrichment in polymer blends." Polymer **34**(16): 3408-3415.
- Sanaeepur, H., A. Ebadi Amooghin, A. Moghadassi, A. Kargari, S. Moradi and D. Ghanbari (2012). "A novel acrylonitrile–butadiene–styrene/poly(ethylene glycol) membrane: preparation, characterization, and gas permeation study." Polymers for Advanced Technologies **23**(8): 1207-1218.

- Schreiber, H. P. and S. H. Storey (1965). "Molecular fractionation in capillary flow of polymer fluids." *Journal of Polymer Science, Polymer Letter* **3**: 723–727.
- Semenov, A. N., J. F. Joanny, A. Johner and J. Bonet-Avalos (1997). "Interaction between Two Adsorbing Plates: The Effect of Polymer Chain Ends." *Macromolecules* **30**(5): 1479-1489.
- Senshu, K., S. Yamashita, H. Mori, M. Ito, A. Hirao and S. Nakahama (1999). "Time-Resolved Surface Rearrangements of Poly(2-hydroxyethyl methacrylate-block-isoprene) in Response to Environmental Changes." *Langmuir* **15**(5): 1754-1762.
- Shan, W. L., J. Du, E. P. Hampp, H. Li, G. Papandreou, C. A. Maryanoff and W. O. Soboyejo (2012). "Adhesion and cohesion in structures containing suspended microscopic polymeric films." *Acta Biomaterialia* **8**(4): 1469-1480.
- Sheth, S. R., N. Efremova and D. E. Leckband (2000). "Interactions of Poly(ethylene oxide) Brushes with Chemically Selective Surfaces." *The Journal of Physical Chemistry B* **104**(32): 7652-7662.
- Shin, B., K. R. Lee, M. W. Moon and H. Y. Kim (2012). "Extreme water repellency of nanostructured low-surface-energy non-woven fabrics." *Soft Matter* **8**(6): 1817-1823.
- Shin, J. S., D. Y. Lee, C. C. Ho and J. H. Kim (1999). "Effect of Annealing on the Surface Properties of Poly(n-butyl methacrylate) Latex Films Containing Poly(styrene/methylstyrene/acrylic acid)." *Langmuir* **16**(4): 1882-1888.
- Sionkowska, A. (2011). "Current research on the blends of natural and synthetic polymers as new biomaterials: Review." *Progress in Polymer Science* **36**(9): 1254-1276.
- Situma, C., Y. Wang, M. Hupert, F. Barany, R. L. McCarley and S. A. Soper (2005). "Fabrication of DNA microarrays onto poly(methyl methacrylate) with ultraviolet patterning and microfluidics for the detection of low-abundant point mutations." *Analytical Biochemistry* **340**(1): 123-135.
- Slepicka, P., A. Vasina, Z. Kolská, T. Luxbacher, P. Malinský, A. Macková and V. Svorcik (2010). "Argon plasma irradiation of polypropylene." *Nuclear Instruments and Methods in Physics Research Section B: Beam Interactions with Materials and Atoms* **268**(11–12): 2111-2114.

- Son, Y. (2001). "Measurement of interfacial tension between polyamide-6 and poly(styrene-co-acrylonitrile) by breaking thread method." Polymer **42**(3): 1287-1291.
- Strobel, M., C. S. Lyons, J. M. Strobel and R. S. Kapaun (1992). "Analysis of air-corona-treated polypropylene and poly(ethylene terephthalate) films by contact-angle measurements and X-ray photoelectron spectroscopy." Journal of Adhesion Science and Technology **6**(4): 429-443.
- Sung, L., D. Hess, C. Jackson and C. Han (1996). "Phase separation kinetics and morphology in a polymer blend with diblock copolymer additive." Journal of Polymer Research **3**(3): 139-150.
- Svanholm, E. (2007). "Printability and Ink-Coating Interactions in Inkjet Printing." Ph.D. Dissertation, Karlstad University, Karlstad, Sweden.
- Taghizadeh, A., P. Sarazin and B. Favis (2013). "High molecular weight plasticizers in thermoplastic starch/polyethylene blends." Journal of Materials Science **48**(4): 1799-1811.
- Takayama, T. and M. Todo (2006). "Improvement of impact fracture properties of PLA/PCL polymer blend due to LTI addition." Journal of Materials Science **41**(15): 4989-4992.
- Tanaka, H. (1993). "Dynamic interplay between phase separation and wetting in a binary mixture confined in a one-dimensional capillary." Physical Review Letters **70**(1): 53-56.
- Tanaka, K., A. Takahara and T. Kajiyama (1998). "Surface Molecular Aggregation Structure and Surface Molecular Motions of High-Molecular-Weight Polystyrene/Low-Molecular-Weight Poly(methyl methacrylate) Blend Films." Macromolecules **31**(3): 863-869.
- Tanaka, K., J. S. Yoon, A. Takahara and T. Kajiyama (1995). "Ultrathinning-Induced Surface Phase Separation of Polystyrene/Poly(vinyl methyl ether) Blend Film." Macromolecules **28**(4): 934-938.
- Tanaka, T., R. Nakatsuru, Y. Kagari, N. Saito and M. Okubo (2008). "Effect of Molecular Weight on the Morphology of Polystyrene/Poly(methyl methacrylate) Composite Particles Prepared by the Solvent Evaporation Method, \ddot{A} †." Langmuir **24**(21): 12267-12271.
- Tang, Y. and M. Lewin (2008). "New aspects of migration and flame retardancy in polymer nanocomposites." Polymer Degradation and Stability **93**(11): 1986-1995.

- Tchoudakov, R., O. Breuer, M. Narkis and A. Siegmann (1996). "Conductive polymer blends with low carbon black loading: Polypropylene/polyamide." Polymer Engineering & Science **36**(10): 1336-1346.
- Ting, Y. H., C. C. Liu, S. M. Park, H. Jiang, P. F. Nealey and A. E. Wendt (2010). "Surface Roughening of Polystyrene and Poly(methyl methacrylate) in Ar/O₂ Plasma Etching." Polymers **2**(4): 649-663.
- Torres, N., J. J. Robin and B. Boutevin (2000). "Study of thermal and mechanical properties of virgin and recycled poly(ethylene terephthalate) before and after injection molding." European Polymer Journal **36**(10): 2075-2080.
- Tsao, C. W. and D. DeVoe (2009). "Bonding of thermoplastic polymer microfluidics." Microfluidics and Nanofluidics **6**(1): 1-16.
- Uyama, Y., K. Kato and Y. Ikada (1998). Surface Modification of Polymers by Grafting. Grafting/Characterization Techniques/Kinetic Modeling. H. Galina, Y. Ikada, K. Kato et al., Springer Berlin Heidelberg. **137**: 1-39.
- Valera, T. S., A. T. Morita and N. R. Demarquette (2006). "Study of Morphologies of PMMA/PP/PS Ternary Blends." Macromolecules **39**(7): 2663-2675.
- Van Oss, C. J., R. J. Good and M. K. Chaudhury (1988). "Additive and nonadditive surface tension components and the interpretation of contact angles." Langmuir **4**(4): 884-891.
- van Zyl, A. J. P., R. D. Sanderson, D. de Wet-Roos and B. Klumperman (2003). "Core/Shell Particles Containing Liquid Cores: Morphology Prediction, Synthesis, and Characterization." Macromolecules **36**(23): 8621-8629.
- Vandencastele, N., B. r. r. Broze, S. p. Collette, C. De Vos, P. Viville, R. Lazzaroni and F. o. Reniers (2010). "Evidence of the Synergetic Role of Charged Species and Atomic Oxygen in the Molecular Etching of PTFE Surfaces for Hydrophobic Surface Synthesis." Langmuir **26**(21): 16503-16509.
- Vicini, S., E. Princi and E. Pedemonte (2008). "Thermodynamic of polymer mixtures: The LCT applied to the poly(styrene)/poly(vinyl methylether) system." Journal of Polymer Science Part B: Polymer Physics **46**(8): 791-797.

- Virgilio, N., P. Desjardins, G. L'Esperance and B. D. Favis (2010). "Modified interfacial tensions measured in situ in ternary polymer blends demonstrating partial wetting." Polymer **51**(6): 1472-1484.
- Virgilio, N., C. Marc-Aurele and B. D. Favis (2009). "Novel Self-Assembling Close-Packed Droplet Array at the Interface in Ternary Polymer Blends." Macromolecules **42**(9): 3405-3416.
- Vrij, A. and J. T. G. Overbeek (1968). "Rupture of thin liquid films due to spontaneous fluctuations in thickness." Journal of the American Chemical Society **90**(12): 3074-3078.
- Wake, W. C. (1978). "Theories of adhesion and uses of adhesives: a review." Polymer **19**(3): 291-308.
- Walters, K. B., D. W. Schwark and D. E. Hirt (2003). "Surface Characterization of Linear Low-Density Polyethylene Films Modified with Fluorinated Additives." Langmuir **19**(14): 5851-5860.
- Wampler, T. P. (1989). "Thermometric behavior of polyolefins." Journal of Analytical and Applied Pyrolysis **15**(0): 187-195.
- Wang, H. and R. J. Composto (2000). "Understanding morphology evolution and roughening in phase-separating thin-film polymer blends." EPL (Europhysics Letters) **50**(5): 622.
- Wang, H. and R. J. Composto (2002). "Kinetics of Surface and Interfacial Fluctuations in Phase Separating Polymer Blend Films." Macromolecules **35**(7): 2799-2809.
- Wang, W., Q. Y. Shi, P. Liu, H. K. Li and T. Li (2009). "A novel way to produce bulk SiCp reinforced aluminum metal matrix composites by friction stir processing." Journal of Materials Processing Technology **209**(4): 2099-2103.
- Warson, H. (1991). "UV & EB curing formulation for printing inks, coatings and paints Edited by R. Holman & P. Goldring, London, Sita-Technology: 47.
- Wei, Q., Y. Liu, D. Hou and F. Huang (2007). "Dynamic wetting behavior of plasma treated PET fibers." Journal of Materials Processing Technology **194**: 89-92.
- Wenzel, R. N. (1948). "Surface Roughness and Contact Angle." The Journal of Physical and Colloid Chemistry **53**(9): 1466-1467.

- Willemse, R. C., A. Posthuma de Boer, J. van Dam and A. D. Gotsis (1999). "Co-continuous morphologies in polymer blends: the influence of the interfacial tension." Polymer **40**(4): 827-834.
- Wu, J. and C. C. Chu (2012). "Block copolymer of poly(ester amide) and polyesters: Synthesis, characterization, and in vitro cellular response." Acta Biomaterialia **8**(12): 4314-4323.
- Wu, S. (1971). "Calculation of interfacial tension in polymer systems." Journal of Polymer Science Part C: Polymer Symposia **34**(1): 19-30.
- Wu, S. (1974). "Interfacial and Surface Tensions of Polymers." Journal of Macromolecular Science, Part C **10**(1): 1-73.
- Wyart, F. B. and J. Daillant (1990). "Drying of solids wetted by thin liquid films." Canadian Journal of Physics **68**(9): 1084-1088.
- Xiaoying, L., C. Wei, H. Yan, Z. Yi and W. Zhigong (2009). "Surface modification on silicon with chitosan and biological research." Biomedical Materials **4**(4): 044103.
- Xing, C.-M., J. P. Deng and W. T. Yang (2005). "Synthesis of antibacterial polypropylene film with surface immobilized polyvinylpyrrolidone-iodine complex." Journal of Applied Polymer Science **97**(5): 2026-2031.
- Xue, M. L., Y. L. Yu, H. H. Chuah, J. M. Rhee, N. H. Kim and J. H. Lee (2007). "Miscibility and compatibilization of poly(trimethylene terephthalate)/acrylonitrile, Äbutadiene, Ästyrene blends." European Polymer Journal **43**(9): 3826-3837.
- Y. Kong, J. N. H. (2002). "The measurement of the crystallinity of polymers by DSC." polymer **43**(14): 6.
- Yang, J., J. L. White and Q. Jiang (2010). "Phase morphology development in a low interfacial tension immiscible polyolefin blend during die extrusion and melt spinning." Polymer Engineering & Science **50**(10): 1969-1977.
- Yekta-Fard, M. and A. B. Ponter (1992). "Factors affecting the wettability of polymer surfaces." Journal of Adhesion Science and Technology **6**(2): 253-277.

- You, J., Y. Liao, Y. Men, T. Shi, L. An and X. Li (2011). "Composition Effect on Interplay between Phase Separation and Dewetting in PMMA/SAN Blend Ultrathin Films." Macromolecules **44**(13): 5318-5325.
- Young Wook, C., K. Dongwoo, M. H. Karen and J. W. Thomas (2009). "The role of polymer nanosurface roughness and submicron pores in improving bladder urothelial cell density and inhibiting calcium oxalate stone formation." Nanotechnology **20**(8): 085104.
- Yu, L., K. Dean and L. Li (2006). "Polymer blends and composites from renewable resources." Progress in Polymer Science **31**(6): 576-602.
- Zenkiewicz, M. (2007). "Methods for the calculation of surface free energy of solids." Journal of Achievements in Materials and Manufacturing Engineering **24**(1): 137-145.
- Zhang, F., E. T. Kang, K. G. Neoh, P. Wang and K. L. Tan (2002). "Reactive coupling of poly(ethylene glycol) on electroactive polyaniline films for reduction in protein adsorption and platelet adhesion." Biomaterials **23**(3): 787-795.
- Zhang, Y., D. Wu, M. Zhang, W. Zhou and C. Xu (2009). "Effect of steady shear on the morphology of biodegradable poly(ϵ -caprolactone)/polylactide blend." Polymer Engineering & Science **49**(12): 2293-2300.
- Zisman, W. A. (1964). Relation of Equilibrium Contact Angle to Liquid and Solid Constitution: 1-51.
- Zollinger, H. (1987). Color Chemistry: Syntheses, Properties and Applications of Organic Dyes and Pigments. New York, VCH.